Title
Cysteine sulfenic acid protein modification regulates protein function in eukaryotic photosynthetic organisms during light stress conditions

Author
Endelman, Benjamin J

Publication Date
2018

Peer reviewed|Thesis/dissertation

Cysteine sulfenic acid protein modification regulates protein function in eukaryotic photosynthetic organisms during light stress conditions

By

Benjamin J Endelman

A dissertation submitted in partial satisfaction of the

requirements for the degree of

Doctor of Philosophy

In

Plant Biology

in the

Graduate Division

of the

University of California, Berkeley

Committee in charge:

Professor Krishna K. Niyogi, Chair
Professor Anastasios Melis
Professor Naomi Ginsberg

Spring 2018

Abstract

Cysteine sulfenic acid protein modification regulates protein function in eukaryotic photosynthetic organisms during light stress conditions

By

Benjamin J Endelman

Doctor of Philosophy in Plant Biology

University of California, Berkeley

Professor Krishna K. Niyogi, Chair

Protein oxidation is ubiquitous throughout the tree of life and is important for all organisms to respond to both biotic and abiotic stress conditions. This is especially true in photosynthetic organisms, because they must contend with a daily onslaught of variable light conditions. Under optimal photon flux densities, a plant or alga can use the majority of the light for photochemistry. However, photosynthetic organisms are often inundated with excess light that cannot all be used photochemically due to sink constraints. This excess absorbed excitation energy must be dissipated or else the oxidative stress, caused by the formation of reactive oxygen species (ROS), would cause detrimental damage. These organisms have evolved a number of different mechanisms to dissipate excess energy, collectively known as non-photochemical quenching (NPQ). However, even with these safeguards, excess energy remains and ROS are still formed. Over the last few decades, research has shown that ROS may be more than just damaging to the cell. In fact, ROS can function in a second level of defense through protein oxidation-induced regulation and signaling. To investigate the effects of protein oxidation in photosynthetic organisms, I completed a proteomic analysis to identify cysteine oxidation sites in both *Nannochloropsis oceanica* cells and *Arabidopsis thaliana* chloroplasts, and I characterized cysteine-modified mutants that affect target proteins identified from the proteomics.

In *N. oceanica*, I identified several hundred proteins containing the primary oxidized state of cysteine, cysteine sulfenic acid (Cys-SOH), from three light conditions: dark, low light (LL), and high light (HL). Additionally, the proteomic analysis showed an increase in the number of Cys-SOH modifications with increases in light intensity. From this screen, several targets were selected for reverse genetics. CRISPR/Cas9 ribonucleoprotein-mediated homologous recombination was used to knockout (KO) these target genes. Four mutants showed an NPQ phenotype, with *lhcx1* standing out above the rest. The *lhcx1* KO exhibited a complete loss of the rapidly reversible, feedback de-excitation component of NPQ (qE), demonstrating that it is central to early NPQ induction. I transformed the mutant with the wild type *LHCX1* gene (*lhcx1*+WT) as well as two modified versions of the gene: a cysteine to alanine mutant (*lhcx1*+C162A) to mimic the reduced state of the cysteine and a cysteine to serine (*lhcx1*+C162S) to

mimic the Cys-SOH state. These modifications were chosen to determine what role the cysteine oxidation plays in the function of this protein.

Analysis of the cysteine-modified transgenics showed that LHCX1 is regulated by the oxidation state of its lone cysteine residue. In the *lhcx1*+WT and *lhcx1*+C162A lines, there was a recovery of qE back to the wild type state. In contrast, this recovery was not complete in the *lhcx1*+C162S line, which showed only ~60% of wild type total NPQ, and there was an additional sustained quenching phenotype: up to 50% of the total NPQ was slowly reversible compared to only 20% in *lhcx1*+WT and *lhcx1*+C162A. This sustained quenching was reminiscent of the qZ type of NPQ, which is slow to relax and dependent on zeaxanthin (Zea) formation. I examined Zea levels to determine if this higher qZ quenching was due to overaccumulation of Zea and found that there were no major differences. To determine if this sustained quenching would occur in the wild type, the period of actinic light was increased to allow for ROS build up. After 20 min, the level of qZ in the *lhcx1*+WT line had increased to ~40%, while qZ in *lhcx1*+C162A, which cannot be oxidized, remained low at 20%. These results strongly suggest that the oxidation of C162 to the Cys-SOH state modulates the quenching dynamics from the qE state to a qZ state. Based on protein modeling, it is possible that this switch is caused by a structural change in LHCX1, which directly alters the Zea binding affinity and causes the relocation of Zea away from the qE site(s) on LHCX1 toward qZ sites most likely on VCP type proteins.

In *A. thaliana*, I focused on the chloroplast proteome, as we are most interested in light-induced oxidation reactions. Hundreds of proteins with the Cys-SOH modification were identified from the three light conditions (dark, LL, and HL). Similar to *N. oceanica*, there was an increase in the number of Cys-SOH modified proteins with increases in light intensity, with the HL samples having twice as many modified proteins as the dark samples. The HL sample has an enrichment of proteins, based on GO term analysis, that are involved in translation, transport, and phosphorylation, which might be linked to downstream responses to oxidative stress. Based on the proteomics results, T-DNA lines were acquired in photosynthesis-associated targets for further characterization of possible Cys-SOH regulation. Three lines (*lhca6, prxq,* and *atr2*) had NPQ phenotypes, and one line (*cyp38*) had a strong growth phenotype. *lhca6* had the strongest NPQ enhancement in both LL-grown and HL-treated conditions, so it was transformed with the wild-type *LHCA6* gene (*lhca6*+WT) as well as the two cysteine-modified versions (*lhca6*+C58A and *lhca6*+C58S). The NPQ phenotype of *lhca6*+WT and *lhca6*+C58A both returned to the wild-type level, but the *lhca6*+C58S stayed at the level of the *lhca6* T-DNA line. This is consistent with the possibility of Cys-SOH oxidation causing inactivation of LHCA6. However, this T-DNA line was only a knockdown with highly variable levels of mRNA, ranging from 20-65% of WT, so for complete confidence in the phenotype analysis of a complete KO is required.

NPQ dissipates excitation energy. If not tightly regulated this process could dissipate usable energy when light levels return to the optimal range. The oxidative regulation of proteins associated with NPQ could represent a second level of control, thereby preventing sustained NPQ quenching during short bursts of HL but allowing for greater overall quenching during longer periods of excess light. Additionally, the activation or inactivation of proteins by Cys-SOH formation could play a major role in

many signaling and direct stress responses, beyond the light-mediated stress response examined here.

Table of Contents

FIGURES AND TABLES

CHAPTER 1

CHAPTER 2

CHAPTER 3

APPENDIX A

APPENDIX B

ACKNOWLEDGEMENTS

This dissertation would not have been possible without the help, support and guidance I received throughout my time here.

I would like to thank both the past and present members of the Niyogi lab who have each in there own way aided my progress, either through their direct advice/assistance or helpful comments at our lively lab meetings. Specifically, I would like to thank Matt Brooks who spurred the idea for this project and who mentored me during my early years. Lauriebeth Leonelli who was always there with sage advice and a smile. Erika Erickson and Robbie Caldron for being the wise graduate students that guided me during the start of my graduate career. Masa Iwai who gave insightful technical advice. Dagmar Lyska who is a great friend and collaborator on many a Nanno project. The rest of team Nanno, Chris Gee and Johan Andersen-Ranberg, who were always there to bounce ideas off of or commiserate when things did not go to plan. The list of helpful labmates could go on for many pages but let me just say that each of you helped make me the scientist I am today. Finally, thank you Kris Niyogi for your mentorship and support throughout my time in your lab. I've learned so much from you and will leave your lab a better scientist.

Thanks to Lori Kohlstaedt at the Vincent J. Coates Proteomics/Mass Spectrometry Laboratory for her technical assistance and data analysis on all my proteomics work.

I'd like to thank the professors who served on my qualifying exam committee, Tasios Melis, Henrik Scheller, Bob Buchanan and Naomi Ginsberg, with special thanks to Tasios and Naomi for continuing on as members of my dissertation committee.

I'd like to thank Mike and Sheamus for being with me and supporting me everyday. Without them none of this would have been possible.

Finally, I want to thank my friends and family for their support, with a special shout out to my cohort, PMB 2012, who are awesome people in so many ways and the Foul Tips! for the summertime softball shenanigans.

Chapter 1

CYSTEINE SULFENIC ACIDS IN BIOLOGY: FOCUS ON PLANT BIOLOGY

1: Introduction/scope of this chapter

Regulation of reduction-oxidation (redox) reactions is fundamental to biology, and cysteine sulfenic acids (Cys-SOH) are central to many of the redox regulatory pathways throughout the cell. Redox reactions occur between an oxidizing agent and a reducing agent. These reactions occur in every cellular compartment and are the driving force of most biosynthetic pathways. Enzymes can catalyze redox reactions, because the protein environment in which the reaction occurs can lower the activation energy of the reaction by stabilizing its transition state. During this chapter I will discuss how the conversion of a thiol group to a sulfenic acid can be achieved both chemically and more importantly in a biological context. I will then describe how the formation of Cys-SOH can affect protein regulation throughout the cell and therefore influence biochemical pathways in every part of cellular metabolism.

2: Thiol/sulfenic acid chemistry

Cysteine sulfenic acid (Cys-SOH) modifications of proteins have emerged as one of the most important post-translational modifications in biological redox regulation. Historically, Cys-SOH has been thought of mostly as a transient intermediate state in pathways leading to further downstream modifications, but this concept has been challenged as evidence has built up showing the regulatory role of stable Cys-SOH residues in both protein activation and deactivation. Recent work also suggests that refunctionalization of a protein by cysteine oxidation during high light stress conditions (discussed in Chapter 2) is possible. Characterization of sulfenic acids began over a century ago in the field of inorganic chemistry when the first sulfenic acid species was isolated in a free acid state in anthraquinone-l-sulfenic acid (Fries, 1912). This early success in the stabilization of the free acid state was not repeated for many decades (Pal et al., 1969; Penn et al., 1978) despite many efforts to do so (reviewed in Kharasch et al., 1946; Gupta & Carroll, 2014), owning to that fact that the sulfenic acid moiety is highly reactive.

The high reactivity of the free acid state of sulfenic acid is quite unique in that it can act as either a nucleophile or an electrophile depending on the environment (reviewed in Yang, 2016). Due to the availability of an empty d orbital, the sulfur atom on the cysteine has a large range of oxidation states from -2, in its thiolate anion state, to +6, in its sulfonic acid state (Reddie & Carroll, 2008). Because of the relatively low redox potential of the thiol, cysteines are readily oxidized, which as will be discussed in this chapter, plays an important role in protein regulation. Sulfenic acid, with an oxidation state of 0, can readily react with other sulfur- or nitrogen-containing molecules (Fig. 1.1), many of which have been implicated in various biological regulatory roles. The most well studied of these reactions is the reaction of Cys-SOH with a second thiol group to form a disulfide bond. This bond has been shown to be important in protein structure and in the redox regulation of proteins, e.g. fructose 1-6-bis-phosphatase via

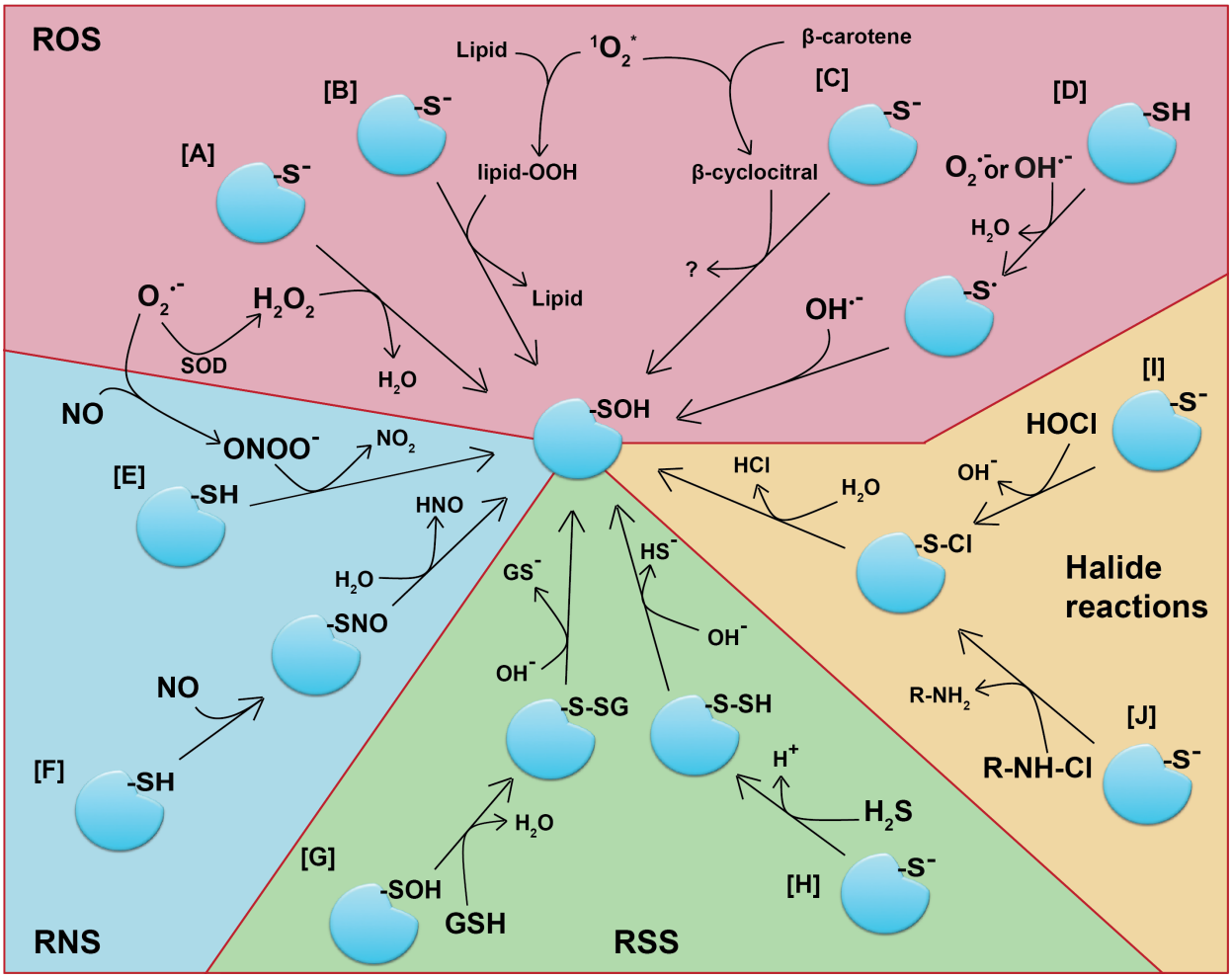

Figure 1.1: Formation of cysteine sulfenic acids in biology.

A. Reaction of cysteine thioloate anion with hydrogen peroxide (H_2O_2) to form Cys-SOH. **B.** Reaction of $^1O_2$ with lipid to form lipid peroxide which then reacts with cysteine thioloate anion to form Cys-SOH. **C.** Reaction of singlet oxygen ($^1O_2$) with β-carotene to form β-cyclocitral which then reacts with cysteine thioloate anion to form Cys-SOH. **D.** Reaction of cysteine thiol with either superoxide ($O_2^{\cdot-}$) or hydroxyl radical ($OH^{\cdot-}$) to form thiyl radical which then reacts with a second $OH^{\cdot-}$ to form Cys-SOH. **E.** Nitic oxide ($^{\cdot}NO$) reacts with $O_2^{\cdot-}$ to form peroxynitrite ($ONOO^-$) which reacts with cysteine thiol to form Cys-SOH. **F.** $^{\cdot}NO$ reacts with cysteine thiol to produce s-nitosolated cysteine, which then hydrolyzes to Cys-SOH. **G.** Glutathione (GSH) binds to Cys-SOH, which then returns to Cys-SOH in alkaline solution. **H.** Hydrogen sulfide (H_2S) binds to cysteine thiolate anion producing a persulfide, which in alkaline solution forms Cys-SOH **I.** Hydrochlorous acid (HOCl) reacts with cysteine thiolate anion to form sulfenyl-chloride, which then hydrolyzes to Cys-SOH. **J.** Chloromine (R-NH-Cl) reacts with cysteine thiolate anion to form sulfenyl-chloride, which then hydrolyzes to Cys-SOH. Modified from Gupta & Carroll, 2014.

thioredoxin (Trx ; Buchanan et al., 1967). Additionally, Cys-SOH can be further oxidized by reactive oxygen species (ROS) to the sulfinic acid (Cys-SO_2H) or sulfonic acid state (Cys-SO_3H). These oxidized states are thought to be irreversible and a signal of oxidative damage that may trigger degradation of the protein (Poole & Nelson, 2008). However, the biological enzyme sulfiredoxin (Srx) can reduce the sulfinic acid back to sulfenic acid, though this is not ubiquitous and is a very specific reaction on only a few proteins (i.e. Peroxiredoxin further discussed below; Biteau et al., 2003; Rey et al., 2007). Additionally, a Cys-SOH residue can interact with glutathione, in a reaction known as a S-glutathionylation (Pihl & Lange, 1962). This reaction is typically considered to be a protective measure to prevent over-oxidation of the cysteine to its more terminally oxidized states. In terms of nitrogen interactions, sulfenic acid can interact with reactive nitrogen species (RNS) to form S-nitrosylation species, which may play a role in biology through RNS signaling (Biswas et al., 2006). Finally, the formation of Cys-sulfonamide through the interaction of the Cys-SOH with an amine or amide can occur with the adjacent protein backbone producing a 5-member ring, acting as an additional hyper-oxidation protection (Poole & Nelson, 2008), although there are other possible biological roles discussed in greater detail below.

Very specific conditions are needed in order to sustain the sulfenic acid on any molecule. The first condition is the requirement to protect the sulfenic acid from interacting with other compounds. Evidence for this was first understood by the development of a few compounds with a sterically hindered sulfenic acid group, one of which had a unique bowl shape to block other reagents' access to the sulfenic acid (Ishii et al, 1996; Goto et al. 1997). Additionally, they showed that direct oxidation of the thiolate anion was possible and that the oxidative product, sulfenic acid, was stable. Also, another group developed a compound, 4,6-dimethoxy-1,3,5-triazine-2-sulfenic acid, with a stable sulfenic acid almost by accident (Tripolt et al., 1993). They saw that the stability of the sulfenic acid, in this case, was directly related to the hydrogen bonding within the molecule. In proteins, the nature of neighboring amino acids also directly influences Cys-SOH stability; polar uncharged amino acids, such as histidine or threonine, can help distribute the electron density around the thiolate anion and sulfenic acid (Salsbury et al., 2008). Additionally, it has been shown that stability requires that there are no proximal cysteine residues (Miller & Claiborne, 1991). The importance of cysteine isolation from other cysteine residues was first implicated in the 1970s (Allison, 1976) and appears to one of the most important factors in sulfenic acid stability *in vivo* as we will see later in this chapter.

3: Protein sulfenic acids

The first evidence that a stable Cys-SOH could be possible in a protein was obtained over 60 years ago when the coat protein of the tobacco mosaic virus was reacted with iodine and retained the stable sulfenyl iodide residue, a very similar oxidative state to Cys-SOH (Fraenkel-Conrat, 1955). This was the first experiment showing the potential that Cys-SOH could be stable and be an important functional group in the formation of disulfide bonds in biology, which led many biologists to explore how cysteine, and its various oxidative states, could be important in redox regulation. Cysteine is unique among the amino acids in that it has a fully available sulfur atom,

which gives it its high reactivity potential. With this high reactivity and the oxidative stress sensitivity of the sulfur group, it makes sense that cysteine is one of the least abundant of the 20 standard amino acids. Protein content of cysteine is exceptionally low in archaea (0.5%) and the highest in mammalian proteins at 2.2%, but this is still lower than an expected 3.8% based on codon usage, with plants and algae falling somewhere in between (Miseta & Csutora, 2000). Additionally, they found that cysteine preferentially exists in a CxxC motif, like those seen in a thioredoxin or metalloproteins, in all species examined except plants. It was also noted that there was an increase in abundance of cysteine with increasing organismal complexity. Miseta and Csutora (2000) speculate that with the increases in oxygen in the environment the eukaryotes evolved a greater capacity to utilize this residue for its redox regulation, allowing them to develop into more complex organisms.

3.1: Formation of sulfenic acids in biology

With the advent of an aerobic atmosphere came many new challenges to the existing and evolving organisms during that era. The increased levels of molecular oxygen, which is far more energetically reactive than the sulfur-rich atmosphere that preceded it, would have been extremely stressful to all organisms during that time, and only those that could evolve mechanisms to deal with the oxygen or stay hidden from it would persist. With this increase in oxygen in the environment, there would also be an increase in ROS, potentially causing detrimental and irreversible damage to cells, leading to death. It would be essential for any organism to be able to manage these highly redox-active compounds and, as research of the last few decades has shown, utilize these oxidants for signaling responses to stress conditions. Firstly, it is important to examine what these potential oxidants are, how they are formed, their localization throughout the cell/organism and, most importantly, how they lead to the formation of Cys-SOH. Additionally, there will be sections on other oxidants, such as RNS and reactive sulfur species (RSS), as well as other ways to form Cys-SOH *in vivo*. I will only go into brief detail on each of these. For a more in-depth examination of reactive species chemistry in biology, see the review by Villamena (2017).

One of the major factors in the formation of Cys-SOH is that the thiol group of cysteine is much less reactive to oxidants than the reduced thiolate anion state. For significant oxidation to occur, the thiol must be deprotonated to the thiolate anion. The pK_a, or logarithmic acid dissociation constant, of a free cysteine is 8.3, higher than standard physiological pH, and therefore the majority of these molecules are retained in the thiol state (Gupta & Carroll, 2014) under this condition. This could pose a problem for many proteins that require the oxidation and, in some cases, further modification of cysteine for their structural and functional regulation. However, due to the specific microenvironment around a cysteine on each protein, the pK_a of many cysteines are changed, ranging from 3-12 (Roos et al., 2013). One of the major factors that determine the individual cysteine's pK_a is the level of hydrogen bonding between the sulfur group and the neighbor hydrogen atoms (Li et al., 2005). A change to a lower pK_a would allow for a thiolate anion dominance at physiological pH, but the hydrogen bonding stabilizing the thiolate comes at a cost on nucleophilicity of that residue. Roos and colleagues note that a very low pK_a may make the reaction with an oxidant less energetically favorable

and could prevent the formation of the Cys-SOH state. Eukaryotic compartmentalization has allowed for high regional changes in pH, which in turn could drive cysteine deprotonation in very specific locations. For example, during the light reactions of photosynthesis the stroma around the thylakoid membrane develops a higher pH (Werdan et al., 1975), in some cases greater than 8. This higher pH would drive deprotonation of many thiols in a light-dependent manner. This could facilitate reaction of those thiols with increased levels of ROS, thereby providing a two-step regulation of protein function and photosynthetic regulation.

Protein structural changes can affect the rate of oxidation by more than just changing the cysteine's pK_a. Hydrogen peroxide (H_2O_2) has a slow oxidative effect on most cellular components, i.e., the second order rate of reaction of free cysteine is fairly low at ~20 $M^{-1}s^{-1}$ (Gupta & Carroll, 2014). However, peroxiredoxins (Prx) have a much higher second order rate of reaction (rate constants ranging as high as 10^8 $M^{-1}s^{-1}$) and would therefore be active at very low levels of ROS (Hall et al., 2010). This is necessary for their roles in the scavenging and management of redox throughout the cell as well as passage of redox potentials in many cellular processes. Hall and colleagues note that this higher reactivity in Prx is likely due to a stabilization of the thiolate anion to hydrogen peroxide intermediate. The changes made to the local environment around oxidizable protein cysteine residues, which increase or decrease the reactivity of these residues with different oxidants would help dictate/regulate the oxidation of the total proteome. Additionally, in plants this directionality of protein oxidation would, in turn, determine the outcome of each photo-oxidative stress event. Hypothetically, if a certain residue has a lower rate of oxidation, then it would require a much higher threshold of ROS for effective oxidation, thereby only allowing regulation of that specific protein, or set of proteins, in extreme stress conditions. The tertiary structure of the cysteine pocket could also dictate which oxidant would be preferentially bound/reacted with, making specific proteins more sensitive to different kinds of stress. For example, the cysteine of Prx2, from human erythrocytes, has a very high specificity for H_2O_2 but a much lower reactivity for other thiol oxidants (Peskin et al., 2007).

3.1.1: ROS

There is a great deal known about the production and signaling aspects of ROS in many different biological systems, from plants and animals to single-celled algae and bacteria (reviewed and referenced in Mullineaux et al., 2018). A complete discussion of how ROS affect regulation and oxidant homeostasis is well beyond the scope of this chapter, so I will instead focus on how the different types of ROS can ultimately end up as Cys-SOH. This will serve as a primer for the discussion of how Cys-SOH impacts biology in every part of the cell during very distinct physiological conditions. Here I will briefly review the role of H_2O_2 in this capacity, with a brief mention of singlet oxygen ($^1O_2$*), superoxide ($O_2^{\cdot-}$), and hydroxyl radical ($OH^{\cdot-}$), which are only indirectly involved in Cys-SOH formation.

The best studied ROS is H_2O_2, which has been implicated in retrograde signaling, cell death, defense response to infection, and high light (HL) stress response, to name a few (Leister, 2017; Mullineaux and Baker, 2010; Kimura et al., 2017; Apel & Hirt, 2004). Some of the sources of H_2O_2 are NADPH oxidase (Nox), superoxide dismutase (SOD),

electron transport chains, chloroplast SOD and ascorbate reaction with singlet oxygen (Sies, 2017; Kramarenko et al., 2006). Many of these sources are cellular compartment specific, which can allow for subcellular microenvironments with drastically different levels of H_2O_2 (Garcia-Santamarina et al., 2014) compared to what is considered the molecular average homeostatic level of H_2O_2, which in animals is around 10 nM (Sies, 2017). In plants, the levels of H_2O_2 can fluctuate dramatically depending on the time of day and light intensity. A local increase in H_2O_2 in all organisms can direct specific responses to stress conditions depending of the source of that stress. This specificity prevents undesired redox responses and allows for the right response at the right time. An excellent example of this is the rapid increase of ROS in the chloroplasts during HL stress in plants.

Rapid increases in H_2O_2 have a strong impact on the cysteine oxidation state of the local environment and in some cases cause a transduction of that oxidation to other regions of the cell. It was shown many years ago (Barton et al., 1973) that H_2O_2 would react with cysteine to form a Cys-SOH (Fig. 1.1A). HL stress in plants and algae causes a dramatic shift in the overall sulfenome, as seen in the coming chapters. These changes can be both fast and, in prolonged exposure, could induce acclimative changes for the new light regime. The Cys-SOH profile alterations of the cell during HL stress are not limited to the chloroplast. Peroxisomes, for example, can sense this change in redox states through the increases in photorespiration, which in turn produces elevated levels of H_2O_2. However, there is still debate as to whether that increase in H_2O_2 has any role in signaling, as the peroxisomal catalase is very effective at scavenging H_2O_2 (Sandalio and Romero, 2015). In the mitochondria, there is evidence that the alternative oxidase (AOX) pathway, which can act as a metabolic sink during light stress, can induce changes to the Cys-SOH profile in the mitochondria through H_2O_2 (Yoshida et al., 2011). Again, there is debate about the relevance to HL stress, as other studies have indicated that AOX can decrease the ROS level in mitochondria and thereby decrease Cys-SOH in that compartment (Møller, 2001). Additionally, due to the relatively low reactivity of H_2O_2, there is evidence suggesting that H_2O_2 could travel to different parts of the cell or to different parts of the organism (Gupta & Carroll, 2014). However, the effectiveness of this *in vivo* is suspect as there are many proteins, e.g. Prx, that can scavenge H_2O_2 and prevent it from building up/traveling to distant parts of the organism. The effectiveness of these scavengers may help keep the redox signal specific to each stress condition.

Singlet oxygen ($^1O_2$*) is formed when an excited state chlorophyll relaxes into the triplet state . Triplet chlorophyll is not energetic enough to donate energy to the reaction centers and is longer lived; its lifetime increases, measured in isolated pigments in pyridine, from 6.3 ns to approximately 400 μs (Niedzwiedzki and Blankenship, 2010). The triplet state is, however, poised to pass its energy to molecular oxygen, which excites it into the highly reactive singlet state. In terms of formation of Cys-SOH there is no evidence that $^1O_2$ can induce this thiol oxidation directly (Triantaphylidès & Havaux, 2009). However, there is evidence that $^1O_2$* can induce the oxidation of β-carotene into β-cyclocitral, and the electrophilic molecule has been speculated to oxidize cysteine thiolate (Fig. 1.1B) in the subsequent transcriptional stress response mechanism (Ramel et al., 2012). Additionally, $^1O_2$* can oxidize lipids into lipid peroxides, which have been shown to effectively oxidize cysteine thiols (Fig. 1.1C; Little & O'Brien, 1968; Kim

et al., 2012). Lipid peroxides have been shown to inactivate proteins through what was presumed to be a Cys-SOH (Wills, 1961). Lipid peroxidation through $^1O_2$* has also been linked to the programmed cell death response associated with Executer 1 and 2, which sense $^1O_2$* through some unknown mechanism, perhaps through a lipid peroxide-specific Cys-SOH formation (Wagner et al., 2004; Lee et al., 2007). This raises an interesting question as to whether or not the formation of a Cys-SOH by β-cyclocitral or lipid peroxides could produce very distinct regulatory responses based on the accessibility and transition state stabilization with the thiolate anion. This is an area of study that has not been explored, to my knowledge, and would help to distinguish a generalized stress response from a more specific one.

The formation of Cys-SOH by superoxide ($O_2^{\cdot-}$) has also not been seen; in fact, the probable reaction of $O_2^{\cdot-}$ with thiolate would produce a thiyl radical not Cys-SOH (Wardman & von Sonntag, 1995). Though there is no direct generation of Cys-SOH, thiyl radical could react with $OH^{\cdot-}$ to form a Cys-SOH (Fig. 1.1D; Wardman, 1998). Also, Cys-SOH formation would be mediated through the activity of the enzyme SOD, which converts the $O_2^{\cdot-}$ into H_2O_2 (Fig. 1.1A; McCord & Fridovich, 1969), as well as spontaneous conversion of $O_2^{\cdot-}$ into H_2O_2. One additional role of $O_2^{\cdot-}$ related to Cys-SOH regulated signaling occurs when a plant senses a pathogenic attack and produces an apoplastic ROS burst, specifically $O_2^{\cdot-}$ through the enzyme NADPH oxidase. This is rapidly converted into H_2O_2 by the apoplastic SOD. This H_2O_2 has been seen to oxidize a cysteine on a receptor-like kinase CRK28 forming a disulfide, through a Cys-SOH, and has been shown to have cysteine-dependent function in producing a defense response (Yadeta et al., 2016). It has also been suggested that this $O_2^{\cdot-}$/H_2O_2 acts directly in defense through anti-microbial action (Kimura et al., 2017). Could the pathogen develop responses to this through its own membrane-bound protein oxidation signals? If so, Cys-SOH could function in the biological arms race between host defenses and pathogen responses. A second indirect source of Cys-SOH from $O_2^{\cdot-}$ is the reaction of nitric oxide ($^{\cdot}NO$) with $O_2^{\cdot-}$ to form peroxynitrite ($ONOO^-$; Marla et al., 1997). This RNS, $ONNO^-$, can directly interact with thiol to form Cys-SOH, which will be discussed in more detail below.

In terms of hydroxyl radical ($OH^{\cdot-}$) most evidence indicates that there is not any appreciable accumulation of this ROS *in vivo*, as the two main ways of forming it are unlikely to occur at any appreciable level. The Haber-Weiss reaction to produce $OH^{\cdot-}$ would be unlikely to occur in any organism due to lack of free transition metal ions in the cell (Stohs & Bagchi, 1995). Additionally, the cell's scavenging power for H_2O_2 and $O_2^{\cdot-}$ would prevent the formation of $OH^{\cdot-}$ in vivo (Hopkins, 2016). And even if there was formation of $OH^{\cdot-}$ in the cell it is thought to be too reactive to induce thiol oxidation directly (Huang et al., 2016). It is interesting to note that it is hypothesized that the reaction of a thiyl radical with a hydroxyl radical could end in a Cys-SOH in what was called a radical sink reaction (Fig. 1.1D), but this was all examined through the eyes of chemistry, which may have no relevance *in vivo* (Wardman, 1998).

3.1.2: RNS

Reactive nitrogen species (RNS) have been receiving more attention in redox biology over the last few decades and are starting to show their promise in Cys-SOH

protein regulation, as well as other reactions not important to our discussion. The two major RNS relevant to Cys-SOH are $^{\cdot}NO$ and $ONOO^-$. Each of these has been implicated in the oxidation of cysteine thiols and could represent different pathways for redox signaling during nitrogen stress.

$^{\cdot}NO$ is the less reactive of the pair but could still lead to Cys-SOH formation both directly or indirectly. $^{\cdot}NO$ is produced in plant and animal cells by the NOS complex and is very important in many developmental responses throughout the organism (Planchet & Kaiser, 2006; East & Garthwaite, 1991). In plants the activity of nitrite reductase can also produce $^{\cdot}NO$ (Yamasaki & Sakihama, 2000). $^{\cdot}NO$ can react to a cysteine to produce Cys-SOH, at least *in vitro*, in both human serum albumin (Demaster et al., 1995) and on cathepsin K (Percival et al., 1999), where a $^{\cdot}NO$ reacted with cysteine thiol to produce a Cys-SOH and a nitrous-oxide (Fig. 1.1F). Although this oxidation was observed, the underlying chemistry is not fully understood. $^{\cdot}NO$ signaling through Cys-SOH could be potentially important, however $^{\cdot}NO$ is fairly unreactive, compared to many of the other oxidants mentioned earlier, so there are limits to what this RNS could do. These limits may provide more clues toward the reoccurring theme of directed oxidation of specific molecules for the correct response to unique stresses. Though there is evidence that $^{\cdot}NO$ can produce Cys-SOH, it is far more likely that the major oxidative contribution of $^{\cdot}NO$ comes from its extremely fast spontaneous reaction with $O_2^{\cdot -}$ to produce $ONOO^-$, which is a much more reactive oxidant (Huie & Padmaja, 1993).

$ONOO^-$ is a fairly strong oxidant that has been shown to directly oxidize cysteine thiols to Cys-SOH (Marla et al., 1997). The only source of $ONOO^-$ known to exist in the cell is from its spontaneous formation by $^{\cdot}NO$ and $O_2^{\cdot -}$ condensation (Radi et al., 2001). This reaction is so fast that it can compete with the reaction of SOD but only when the less reactive $^{\cdot}NO$ is in close proximity to the site of $O_2^{\cdot -}$ formation (Pacher et al., 2007). $ONOO^-$ has been shown to be far more stable than $O_2^{\cdot -}$ and much more reactive then $^{\cdot}NO$, characteristics which make $ONOO^-$ a far better messenger molecule than either of the precursor reactive species. This stability is due to its conformation and hydrogen bonding with adjacent water molecules (Tsai et al, 1994), and it allows $ONOO^-$ to travel much further and aids in some of its oxidative specificity. This reactivity and specificity allows $ONOO^-$ to directly oxidize thiol groups (Fig. 1.1E; Quijano et al., 1997), rather than the reduced thiolate anion. This could induce the oxidative signal of some protein cysteine thiols with pK_a's too high to normally react with H_2O_2, providing a nitrogen-specific stress response. However, this oxidant is not unchecked. It has been shown that a bacterial Prx can scavenge $ONOO^-$ thereby producing a Cys-SOH intermediate, giving additional evidence of its activity in sulfenic acid modifications, and reducing the nitrogen to a nitrite (Bryk et al., 2000). As an interesting side note, $ONOO^-$ has been shown to be extremely important in disease progression in mammalian systems (Pacher et al., 2007).

3.1.3: RSS

It was only recently that the term reactive sulfur species (RSS) started appearing in the literature (Giles et al., 2001). When one discusses RSS in biology, they are usually talking about the family of thiol oxidation states, i.e., thiolate anion, and yes that includes Cys-SOH, which I would say is the most important RSS. However, since we

are discussing the different reactive species in terms of how they can form Cys-SOH, it should be mentioned that the reduced forms of cysteine are very important in the formation of Cys-SOH. A Cys-SOH cannot be formed without the thiol or thiolate first, as discussed above (Fig. 1.1). Additionally, disulfides are within this category. Beyond the thiol derivatives, there are a few other molecules worth mentioning including, H_2S and glutathione.

H_2S and glutathione have the potential to create a Cys-SOH through a secondary reaction with their thiol derivatives through an alkaline-mediated hydrolysis of the sulfur-sulfur bond (Fig. 1.1G & H; Gruhlke & Slusarenko, 2012). This disulfide breaking to form a Cys-SOH has also been seen between protein thiol disulfides, but it needs a high level of alkalinity in the media (Andersson, 1970; Wu et al., 1987; Lay et al., 2000). While this might be possible *in vivo*, most of these reactions seen *in vitro* used higher than physiological pH and some ended in an unstable Cys-SOH. More often the reaction of a H_2S or glutathione with a thiolate or Cys-SOH, respectively, does not result in hydrolysis, and Cys-SOH formation, but rather the formation of a protein inactivation or protection modification (Krishnan et al., 2011; Rouhier et al., 2008). Both of these reactions could play a role in redox regulation under may stress conditions.

3.1.4: Other Cys-SOH forming reactions

There are two additional ways to produce a Cys-SOH: through reaction of a hypohalous acid, e.g. hydrochlorous acid (HOCl), and chloramine reactions with thiolate anion followed by water hydrolysis of the resulting sulfenyl halide (Fig 1.1I & J; Nagy & Ashby, 2007). The hypohalous acid reaction is very fast (second order rates $>10^7$ $M^{-1}s^{-1}$) compared to the chloramine reaction, which can be 20 times slower. Despite this slow reaction it is thought to still be biologically relevant, because chloramine is produced via the reaction of hypochlorous acid with amines, which are significantly more abundant than thiols in the cell (Gupta & Carrol, 2014). Similar to many of the other oxidation reactions mentioned earlier, both of these reactions require the reduced thiolate anion to react effectively so all of the factors for thiolate production and stability would play a role in these reactions. It is worth mentioning, again, that the cysteine local protein environment could impart some specificity in the reaction of either of the halide reactions if their transition state is stabilized by the adjacent amino acids.

3.2: Cys-SOH as a reaction intermediate

3.2.1: Disulfide bond formation

Probably the most studied thiol redox regulation of proteins is the formation and reduction of disulfide bonds. One of the first experiments, in chemistry, that first determined a mechanism of disulfide bond formation showed that it proceeded through a Cys-SOH (Pirie, 1933). This set the stage for many more experiments that eventually showed the transition from the Cys-SOH to a disulfide in a ribonuclease (Haber E, Anfinsen, 1962). Later a different group showed that four separate disulfide bonds were necessary for the three-dimensional structure of the protein in the crystal structure of an egg white lysozyme (Blake et al., 1965). This started a major surge in the work to

understand the effects of disulfides as structural components of proteins and Cys-SOH's role in the disulfide regulation *in vivo* (Wedemeyer et al., 2000). Interestingly, it was recently found that formation of the disulfide for proper folding of a protein can occur spontaneously if there is an oxidant present to produce the Cys-SOH in one member of the thiol pair (Rehder & Borges, 2010). This shows that the Cys-SOH is not only necessary for proper protein structure but also for the act of proper protein folding.

Disulfides, and therefore Cys-SOH, are not only important for protein structure but are also important in both signaling and redox potential relaying. It has already been mentioned that the oxidative state of a proteome can drastically change the physiology of the organism through the action of redox signaling. One of the ways this redox signal is perceived is through the formation of inter- or intra-molecular disulfide bonds. In addition to the CRK28 pathogen response directed by the ROS burst (Yadeta et al., 2016) discussed earlier, the GRIM REAPER ROS sensor protein in the host defense response pathway can bind to a receptor kinase and trigger cell death when its cysteine is oxidized to Cys-SOH and forms the regulatory disulfide (Wrzaczek et al., 2015). This redox signaling also occurs inside the cell. A good example of this is the AtHSFA8 that responds to H_2O_2 through the oxidation of a cysteine residue and translocation from the cytosol to the nucleus (Giesguth et al., 2015). This translocation requires two cysteine residues and is most likely driven by disulfide bond formation. For a more comprehensive review of the redox signaling potential of cysteine see Nagahara (2011).

In cyanobacteria the oxidation of the elongation factor Tu (EF-Tu), which in need for the translation of plastid encoded proteins, inactivates the protein through a disulfide bond formation (Yutthanasirikul et al., 2016). This inactivation phenotype was seen by activity assess in both reducing (added DTT) and oxidizing (added H_2O_2) conditions. They found that C82 was responsive to the H_2O_2 and when oxidized the WT protein would loss translational activity. However, when they modified this cysteine to serine, which would mimic the Cys-SOH state, they do not see the deactivation of EF-Tu. This shows that Cys-SOH is not inactivating the protein, in fact it is constitutively activating the protein, and most likely it is the formation of an intermolecular disulfide homodimer, see through non-reducing SDS-PAGE, responsible for this proteins inactivation.

The vast amount of literature on the subject of redox potential relaying has filled entire books and has also been extensively reviewed (Yang, 2016; Villamena, 2017). Therefore, I will only briefly discuss some of the important players in the next few subsections and try to focus on Cys-SOH related PTMs and how they act in the transfer of redox potentials and signals. The main focus will be on the families of thiol oxidoreductases as they have been extensively studied over the past half-century and they play a major role in biology.

3.2.2: Peroxiredoxin

Prxs are one of the most abundant antioxidant proteins in cells (Chae et al., 1999). In addition to this well-studied function, recent evidence shows that a peroxiredoxin may play a role in the directed oxidation of specific protein cysteine residues to Cys-SOH in the cytosol (Stöcker et al., 2018). There are 3 types of Prx: 2-Cys Prx, atypical 2-Cys Prx and 1-Cys Prx, named according to the number of cysteine residues in each Prx active site that are important to their redox scavenging function.

The typical 2-Cys Prx has an antiparallel homodimer with two active sites formed between the N-terminal cysteine of one monomer and the C-terminal cysteine of the other. This differs from the atypical 2-Cys Prx, which is always a monomer; it has two active site cysteines coming together from separate helixes of the same protein. The 1-Cys Prx can form a dimer like the typical 2-Cys Prx, but it lacks the C-terminal cysteine and only has a single cysteine in its active site (Choi et al., 1998).

Despite their different structures, all of the Prx function through the same mechanism in the scavenging of hydroperoxides and peroxynitrites through the intermediate formation of a Cys-SOH in their active sites (Fig. 1.2A; reviewed in Rhee et al., 2005). This mode of action involves the interaction of the peroxidatic cysteine, which is situated in a domain conserved in all three types, with a peroxide or peroxynitrite to form a Cys-SOH and reduce the oxidant to water, an alcohol or nitrite, respectively. This Cys-SOH must then be reduced to reactivate the Prx. In the 2-Cys Prxs, after Cys-SOH formation, a conformational change occurs that allows a disulfide bond to form between the two reaction center cysteine residues. A Trx or other disulfide oxidoreductase will then reduce this disulfide renewing the Prx (Fig. 1.2B; Rhee et al., 2005). In the 1-Cys Prx the Cys-SOH, which is slightly more stable, will react first with a free small molecule thiol, such as glutathione, before being resolved by a Trx or Grx (Fig. 1.2C; Hugo et al., 2009). In both cases there is the possibility of over-oxidation at the Cys-SOH, which may function in its own regulatory role (Rey et al., 2007).

3.2.3: Thioredoxin

Trx is a broad family of proteins that are important in redox regulation of many biological processes. The term thioredoxin originates from over 50 years ago from the discovery of an enzyme involved in disulfide reduction in bacteria (Laurent et al., 1964). At the same time, Bob Buchanan was working on how ferredoxin regulates the Calvin-Benson cycle, leading him to discover that Ferredoxin-thioredoxin reductase and Trx f were needed for the regulation of FBPase (Wolosiuk & Buchanan, 1977). This discovery was probably the first real example of redox regulation in biology. Since the early years, Trx has expanded to every part of the cell and seems to be involved in many different processes. In mammals there are only a few types of Trx, each of which is associated to a specific compartment or set of compartments, but in plants there are 22 potential Trx genes that represent at least seven types (Meyer et al., 2012). In plants the expansion of this class of enzymes is probably in part due to the chloroplast, which has five potential Trxs. This expansion is not specific to land plants, as genome studies in *Chlamydomonas* have shown a similarly large pool of Trx genes (Lemaire et al., 2003).

Trx is important in the resolution of Cys-SOH-mediated disulfides on Prx proteins. The mechanism behind this reaction is the formation of what is called the ‘forbidden’ disulfide between adjacent cysteines in a CGPC motif (Wouters et al., 2007). This forbidden nature is due to physical constraints on the formation of this disulfide that were thought to be too great to overcome (Thornton, 1981). This was later found to not be the case in relationship to Trx as this constrained disulfide is key to its function. Since the first discovery of the constrained pair of cysteines, the mechanism of this reaction has been very well studied and is now mostly understood (reviewed in Collet & Messens, 2010). Fundamentally, reduced Trx reacts with a disulfide bond on a protein

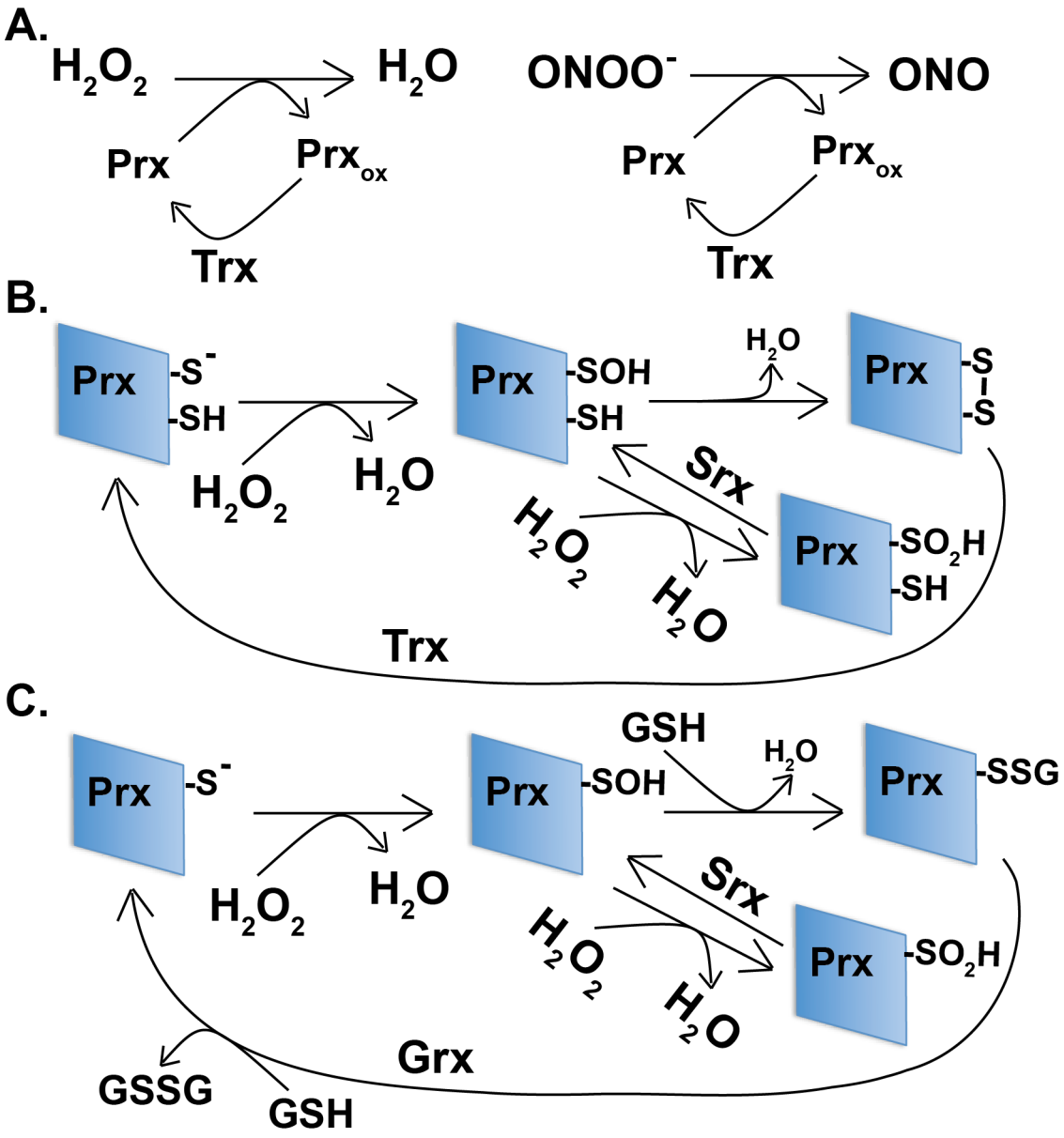

Figure 1.2: Schematic of Prx reduction of hydrogen peroxide and peroxynitrite.

A. General reaction of H2O2 reduction to water via Prx and ONNO- reduction to nitrite. **B.** Specific reaction of 2-cys Prx with H2O2 followed by disulfide bond formation and reduction back to active Prx by Trx; over-oxidation reaction and reduction by Srx also shown. **C.** Specific reaction of 1-cys Prx with H2O2 followed by glutathionylation and reduction back to active Prx by Grx; over-oxidation reaction and reduction by Srx also shown.

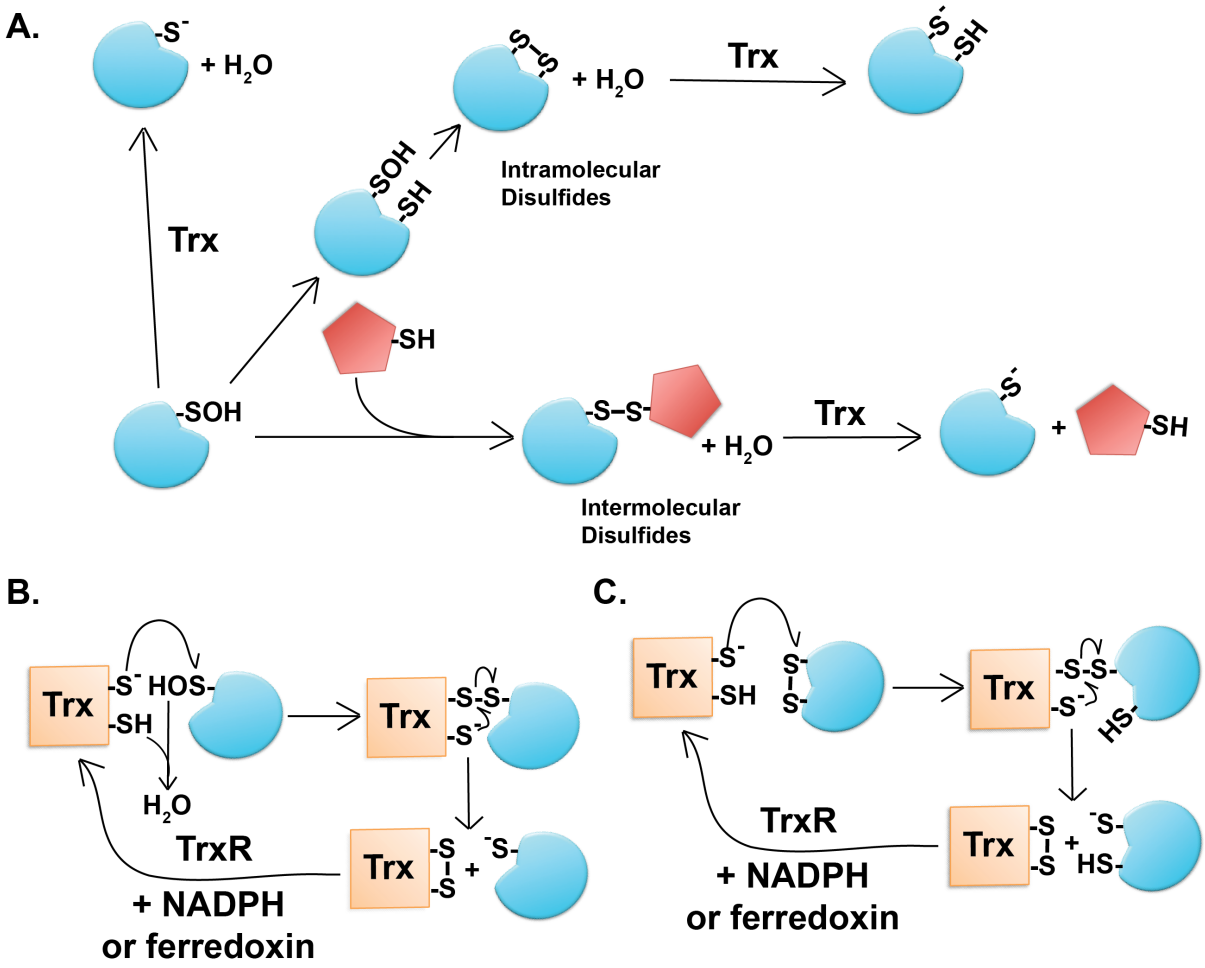

Figure 1.3: Schematic of Trx reduction of disulfide bonds and Cys-SOH.

A. General reaction from Cys-SOH to disulfide bond and reduction of Cys-SOH or the disulfide bond back to thioloate anion by Trx. **B.** a closer look at the reaction of Trx with a Cys-SOH and recover of Trx by a TrxR and NADPH or Ferridoxin **C.** a closer look at the reaction of Trx with a disulfide bond and recover of Trx by a TrxR and NADPH or Ferridoxin.

producing a transient intermolecular disulfide, which is then transferred to the constrained pair, leaving the target protein reduced (Fig. 1.3C). Thioredoxin reductase (TrxR) can then reduce the constrained disulfide with the energy of NADPH or Ferredoxin. It is interesting to note that the two cysteine in the Trx domain have different pK_a values (~7 and 9), and this is why one can be a stable thiolate and attack the target and the other remains a thiol until the intermolecular disulfide is formed. Once the attack has occurred, the pK_a of the resolving cysteine is reduced due to the changes to the local environment, which allows for a thiolate to form and complete the disulfide cycle. Additionally, it has been shown in plants that a Cys-SOH can be directly targeted and reduced by a Trx through the attack of the Cys-SOH by the stable Trx thiolate and resolution by the second cysteine (Fig 1.3B; Tarrago et al., 2010).

I will focus on the chloroplast in oxygenic photosynthetic organisms to give a snapshot of how the great diversity of Trxs provides unique downstream regulation through very similar means. The five chloroplast Trx types are involved in a wide range of regulation from anabolic processes (Trx f and m), protection against oxidative stress (Trx x and y) and transcription (Trx z; Buchanan, 2016). In addition to all the types of Trx, there have been a number of proteomic studies to examine the Trx interaction partners and as of 2009 there were already 500 potential targets (Montrichard et al., 2009). This fairly large pool of Trxs and targets start to form a broader network of redox regulation that spreads throughout the cell and outside the cell. It is also worth mentioning another unique Trx of plant/algal chloroplasts known as NTRC. This enzyme has both the Trx reductase (TrxR) domain, which uses the energy of NADPH to reduce/recycle the Trx (Kuriyan et al., 1991), and a Trx domain (Serrato et al., 2004), essentially housing two steps in a redox cycle within a single protein. NTRC is of special interest in our lab because of its involvement with the reduction of photosynthetic components in plants and knockouts of this gene showed sensitivity to fluctuating light (Carrillo et al., 2016; Nikkanen et al., 2018). Also, a knockout line in *N. oceanica* shows changes in the photoprotective capacity of the cell (unpublished data from our lab), potentially showing its involvement in the reduction of high-light-oxidized proteins during the relaxation of photoprotection. Even with all of this diversity in the family of Trx, they are all still very functionally similar in their resolution of Cys-SOH mediated disulfide bonds.

3.2.4: Glutaredoxin

Glutathione (GSH) is a small thiol containing peptide that can directly react with Cys-SOH residues on proteins and is fairly abundant throughout the cell (Noctor et al., 2011). This direct reaction of GSH with Cys-SOH is known as S-glutathionylation and is thought to play a role in protecting Cys-SOH residues from over-oxidation, though more recent studies have shown that the GSH addition could have its own functional role (Rouhier et al., 2008). Once GSH is bound to cysteine, a special enzyme glutaredoxin (Grx) can reduce the cysteine residue, returning it to a thiolate anion and transferring the GSH to one of the Grx active site cysteine residues (Fig. 1.4). Similar to the other thiol oxidoreductases mentioned so far, the active site of Grx is relatively conserved and retains a Trx-fold domain with sequence specificity of CxxC/CxxS. The mechanism for

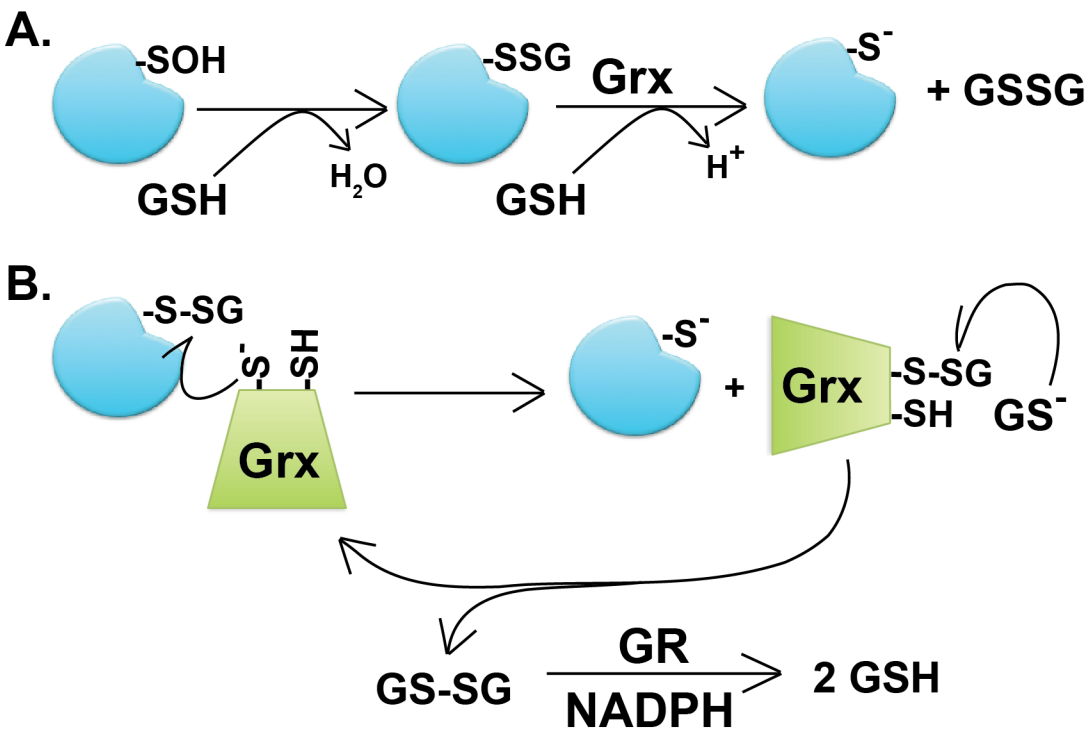

Figure 1.4: Schematic of Grx reduction of Cys-SOH with glutathione adduction.

A. Cys-SOH reacts with GSH to form glutathionylated cysteine, which reacts with a second GSH with the help of Grx to get a oxidized glutathione and reduced cysteine thiolate anion. **B.** Reaction of Grx on the glutathionylated cysteine and recovery of active Grx by second GSH followed by reduction of GSSG to GSH by glutathione reductase (GR) and NADPH.

the recovering Grx is through the deglutathionylation of its active site Cys by the disulfide exchange to a second free GSH molecule forming a GSSG disulfide (Lillig et al., 2008). This oxidized glutathione can then be reduced by glutathione reductase using the energy of an NADPH molecule. An example in plants of the functional regulation of glutathionylation is in the methionine sulfiredoxin-B (MSRB) protein, where it was seen that cysteine oxidation to Cys-SOH inactivated the protein and the addition of glutathione was important for the reduction and reactivation (Vieira Dos Santos et al., 2007). A genome wide examination in plants found that there were potentially 40 Grx adding a great deal of diversity to the already large pool of thiol oxidoreductases (Rouhier et al., 2006). This adds more stock into the vast redox potential under constant management throughout the cell.

3.2.5: Other transient Cys-SOH regulation pathways

I want to briefly mention a few other interesting modifications that are mediated by Cys-SOH. Firstly, the induction of an amide ring by Cys-SOH on the peptide backbone has been shown in a few cases to be important in protein regulation. Tyrosine phosphatases (PTPs), which are a large class of proteins that function antagonistically to tyrosine kinases to control signaling cascades, have been shown to be redox sensitive through a Cys-SOH to amide ring formation pathway (Fig. 1.5A). PTPs were shown to have a very highly conserved domain with Cys and Arg residues that are necessary for the amide ring formation (Yang et al, 2007). This ring formation inactivates the PTP and has been shown to be important in a number of different ROS mediated redox regulations directed through the integrin surface receptor signaling pathways (Ostman et al., 2011).

A different example of cysteine oxidation regulation comes from the hypoxia, low oxygen, sensing mechanism in plants. During hypoxia, plants are able to sense this lack of oxygen and send a signal to the nucleus to alter transcription to acclimate. This sensing is done through an ERF VII transcription factor (TF), which has a conserved cysteine residue on its N-terminus that during aerobic conditions is oxidized to Cys-SOH. This Cys-SOH directs N-end rule pathway regulation (Licausi et al., 2011). This form of regulation involves the arginylation of the N-terminus, which is then recognized by an N-recognin that directs the protein for proteolytic degradation (Fig. 1.5B; Graciet & Wellmer, 2010). Under normal conditions this TF is bound to the plasma membrane by an acyl-CoA binding protein where it is protected from oxidation, but during hypoxic conditions the TF is released and can relocate to the nucleus and induce the transcriptional response need for acclimation. When the oxygen level returns to normal, the Cys residue can be oxidized, triggering the N-end rule pathway and degradation of the TF.

Finally, further oxidation of Cys-SOH to sulfinic acid and sulfonic acid plays an important role during high oxidative stress conditions (Fig. 1.5C). It is important to mention that the rate for over-oxidation of cysteine is at least two orders of magnitude slower than thiolate oxidation (Hugo et al., 2009). Because of this slower rate of oxidation, stabilization of the Cys-SOH would be required for the formation of these higher oxidation states. The over-oxidation has been observed in a number of crystal structures (PrxII for example; Schröder et al., 2000) and is thought to play one of two

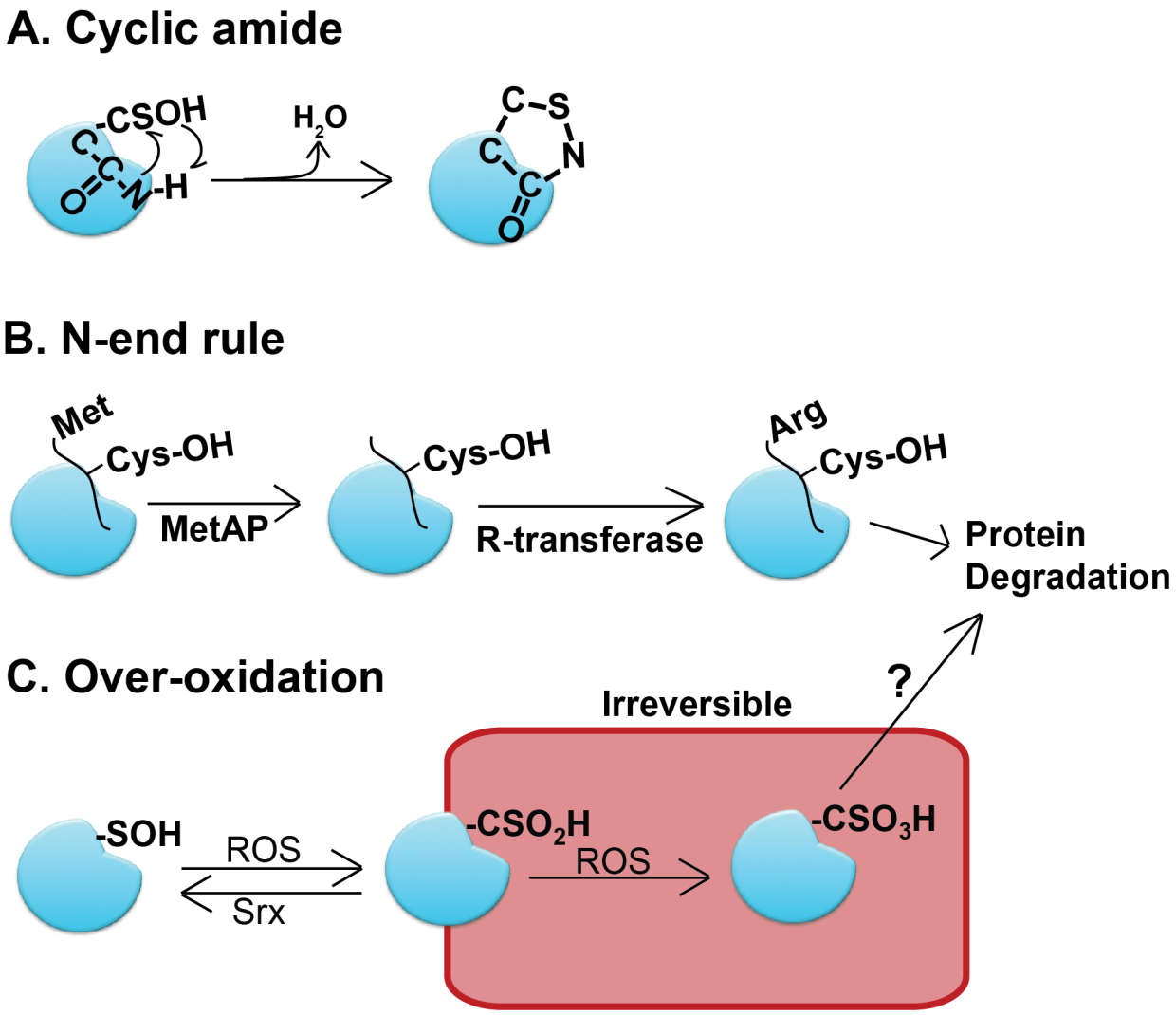

Figure 1.5: Other Cys-SOH modification reactions.

A. Cyclic amide formation by reaction of Cys-SOH with nitrogen atom in the protein backbone. **B.** N-end rule pathway reaction with removal of methionine upon cysteine oxidation followed by arginine replacement and protein degradation. **C.** Over-oxidation of Cys-SOH by additional ROS leading to mostly irreversible cysteine sulfinic acid, with an sulfiredoxin reactions being the exception, and further oxidation to the completely irreversible sulfonic acid possibly leading to protein degradation.

roles. In terms of sulfinic acid on Prx this modification is thought to be a signal for inactivation, perhaps a way to induce downstream signaling in high oxidative conditions by inactivating the scavenger (Jang et al., 2004). This inactivation is reversible by Srx, which is specialized in reduction of sulfinic acid to sulfenic acids in this protein (Lowther & Haynes, 2011). Secondly, these over-oxidations can be irreversible and may trigger proteolysis. If specific proteins were more labile to this irreversible oxidation, this degradation would act as an inhibitor of that set of proteins changing the downstream signaling pathways.

3.3: Stable Cys-SOH in biology

It has only recently been shown that a Cys-SOH can act as a stable group on a protein that can cause regulatory changes to those proteins. In chemistry the idea of a stable sulfenic acid is over a century old, but even then it was thought to be uncommon due to sulfenic acid's reactivity, as mentioned above. In the early 1970's it was hinted that a Cys-SOH could be involved in inactivating proteins (Ehring & Colowick, 1969; Allison & Connors, 1970); in the 1990's, a stable Cys-SOH in a biological system was shown to be possible (Radi et al., 1991). With the improvement of protein technologies, many additional examples of stable sulfenic acid residues in proteins have been identified. For example, in human serum albumin there are 17 cys, 16 of which form disulfides and the last, which is secluded from the others, could be stably sulfenylated for hours (Turell et al., 2008). Experimental evidence has also shown that these stable Cys-SOH residues can have an average calculated lifetime ranging from 4 to12 min via GSH-mediated relaxation *in vivo* (Gupta V & Carroll KS. 2014). This analysis was limited since there is additional evidence that the Cys-SOH modification can be reduced by other Trx-like proteins (Couturier et al., 2013), and the calculations were only done for a few proteins, but it does show that these Cys-SOH can be stable enough to have an effect on the cell.

As of 2012, there have been over 400 different proteins from different organisms that have been crystalized with a Cys-SOH residue (reviewed in Furdui and Poole, 2013). There have also been a number of experiments utilizing mass spectroscopy to identify even more Cys-SOH locations (Ellis & Poole, 1997; Saurin et al., 2004). Whether those stable Cys-SOH are all functionally relevant is yet to be determined. However, over the last few decades a number of stable Cys-SOH residues have been shown to function in regulation of many different biological processes in bacterial and mammalian systems. For example, a stable Cys-SOH inactivates the previously mentioned PTP and the use of the cyclic amide is only used in the recovery of the enzyme (Van Montfort et al., 2003). Over the next few subsections I will explore a few more examples of this Cys-SOH-directed protein regulation in greater detail.

3.3.1: Kinase activity and transduction

Kinases are ubiquitous throughout the tree of life and are essential for the propagation of many cellular signals. Kinases are able to sense a signal and convey a message via protein phosphorylation transduction pathways. This works through the activation of the kinase by either directly perceiving a signal or by its phosphorylation via

another kinase in the signaling cascade (reviewed in Johnson et al., 1996). After it has been activated it directs the signal by phosphorylating its specific targets and regulates their function. Because of their importance in many signaling pathways, it should not be surprising that in humans there are over 500 genes that code for kinases, making up to 2% of the entire gene pool (Manning et al., 2002). In plants, the Arabidopsis Genome Initiative (2000) reported upwards of 1000 potential kinase genes. Considering the broad diversity of kinases and their role in signal perception and transduction, much work has been done to understand how they function in the cell under various stress conditions. Oxidative stress can to be perceived by kinases and in the next few examples I will explain how the Cys-SOH plays a role in these proteins' activity. One other note on kinases is that there is evidence that a Prx1 can be inactivated by phosphorylation, indicating that a kinase could be involved in a localized H_2O_2 increase beyond what would be possible if the Prx ROS scavenging were still active (Woo et al., 2010).

In humans, Cys-SOH increases the phosphorylation activity of the epidermal growth factor receptor (EGFR) by modifying the ATP binding site (Paulsen et al., 2011). Previous work had shown that Cys-SOH is involved in the perception of epidermal growth factor (EGF), phosphorylation of 'prosurvival pathways' and an increase in H_2O_2 caused by an association with a NOX protein (Woo et al., 2010). It was noted that there was an increase in kinase activity but the inactivation of phosphatase activity, through Cys-SOH mediated cyclic amide formation, did not account for all of the kinase activity. However, the presence of Cys-SOH on EGFR could account for the rest of the increased in activity. The authors utilized kinetic assays using H_2O_2 and EGF as well as a dimedone chemical binding assay and MS/MS to show that the specific cysteine was sulfenylated. This was one of the first examples that specifically showed a stable Cys-SOH was important in the function of a protein, showing that this modification can stand-alone.

In bacteria, Cys-SOH was shown to inactivate the RegB membrane bound kinase in the anoxygenic photosynthetic organism *Rhodobacter capsulatus* which in turn down regulates RegA, which is a TF involved in many metabolic processes including photosystem synthesis (Wu et al., 2013). It has been known that the inactivation of RegB occurs in oxygenic stress conditions, but only about 20% of the 95% kinase inactivation had been accounted for by disulfide bond formation between the dimers (Swem et al., 2003). To determine how the rest of the kinase was being inactivated, they completed a set of experiments similar to those that elucidated EGFR function in 2011. They used a chemical binding to show that under oxidized conditions there was an increase in the Cys-SOH presence in RegB. The labeling was completely abolished in a C265A mutant, indicating that C265 was the site of oxidation. This Cys-SOH presence and location was confirmed using MS/MS. They also showed that the activity of this protein was increased in the presence of the reducing agent DTT. These data show the importance of the Cys-SOH in the inactivation of RegB.

In photosynthetic eukaryotic organisms, there have been no reports that show a role for a stable Cys-SOH in the functional regulation of a protein kinase.

3.3.2: Transcription

Redox regulation of transcription factors has been extensively studied (reviewed in Marinho et al., 2014), but few have been shown to be directly regulated by a stable Cys-SOH modification. Work on ROS regulation of TF have shown that certain cysteines are required for regulation and that they are sensitive to H_2O_2. An example in plants showed that on a homeodomain TF there are three cysteines and two of them are required for DNA binding regulation by oxidative stress (Comelli & Gonzalez, 2007). It also appears that the oxidation of the third cysteine residue affects the DNA-binding specificity and may change the DNA targets. However, it is not clear if this is mediated by a Cys-SOH or other oxidative modification and with the requirement of two proximal cysteine residues for regulation it suggests formation of a disulfide bond. In another example, HspA8 translocates to the nucleus from the cytosol upon oxidation, but again the specific oxidation modification was not reported/known (Dietz, 2015). However, in recent years there have been a few examples that show the presence of a stable Cys-SOH in regulating TF function.

OhrR is one of the earliest examples of a stable Cys-SOH modification in biology that directly changes a protein's reactivity (Fuangthong & Helmann, 2002). OhrR is a TF in *Bacillus subtilis* that is involved in the repression of the *ohrA* control region, which encodes peroxide resistance genes. Upon exposure to ROS, OhrR Cys15 oxidizes to a Cys-SOH, and this modified TF can no longer bind to the *ohrA* control region, allowing OhrA to be expressed. They determined Cys15 was involved using chemical labeling, MS analysis, and cysteine mutation complementation experiments. Dimerization was not detected in native PAGE, suggesting that an intermolecular disulfide bond was not formed. Also, they used a chemical that produced a unique signal depending on whether it was bound to thiol or sulfenic acid to show that upon ROS addition the thioester sulfenic acid product was produced.

A second example is the transcriptional regulator CrtJ of *Rhodobacter* has been shown to have a stable Cys-SOH that can change the DNA-binding affinity of the TF (Cheng et al., 2012). Oxidation of the cysteine residue increased the binding affinity of the protein by almost 20 times. To determine if Cys-SOH was involved in the oxidative increase in binding, they used chemical labeling as well as MS/MS to determine that Cys420 was oxidized to Cys-SOH during stress conditions both *in vitro* and *in vivo*. They also showed that a Cys to Ala mutation at Cys420, to mimic the null state, had 60-fold reduction in DNA binding activity and a Cys to Ser, to mimic the oxidized state, had a 4-fold increase in binding activity relative to CrtJ in aerobic conditions. These data provide very strong evidence that a Cys-SOH at Cys420 dramatically increases the activity of CrtJ, showing that this modification is important for fully activating this protein.

4: Concluding remarks

Nearly all of the previous advances in the field of Cys-SOH-directed protein regulation have been done in either prokaryotic cells or mammalian systems leaving our beloved plants unattended. One exception is the recent work in *Arabidopsis thaliana* that found 67 proteins that are liable to oxidation by H_2O_2 (Waszczak et al., 2014). This sulfenome examination was, however, limited to cytosolic proteins that were oxidized during one hour with H_2O_2 exogenously applied to protoplast cells. Additionally, these oxidized proteins had to be able to react in vivo with the Yap-1 protein, which was

previously show to bind directly to Cys-SOH in yeast (Ma et al., 2007). This was a good start in the examination of cysteine liability to oxidative stress in a plant, but what about physiological conditions, such as high light stress, or the proteins in the chloroplast, the source of much of the ROS in plants/algae? Also, do any of those Cys-SOH impart regulation on the proteins identified? These questions motivated my dissertation research. Hopefully by the end of the next few chapters, I will have begun to answer some of these questions and helped to open up an exciting new field of research in the redox regulation of photosynthetic eukaryotes.

References

Allison WS & Connors MJ. 1970. The activation and inactivation of the acyl phosphatase activity of glyceraldehyde-3-phosphate dehydrogenase. Arch. Biochem. Biophys. 136: 383-391.

Allison WS. 1976. Formation and reactions of sulfenic acids in proteins. Acc. Chem. Res. 9, 293-299.

Andersson L-O. 1970. Hydrolysis of disulfide bonds in weakly alkaline media II. Bovine serum albumin dimer. Biochim Biophys Acta, Protein Struct. 1970; 200:363–369.

Apel K & Hirt H. 2004. Reactive oxygen species: metabolism, oxidative stress, and signal transduction. Annu Rev Plant Biol. 55, 373-99.

Barton JP, Packer JE, Sims RJ. 1973. Kinetics of the reaction of hydrogen peroxide with cysteine and cysteamine. J. Chem. Soc. Perkin Trans. 2: 1547-1549.

Biswas S, Chida AS, Rahman I. 2006. Redox modifications of protein- thiols: emerging roles in cell signaling. Biochem Pharmacol, 71, 551-564.

Biteau B, Labarre J & Toledano MB. 2003. ATP-dependent reduction of cysteine-sulphinic acid by *S. cerevisiae* sulphiredoxin. Nature. 425, 980-984.

Blake CC et al. 1965. Structure of hen egg-white lysozyme. A three-dimensional Fourier synthesis at 2 Angstrom resolution. Nature 206, 757–761.

Bob B. Buchanan. 2016. The Path to Thioredoxin and Redox Regulation in Chloroplasts. Ann Review Plant Bio, 67(1), 1-24.

Bryk R, Griffin P, Nathan C. 2000. Peroxynitrite reductase activity of bacterial peroxiredoxins. Nature, 407: 211-215.

Buchanan B, Kalberer P, Arnon D. 1967. Ferredoxin-activated fructose diphosphatase in isolated chloroplasts. *Biochem Biophys Res Comm* 29: 74–9.

Carrillo LR, Froehlich JE, Cruz JA, Savage LJ & Kramer DM. (2016), Multi-level regulation of the chloroplast ATP synthase: the chloroplast NADPH thioredoxin reductase C (NTRC) is required for redox modulation specifically under low irradiance. Plant J, 87: 654–663.

Chae HZ, Kim HJ, Kang SW & Rhee SG. 1999. Characterization of three isoforms of mammalian peroxiredoxin that reduce peroxides in the presence of thioredoxin. Diabetes Res. Clin. Pract. 45, 101–112.

Cheng Z, Wu J, Setterdahl A, Reddie K, Carroll K, Hammad LA, et al. 2012. Activity of the tetrapyrrole regulator CrtJ is controlled by oxidation of a redox active cysteine located in the DNA binding domain. Molecular Microbiology, 85(4), 734–746.

Choi HJ, Kang SW, Yang CH, Rhee SG, & Ryu SE. (1998) Crystal structure of a novel human peroxidase enzyme at 2.0 A˚ resolution. Nat. Struct. Biol. 5, 400–406.

Collet J-F & Messens J. 2010. Structure, Function, and Mechanism of Thioredoxin Proteins. Antioxidants & Redox Signaling, 13(8), 1205-1216.

Comelli RN and Gonzalez DH. 2007. Conserved homeodomain cysteines confer redox sensitivity and influence the DNA binding properties of plant class III HD-Zip proteins. Arch Biochem Biophys 467: 41–47.

Couturier J, Chibani K, Jacquot J-P, & Rouhier N. 2013. Cysteine-based redox regulation and signaling in plants. *Frontiers in Plant Science*, *4*, 105–105.

Demaster EG, Quast BJ, Redfern B, Nagasawa HT. 1995. Reaction of nitric-oxide with the free sulfhydryl-group of human serum-albumin yields a sulfenic acid and nitrous-oxide. Biochemistry. 34: 11494-11499.
Demenstrated the importance of hydrogen bonding in the stabilization of sulfenic acids. Tripolt R, Belaj F, Nachbaur E. 1993. Unexpectedly stable sulfenic acid—4,6-dimethoxy-1,3,5-triazine-2-sulfenic acid—synthesis, properties, molecular and crystal-structure. Z. Naturforsch., B: Chem. Sci. 48: 1212-22.
Dietz KJ. 2014. Redox regulation of transcription factors in plant stress acclimation and development. Antioxidants & Redox Signaling, 21, 1356–1372.
East SJ, Garthwaite J. 1991. DA receptor activation in rat hippocampus induces cyclic GMP formation through the L-arginine-nitric oxide pathway. Neurosci Lett., 123, 17-9.
Ehring R & Colowick SP. 1969. The two-step formation and inactivation of acylphosphatase by agents acting on glyceraldehyde phosphate dehydrogenase. J. Biol. Chem. 244: 4589-4599.
Ellis HR & Poole LB. 1997. Novel application of 7-chloro-4-nitrobenzo-2-oxa-1,3-diazole to identify cysteine sulfenic acid in the AhpC component of alkyl hydroperoxide reductase. Biochem., 36, 15013–15018.
Formation of Cys-SOH by hydrolyzing a disulfide bond. Pal BC, Uziel M, Doherty DG, Cohn WE. 1969. Isolation and characterization of a pyrimidine sulfenic acid via scission of the sulfur–sulfur bond in the methyl analog of bis(4-thiouridine) disulfide. J. Am. Chem. Soc. 91: 3634-3638.
Fraenkel-Conrat H. 1955. The reaction of tobacco mosaic virus with iodine. J. Biol. Chem. 217: 373-381.
Fries, K. 1912. Über α-Anthrachinon-sulfensäure. Ber. Dtsch. Chem. Ges., 45: 2965–2973.
Fuangthong M, Helmann JD. 2002. The OhrR repressor senses organic hydroperoxides by reversible formation of a cysteine-sulfenic acid derivative. Proc. Natl. Acad. Sci. U. S. A. 99: 6690-6695.
Garcia-Santamarina S, Boronat S & Hidalgo E. 2014. Reversible cysteine oxidation in hydrogen peroxide sensing and signal transduction. Biochemistry 53, 2560–2580.
Giles GI, Tasker KM & Jacob C. 2001. Hypothesis: The role of reactive sulfur species in oxidative stress. Free Radic. Biol. Med., 31, 1279–1283.
Goto K, Holler M, Okazaki R. 1997. Synthesis, structure, and reactions of a sulfenic acid bearing a novel bowl-type substituent: the first synthesis of a stable sulfenic acid by direct oxidation of a thiol. J. Am. Chem. Soc. 119: 1460-1461
Graciet E & Wellmer F. 2010. The plant N-end rule pathway: structure and functions. *Trends Plant Sci.* **15**, 447–453.
Gruhlke MCH & Slusarenko AJ. 2012. The biology of reactive sulfur species (RSS). Plant Phys & Biochem. 59, 98-107.
Gupta V & Carroll KS. 2014. Sulfenic acid chemistry, detection and cellular lifetime. BBA. 1840 (2), 847-875.
Haber E, Anfinsen CB. 1962. Side-chain interactions governing the pairing of half-cystine residues in ribonuclease. J Biol Chem., 237, 1839–1844.

Hall A, Parsonage D, Poole LB & Karplus PA. 2010. Structural evidence that peroxiredoxin catalytic power is based on transition-state stabilization. J. Mol. Biol. 402, 194-209.
Hopkins R. 2016. Superoxide in biology and medicine: an overview. React. Oxyg. Species, 1, pp. 99-109.
Huang S, Van Aken O, Schwarzländer M, Belt K & Millar AH. 2016. The roles of mitochondrial reactive oxygen species in cellular signaling and stress response in plants. Plant Physiol., 171, 1551-1559.
Hugo MN, Turell LA, Manta B, Botti H, Monteiro G, Netto LES, Alvarez B, Radi R & Trujillo M. 2009. Thiol and sulfenic acid oxidation of AhpE, the one-cysteine peroxiredoxin from mycobacterium tuberculosis: kinetics: acidity constants, and conformational dynamics Biochemistry. 48, 9416-9426
Huie RE, Padmaja S. 1993. The reaction of no with superoxide. Free Radic Res Commun., 18, 195-9.
Ishii A, Komiya K & Nakayama J. 1996. Synthesis of a Stable Sulfenic Acid by Oxidation of a Sterically Hindered Thiol (Thiophenetriptycene-8-thiol)1 and Its Characterization. *J. Am. Chem. Soc. 118* (50), 12836–12837.
Jang HH, et al. 2004. Two enzymes in one: two yeast peroxiredoxins display oxidative stressdependent switching from a peroxidase to a molecular chaperone function. Cell 117, 625–635
Johnson LN, Noble ME, & Owen DJ. 1996. Active and inactive protein kinases: structural basis for regulation. Cell 85, 149–158.
Kharasch, N., Potempa, S. J., & Wehrmeister, H. L. (1946). The Sulfenic Acids and their Derivatives. *Chemical Reviews*, *39*(2), 269–332.
Kim C, Meskauskiene R, Zhang S, Lee KP, Ashok ML, Blajecka K, Herrfurth C, Feussner I & Apel K. 2012. Chloroplasts of Arabidopsis Are the Source and a Primary Target of a Plant-Specific Programmed Cell Death Signaling Pathway. The Plant Cell. (7) 3026-3039.
Kimura S, Waszczak C, Hunter K & Wrzaczek M. 2017. Bound by Fate: The Role of Reactive Oxygen Species in Receptor-Like Kinase Signaling. The Plant Cell, 29 (4), 638-654.
Kramarenko GG, Hummel SG, Martin SM, Buettner GR. 2006. Ascorbate reacts with singlet oxygen to produce hydrogen peroxide. Photochem. Photobiol., 82, 1634.
Krishnan N, Fu C, Pappin DJ & Tonks NK. 2011. H2S-Induced sulfhydration of the phosphatase PTP1B and its role in the endoplasmic reticulum stress response. *Sci. Signal.* 4, 86.
Kuriyan J, et al. 1991. Convergent evolution of similar function in two structurally divergent enzymes. Nature, 352, 172-174.
L.H. Ma, C.L. Takanishi, M.J. Wood, Molecular mechanism of oxidative stress perception by the Orp1 protein, J. Biol. Chem. 282 (2007) 31429–31436.
Laurent TC, Moore EC & Reichard P. 1964. Enzymatic synthesis of deoxyribonucleotides. IV. Isolation and characterization of thioredoxin, The hydrogen donor from Escherichia coli. J. Biol. Chem., 239, 3436-3444.
Lay AJ, Jiang XM, Kisker O, Flynn E, Underwood A, Condron R, Hogg PJ. 2000. Phosphoglycerate kinase acts in tumour angiogenesis as a disulphide reductase. Nature. 408, 869–873.

Lee KP, Kim C, Landgraf F & Apel K. (2007) EXECUTER1- and EXECUTER2-dependent transfer of stress-related signals from the plastid to the nucleus of *Arabidopsis thaliana*. Proc. Natl. Acad. Sci. U.S.A. 104, 10270–10275

Leister D. 2017. Piecing the Puzzle Together: The Central Role of Reactive Oxygen Species and Redox Hubs in Chloroplast Retrograde Signaling. Antioxidants & Redox Signaling Epub: doi.org/10.1089/ars.2017.7392.

Lemaire SD, Collin V, Keryer E, Issakidis-Bourguet E, Lavergne D, Miginiac-Maslow M. 2003. Chlamydomonas reinhardtii: a model organism for the study of the thioredoxin family. Plant Physiol Biochem, 41, 513-521.

Li H, Robertson AD & Jensen JH. 2005. Very fast empirical prediction and rationalization of protein pK_a values. Proteins, 61, 704–721.

Licausi F, Kosmacz M, Weits DA, Giuntoli B, Giorgi FM, Voesenek LA, Perata P, van and Dongen JT. 2011. Oxygen sensing in plants is mediated by an N-end rule pathway for protein destabilization. Nature 479: 419–422.

Lillig CH, Berndt C & Holmgren A. 2008. Glutaredoxin systems. BBA, 1780 (11), 1304-17.

Little C & O'Brien PJ. 1968. The effectiveness of a lipid peroxide in oxidizing protein and non-protein thiols. Biochem. J. 106, 419–423.

Lowther WT & Haynes AC. 2011. Reduction of cysteine sulfinic acid in eukaryotic, typical 2-Cys peroxiredoxins by sulfiredoxin. Antioxid. Redox Signal. 15, 99–109

M. Giesguth, A. Sahm, S. Simon, K.J. Dietz. 2015. Redox-dependent translocation of the heat shock transcription factor AtHSFA8 from the cytosol to the nucleus in Arabidopsis thaliana. FEBS Lett., 589, 718-725.

Manning G, Whyte DB, et al. 2002. The protein kinase complement of the human genome. Science, 298 (5600), 1912–1934.

Marinho HS, Real C, Cyrne L, Soares H & Antunes F. 2014. Hydrogen peroxide sensing, signaling and regulation of transcription factors. Redox. Biol. 2, 535–562.

Marla SS, Lee J, Groves JT. 1997. Peroxynitrite rapidly permeates phospholipid membranes. PNAS, 94, 14243–14248.

McCord JM & Fridovich I. 1969. Superoxide Dismutase: An enzymatic function for erythrocuprein (hemocuprein). J Bio Chem. 244, 6049-6055.

Meyer Y, Belin C, Delorme-Hinoux V, Reichheld JP & Riondet C. 2012. Thioredoxin and glutaredoxin systems in plants: molecular mechanisms, crosstalks, and functional significance. Antioxid. Redox Signal., 17, 1124-1160.

Meyer Y, Reichheld JP, Vignols F. 2005. Thioredoxins in Arabidopsis and other plants. Photosynthesis Res, 86, 419-433.

Miller H & Claiborne A. 1991. Peroxide modification of monoalkylated glutathione reductase. Stabilization of an active-site cysteine-sulfenic acid. J. Biol. Chem. 266, 19342-19350.

Miseta A and Csutora P. 2000. Relationship Between the Occurrence of Cysteine in Proteins and the Complexity of Organisms, *Mol Bio and Evo*. 17(8), 1232–1239.

Møller IM. 2001. Electron transport, NADPH turnover, and metabolism of reactive oxygen species. Annu. Rev. Plant Physiol. Plant Mol. Biol., 52, 561-591.

Montrichard F, Alkhalfioui F, Yanoc H, Vensel WH, Hurkman WJ & Buchanan BB. 2009. Thioredoxin targets in plants: The first 30 years. J Prot. 72(3), 452-474.

Mullineaux PM & Baker NR. 2010. Oxidative stress: antagonistic signaling for acclimation or cell death? Plant Phys., 154.
Mullineaux PM, Exposito-Rodriguez M, Laissue PP &Smirnoff N. 2018. ROS-dependent signalling pathways in plants and algae exposed to high light: Comparisons with other eukaryotes. Free Rad. Bio. Med. https://doi.org/10.1016/j.freeradbiomed.2018.01.033
Nagahara, N. 2011. Intermolecular disulfide bond to modulate protein function as a redox-sensing switch. Amino Acids 41, 59-72.
Nagy P & Ashby MT. 2007. Reactive sulfur species: kinetics and mechanisms of the oxidation of cysteine by hypohalous acid to give cysteine sulfenic acid. J. Am. Chem. Soc. 129: 14082-14091.
Nikkanen L, Toivola J, Trotta A, Diaz MG, Tikkanen M, Aro EM & Rintamaki E. 2018. Regulation of chloroplast NADH dehydrogenase-like complex by NADPH-dependent thioredoxin system. bioRxiv (preprint - unreviewed article)
Noctor G, Queval G, Mhamdi A, Chaouch S, and Foyer CH. 2011. Glutathione. The Arabidopsis Book 9:e0142.
Ostman A, et al. 2011. Regulation of protein tyrosine phosphatases by reversible oxidation. J. Biochem., 150 (4), 345-356.
Pacher P, Beckman JS & Liaudet L. 2007. Nitric oxide and peroxynitrite in health and disease. Physiol Rev., 87, 315–424.
Paulsen CE, Truong TH, Garcia FJ, Homann A, Gupta V, Leonard SE & Carroll KS. 2011. Peroxide-dependent sulfenylation of the EGFR catalytic site enhances kinase activity. Nat. Chem. Biol. 8, 57-64.
Penn RE, Block E, Revelle LK. 1978. Flash vacuum pyrolysis studies 5-Methanesulfenic acid. J. Am. Chem. Soc., 100: 3622-3623
Percival MD, Ouellet M, Campagnolo C, Claveau D, Li C. 1999. Inhibition of cathepsin K by nitric oxide donors: evidence for the formation of mixed disulfides and a sulfenic acid. Biochemistry. 38, 13574–13583.
Peskin AV, Low FW, Paton LN, Maghzal GJ, Hampton MB & Winterbourn CC. 2007. The High Reactivity of Peroxiredoxin 2 with H2O2 Is Not Reflected in Its Reaction with Other Oxidants and Thiol Reagents. J. Biol. Chem., 282 (16), 11885–11892.
Pihl A & Lange R. 1962. The interaction of oxidized glutathione, cystamine monosulfoxide, and tetrathionate with the-SH groups of rabbit muscle D-glyceraldehyde 3-phosphate dehydrogenase. J. Biol. Chem. 237: 1356-1362.
Pirie NW. 1933. The oxidation of sulphydryl compounds by hydrogen peroxide: catalysis of oxidation of cysteine by thiocarbamides and thiolglyoxalines. Biochem. J. 27: 1181-1188.
Planchet E & Kaiser WM. 2006. Nitric Oxide Production in Plants: Facts and Fictions. Plant Signal Behav. 1(2), 46–51.
Quijano C, Alvarez B, Gatti RM, Augusto O & Radi R. 1997. Pathways of peroxynitrite oxidation of thiol groups. Biochem. J., 322: 167-173.
Radi R, Beckman JS, Bush KM, Freeman BA. 1991. Peroxynitrite oxidation of sulfhydryls. The cytotoxic potential of superoxide and nitric oxide. J Biol Chem., 266(7), 4244-50.

Radi R, Bush KM, Cosgrove TP & Freeman BA. 1991. Reaction of xanthine oxidase-derived oxidants with lipid and protein of human plasma. Arch. Biochem. Biophys. 286: 117-125.
Ramel F, Birtic S, Ginies C, Soubigou-Taconnat L, Triantaphylidès C & Havaux M. 2012. Carotenoid oxidation products are stress signals that mediate gene responses to singlet oxygen in plants. Proc. Natl. Acad. Sci. USA, 109 (2012), pp. 5535-5540.
Reddie KG, & Carroll KS. 2008. Expanding the functional diversity of proteins through cysteine oxidation. *Current Opinion in Chemical Biology*, *12*(6), 746–754.
Rehder DS & Borges CR. 2010. Cysteine sulfenic Acid as an Intermediate in Disulfide Bond Formation and Nonenzymatic Protein Folding. *Biochemistry*. *49* (35), 7748-7755.
Rey P, Becuwe N, Barrault MB, Rumeau D, Havaux M, Biteau B, et al. 2007. The *Arabidopsis thaliana* sulfiredoxin is a plastidic cysteine- sulfinic acid reductase involved in the photooxidative stress response. *Plant J.* 49, 505–514.
Rhee SG, Chae, H. Z., and Kim, K. 2005. Peroxiredoxins: a historical overview and speculative preview of novel mechanisms and emerging concepts in cell signaling. Free Radical Biol. Med. 38, 1543– 1552.
Rhee SG, Chae, H. Z., and Kim, K. 2005. Peroxiredoxins: a historical overview and speculative preview of novel mechanisms and emerging concepts in cell signaling. Free Radical Biol. Med. 38, 1543– 1552.
Roos G, Foloppe N & Messens J. 2013. Understanding the pK(a) of redox cysteines: the key role of hydrogen bonding. Antioxid. Redox Signal. 18, 94-127
Rouhier N, Couturier J & Jacquot JP. 2006. Genome-wide analysis of plant glutaredoxin systems. J. Exp. Bot., 57, 1685-1696.
Rouhier N, Lemaire SD, Jacquot JP. 2008. The role of glutathione in photosynthetic organisms: emerging functions for glutaredoxins and glutathionylation. Annu. Rev. Plant Biol., 59, 143-166.
Salsbury Jr FR, Knutson ST, Poole LB & Fetrow JS. 2008. Functional site profiling and electrostatic analysis of cysteines modifiable to cysteine sulfenic acid. Protein Sci. 17, 299-312.
Sandalio LM & Romero-Puertas MC. 2015. Peroxisomes sense and respond to environmental cues by regulating ROS and RNS signalling networks. Ann. Bot., 116, 475-485.
Saurin AT, Neubert H, Brennan JP & Eaton P. 2004. Widespread sulfenic acid formation in tissues in response to hydrogen peroxide, Proc. Natl. Acad. Sci., 101, 17982–17987.
Schröder E, et al. 2000. Crystal structure of decameric 2-Cys peroxiredoxin from human erythrocytes at 1.7 Å resolution. Structure, 8, 605-615.
Serrato AJ, Pérez-Ruiz JM, Spínola MC & Cejudo FJ. 2004. A Novel NADPH thioredoxin reductase localized in the chloroplast, which deficiency causes hypersensitivity to abiotic stress in Arabidopsis thaliana. J. Biol. Chem., 279, 43821-43827
Sies H. 2017. Hydrogen peroxide as a central redox signaling molecule in physiological oxidative stress: oxidative eustress. Redox Biol., 11, 613-619.

Stöcker S, Maurer M, Ruppert T, & Dick TP. 2018. A role for 2-Cys peroxiredoxins in facilitating cytosolic protein thiol oxidation. *Nature Chemical Biology*, *14*(2), 148–155.
Stohs SJ & Bagchi D. 1995. Oxidative mechanisms in the toxicity of metal ions. Free Radic. Biol. Med., 18, 321-336.
Swem LR, Kraft BJ, Swem DL, Setterdahl AT, Masuda S, Knaff DB, Zaleski JM, & Bauer CE. 2003. Signal transduction by the global regulator RegB is mediated by a redox-active cysteine. EMBO J. 22, 4699–4708.
Tarrago L, Laugier E, Zaffagnini M, Marchand CH, Le Maréchal P, Lemaire SD & Rey P. 2010. Plant thioredoxin CDSP32 regenerates 1-cys methionine sulfoxide reductase B activity through the direct reduction of sulfenic acid. J Biol Chem., 285(20), 14964-72.
The Arabidopsis Genome Initiative. 2000. Analysis of the genome sequence of the flowering plant Arabidopsis thaliana. Nature, 408, 796-815.
Thornton JM. 1981. Disulphide bridges in globular proteins. J. Mol. Biol., 151, 261-287.
Triantaphylidès C & Havaux M. 2009. Singlet oxygen in plants: production, detoxification and signaling. Trends plant sci. 14 (4), 219-228.
Tsai JHM, Harrison JG, Martin JC, Hamilton TP, van der Woerd M, Jablonsky MJ, Beckman JS. Role of conformation of peroxynitrite anion ($ONOO^-$) in its stability and toxicity. J Am Chem Soc. 1994;116:4115–4116.
Turell L, Botti H, Carballal S, Ferrer-Sueta G, Souza JM, Duran R, Freeman BA, Radi R & Alvarez B. 2008. Reactivity of sulfenic acid in human serum albumin. Biochem. 47, 358-367.
Van Montfort RL, Congreve M, Tisi D, Carr R, Jhoti H. 2003. Oxidation state of the active-site cysteine in protein tyrosine phosphatase 1B. *Nature 423*:773–777.
Vieira Dos Santos C, Laugier E, Tarrago L, Massot V, Issakidis-Bourguet E, Rouhier N & Rey P. 2007. Specificity of thioredoxins and glutaredoxins as electron donors to two distinct classes of arabidopsis plastidial methionine sulfoxide reductases B. FEBS Lett., 581, 4371-4376.
Villamena FA. 2017. Chapter 2- Chemistry of Reactive Species. Reactive species detection in biology, 12-64.
Wagner D, Przybyla D, Op den Camp R, Kim C, Landgraf F, Lee KP, Würsch M, Laloi C, Nater M, Hideg E & Apel K. 2004. The genetic basis of singlet oxygen-induced stress responses of Arabidopsis thaliana. Science 306, 1183–1185.
Wardman P & von Sonntag C. 1995. Kinetic factors that control the fate of thiyl radicals in cells. Methods Enzymol, 251, 31–45.
Wardman P. 1998. Evaluation of the “radical sink” hypothesis from a chemical-kinetic viewpoint. J. Radioanal. Nucl. Chem. 232, 23-27.
Waszczak C, Akter S, Eeckhout D, Persiau G, Wahni K, Bodra N, et al. 2014. Sulfenome mining in Arabidopsis thaliana. PNAS USA, 111(31), 11545–11550.
Wedemeyer WJ, Welker E, Narayan M & Scheraga HA. 2000. Disulfide Bonds and Protein Folding. Biochemistry 39, 4207-4216.
Werdan K, Heldt HW & Milovancev M. 1975. The role of pH in the regulation of carbon fixation in the chloroplast stroma. Studies in CO_2 fixation in the light and dark. Biochimica et Biophysica Acta, 396, 276-292.

Wills ED. 1961. Effect of unsaturated fatty acids and their peroxides on enzymes. Biochem. Pharmacol. 7: 7-16.
Wolosiuk RA & Buchanan BB. 1977. Thioredoxin and glutathione regulate photosynthesis in chloroplasts. Nature, 266, 565-567.
Woo, H.A. et al. 2010. Inactivation of peroxiredoxin I by phosphorylation allows localized H2O2 accumulation for cell signaling. Cell, 140, 517–528.
Wouters MA, George RA, and Haworth NL. 2007. "Forbidden" disulfides: Their role as redox switches. Curr Protein Pept Sci, 8, 484–495.
Wrzaczek, M., et al. 2015. GRIM REAPER peptide binds to receptor kinase PRK5 to trigger cell death in Arabidopsis. EMBO J. 34: 55–66
Wu HL, Shi GY, Wohl RC, Bender ML. 1987. Structure and formation of microplasmin. Proc Natl Acad Sci, 84, 8793–8795.
Wu J, Cheng Z, Reddie K, Carroll K, Hammad LA, Karty JA, & Bauer CE. 2013. RegB Kinase Activity Is Repressed by Oxidative Formation of Cysteine Sulfenic Acid. Journal of Biological Chemistry, 288(7), 4755–4762.
Yadeta, K.A., Elmore, J.M., Creer, A.Y., Feng, B., Franco, J.Y., Rufian, J.S., He, P., Phinney, B.S., Coaker, G.L. (2016). An extracellular cysteine-rich protein kinase associates with a membrane immune complex and is required for cell death. Plant Physiol. 173: 773–789.
Yamasaki H & Sakihama Y. 2000. Simultaneous production of nitric oxide and peroxynitrite by plant nitrate reductase: in vitro evidence for the NR-dependent formation of active nitrogen species. FEBS Letters 468, 1873-3468.
Yang J, et al. 2007. Reversible oxidation of the membrane distal domain of receptor PTPalpha is mediated by a cyclic sulfonamide. Biochemistry, 46 (3), 709-719.
Yang Y. 2016. Chapter 9- peptide oxidation/reduction side reactions. Side reactions in peptide synthesis. Academic press. 217-233.
Yoshida K, Terashima I & Noguchi K. 2011. How and why does the mitochondrial respiratory chain respond to light? Plant Signal. Behav., 6, 864-866.
Yutthanasirikul R, Nagano T, Jimbo H, Hihara Y, Kanamori T, Ueda T, et al. 2016. Oxidation of a Cysteine Residue in Elongation Factor EF-Tu Reversibly Inhibits Translation in the Cyanobacterium Synechocystis sp. PCC 6803. *Journal of Biological Chemistry*, *291*(11), 5860–5870.

Chapter 2

NON-PHOTOCHEMICAL QUENCHING IS MODULATED BY CYSTEINE SULFENIC ACID MODIFICATION OF LHCX1 IN *NANNOCHLOROPSIS OCEANICA*

Abstract:

Oxidation of proteins during environmental stress plays an important role in regulating protein function. Oxidation of cysteine residues to disulfides is well studied as a regulatory mechanism in biology, but relatively little is known about the role of non-disulfide cysteine oxidation in eukaryotic photosynthetic organisms. Because molecular oxygen and reactive oxygen species (ROS) are inevitable byproducts of the light reactions of photosynthesis, we examined which proteins have cysteine sulfenic acid modifications in the emerging model photosynthetic stramenopile, *Nannochloropsis oceanica.* Comparing three light conditions (dark, low light, and high light) by immunoblot analysis and LC-MS/MS, we observed an overall increase in cysteine sulfenic acid residues with increasing light intensity. One of the proteins identified to contain cysteine sulfenic acid in high light was LHCX1, a protein involved in photoprotective non-photochemical quenching of chlorophyll fluorescence (NPQ). To determine the possible role of cysteine oxidation in the regulation/function of LHCX1, we expressed either of two mutant alleles of *LHCX1* in the *lhcx1* mutant: cysteine to alanine (*lhcx1*+C162A) to mimic the constitutively reduced state and cysteine to serine (*lhcx1*+C162S) to mimic the constitutively oxidized state; expression of the wild-type gene (*lhcx1*+WT) served as the control. A complete recovery of NPQ was observed in low-light-grown cells of the *lhcx1*+WT and *lhcx1*+C162A lines, indicating that in low light the reduced cysteine form of LHCX1 is predominant. On the other hand, the *lhcx1*+C162S line showed only a partial (~60%) recovery of NPQ, which exhibited altered kinetics and a more prominent slowly relaxing component. Upon longer exposure to high light, the *lhcx1*+C162A line retained a low level of slowly reversible NPQ, while that of *lhcx1*+WT approached the level of *lhcx1*+C162S. Additionally, overexpression of LHCX1 led to higher overall NPQ and a lower level of slowly relaxing NPQ compared to wild type. We hypothesize that oxidation of C162 in the native LHCX1 protein acts as a switch, which redirects zeaxanthin from LHCX1 to sites of slowly reversible NPQ by decreasing the zeaxanthin binding affinity near C162 when there is greater oxidative stress in excess light.

Significance:

Global proteomic analysis shows that cysteine sulfenic acid modifications increase with higher light intensities in the photosynthetic eukaryote *Nannochloropsis oceanica.* We demonstrate that the activity of the LHCX1 protein in rapidly reversible photoprotection is affected by its oxidation state. Oxidation of the single cysteine in LHCX1 appears to favor a switch to a sustained, slowly reversible type of photoprotection. More broadly, this work identifies a vast resource of proteins with cysteine sulfenic acid modifications that can be further examined to determine to what

extent this post-translational modification can regulate photosynthesis and many other metabolic functions throughout the cell.

Introduction:

A major challenge in plant biology has been to better understand how photosynthesis is regulated and controlled with the goal of improving crop yields, production of biofuels, and resistance to environmental stresses. Much of the light absorbed by photoautotrophs in full sunlight is dissipated by photoprotective mechanisms, and a greater understanding of these mechanisms is critical for increasing photosynthetic efficiency and biomass productivity (Zhu et al., 2004). One type of photoprotection, thermal dissipation of excess absorbed light energy, is measured as non-photochemical quenching (NPQ) of chlorophyll fluorescence (Müller et al., 2001). There have been many advances in research on photoprotection in the last few decades that have identified the network of proteins that are necessary for NPQ (Li et al., 2000; Depège et al., 2002; Bellafiore et al., 2005; Peers et al., 2009; Brooks et al., 2013; Malnoe et al., 2018). Recent work has shown that overexpressing genes involved in NPQ relaxation in a model crop plant resulted in up to a 20% increase in biomass over the growing season (Kromdijk et al., 2016). This is only the beginning of what can be achieved if the processes that regulate photosynthesis can be identified and optimized for crop production.

NPQ has many components that range in kinetics from fast-acting responses that can be activated and relaxed in seconds to minutes to slower acclimation responses that turn on and off on a timescale of several minutes to hours (Muller et al., 2001). Here we focus on two of the NPQ components, qE and qZ. The fastest known NPQ component, qE, responds to the high ΔpH that is built up across the thylakoid membrane in excess light (Krause et al., 1982; Noctor et al., 1991). Stress response proteins involved in induction of qE are hypothesized to be sensitive to the change in thylakoid lumen pH: PsbS in plants (Li et al., 2000), LHCSR in green algae (Peers et al., 2009; Liguori et al., 2013; Ballottari et al., 2016), and LHCX in photosynthetic stramenopiles (Bailleul et al., 2010; Chukhutsina et al., 2017; Lyska et al., 2018). It has also been shown that qE is dependent on the de-epoxidation state of the xanthophyll cycle pool (Demmig-Adams, 1990; Niyogi et al., 1998; Lavaud et al., 2012). The second type of NPQ, which activates on a timescale of minutes to tens of minutes, is qZ, so named because of its dependence on zeaxanthin; qZ is distinct from qE due to its independence from ΔpH when zeaxanthin is present (Dall'Osto et al., 2005; Nilkens et al., 2010). It is believed that this more slowly relaxing quenching takes place in the photosystem II antenna, but the specific sites and regulation of qZ are still unknown (Demmig-Adams et al, 2014).

Despite the multiple mechanisms to dissipate excess energy, reactive oxygen species (ROS; e.g. singlet oxygen, superoxide, hydrogen peroxide, hydroxyl radical, etc.) are still formed. In photosynthesis, ROS can be produced when excitation energy is not used or dissipated by photochemistry, chlorophyll fluorescence, or NPQ (reviewed by Foyer and Shigeoka, 2011). ROS can oxidize cellular components such as lipids, DNA, and proteins. However, not all oxidation of proteins is damaging, and it has been increasingly appreciated that ROS can act as signaling molecules throughout the cell

(Jones, 2006; Foyer and Noctor, 2009; reviewed in Mullineaux et al., 2018). Oxidation of cysteine residues to form cysteine sulfenic acid (Cys-SOH) plays a crucial role in many redox reactions and has been studied in plants since the discovery of ferredoxin (Buchanan et al., 1967). A number of functionally related proteins, such as thioredoxins, have been found that undergo similar oxidative modifications during redox reactions in other pathways (reviewed in Montrichard et al., 2009). The Cys-SOH residues on most of these proteins are short-lived and tend to act as intermediates in the formation and reduction of disulfide bonds (Couturier et al., 2013). Additionally, Cys-SOH can be further oxidized to a sulfinic acid (Cys-SO_2H) and a sulfonic acid (Cys-SO_3H) state. Cys-SO_2H has been shown to be reversible by a single enzyme, Srx (Rey, et al., 2007; Woojin et al., 2012). The biological reversal of Cys-SO_3H has never been observed, and it may represent a terminally oxidized state (Fig. 2.1a).

Recent work has shown that oxidation of a cysteine to Cys-SOH on a protein can be stable yet reversible and induce a change in protein activity (Chiang et al., 2010). For example, in the anaerobic photosynthetic prokaryote *Rhodobacter*, stable Cys-SOH residues were shown to negatively regulate the function of RegB, a membrane-bound kinase that activates a transcription factor for photosynthetic gene expression, RegA (Wu et al., 2013). In the presence of oxidative stress, the cysteine residues of RegB are oxidized to stable sulfenic acids, which results in inactivation of the transcription of photosynthetic genes. Further evidence of stable Cys-SOH comes from x-ray crystallography, which has revealed more than 400 proteins that maintain a stable Cys-SOH residue in many different organisms (reviewed in Furdui and Poole, 2013).

Not all Cys-SOH modifications negatively regulated protein function. The transcriptional regulator CrtJ of *Rhodobacter* requires Cys-SOH to have high binding affinity, up to 20 times higher than the reduced form (Cheng et al., 2012). Similar to other post-translational modifications, such as phosphorylation, it would also be reasonable to predict that Cys-SOH might refunctionalize proteins, e.g. from a light harvesting to a quenching state. For example, STN7, a kinase involved in state transitions, phosphorylates LHCB antenna proteins to induce movement of these complexes away from PSII supercomplexes (Bellafiore et al., 2005). In this example, the phosphorylation refunctionalizes the antenna from a light-harvesting complex for PSII to either an antenna for PSI or a quencher, depending on where it moves. Compared to phosphorylation, which is entirely dependent on a kinase delivering the phosphate group, the sulfenylation of a protein could occur by direct oxidation without a protein catalyst, although recent evidence in a mammalian system has shown that a peroxiredoxin may play a role in the directed oxidation of specific proteins in the cytosol (Stöcker et al., 2018). Additionally, Cys-SOH formation would be fast due to reactivity of cysteine residues with ROS or molecular oxygen and probably reversible through a thioredoxin-like protein (Couturier et al., 2013).

Most work on Cys-SOH has been done in bacterial or mammalian systems, leaving a vast unexplored area of research on eukaryotic photosynthetic organisms (examples in: Van Montfort et al., 2003; Cheng et al., 2012; Wu et al., 2013). One exception is the cytosolic sulfenome established for *Arabidopsis thaliana,* in which 67 proteins with Cys-SOH were identified after exposure to exogenous H_2O_2 (Waszczak et al., 2014). Among the changes in the protein oxidation landscape of the cell, we hypothesize that specific Cys-SOH modifications might change the activity of target

proteins, leading to acclimation to photo-oxidative stress. ROS generated by photo-oxidative stress increase oxidized pressure in the cell and as such, overall Cys-SOH modifications are presumed to increase.

To test this hypothesis, we examined Cys-SOH modifications of proteins in the model photosynthetic stramenopile, *Nannochloropsis oceanica*. *N. oceanica* is an ideal system for this work as many tools have recently been developed to allow genetic manipulation of this haploid organism (Kilian et al, 2012; Wang et al., 2016; Poliner et al., 2018; Lyska et al, 2018), which possesses a doubling time of 22 h to enable rapid experimentation. *N. oceanica* is also important to the biofuels industry as a possible feedstock for lipid-based biofuel production due to its ability to accumulate ~60% of its biomass as oil upon nitrogen or osmotic stress (Rodolfi et al., 2009). Additionally, *Nannochloropsis sp.* have been used for food enrichment as a source of omega-3 fatty acids (Babuskin et al, 2014). By examining how oxidative stress affects regulation of photosynthesis and photoprotection, we might be able to improve photosynthetic efficiency, which would have positive downstream effects on growth and oil production.

To identify sulfenylated proteins in *N. oceanica*, we performed a global sulfenome analysis utilizing immunoblotting and mass spectrometry (MS) (Willett & Copley, 1996; Ellis & Poole, 1997). From this analysis we identified a target protein, LHCX1, to further examine the impact of cysteine oxidation. Cell lines were generated with modified LHCX1 to mimic a constitutively reduced state (C162A) or a Cys-SOH state (C162S). Characterization of these mutant lines showed that the oxidation state of the cysteine on LHCX1 affects the function of this protein in NPQ. We suggest that oxidation of C162 affects the binding affinity of zeaxanthin to LHCX1, which shifts the overall NPQ of the cell in favor of slowly reversible qZ versus rapidly reversible qE. These results demonstrate, for the first time, Cys-SOH regulation of protein function and photoprotection in a eukaryotic photosynthetic organism.

Results:

Identification of Cys-SOH modifications in response to increased light intensity and hydrogen peroxide

To examine the gross changes in Cys-SOH in increasing light intensities, wild-type *N. oceanica* cells were exposed to three light treatments for 2 h: dark, low light (LL; 100 µmol photons m^{-2} s^{-1}), and high light (HL; 600 µmol photons m^{-2} s^{-1}). The proteins were extracted and treated with the Cys-SOH-binding reagent dimedone, a chemical that specifically alkylates only the Cys-SOH state of cysteine, not other oxidized states (Fig. 2.1A; Benitez and Allison, 1974; Furdui and Poole, 2013). Proteins with Cys-SOH were subsequently detected with an anti-dimedone antibody by immunoblotting (Maller et al., 2011), which revealed a higher number of bands as well as higher intensity of the bands with increasing light intensity (Fig. 2.1B). A similar pattern was observed with cells treated with hydrogen peroxide (H_2O_2) (Fig. 2.1C).

We then used LC-MS/MS to identify proteins prone to cysteine oxidation after treatment of *N. oceanica* cells with the three light levels listed above, with and without dimedone treatment (Fig. 2.2A). Consistent with the immunoblot analysis, Cys-SOH modifications increased with the increasing light intensity. The number of Cys-SOH

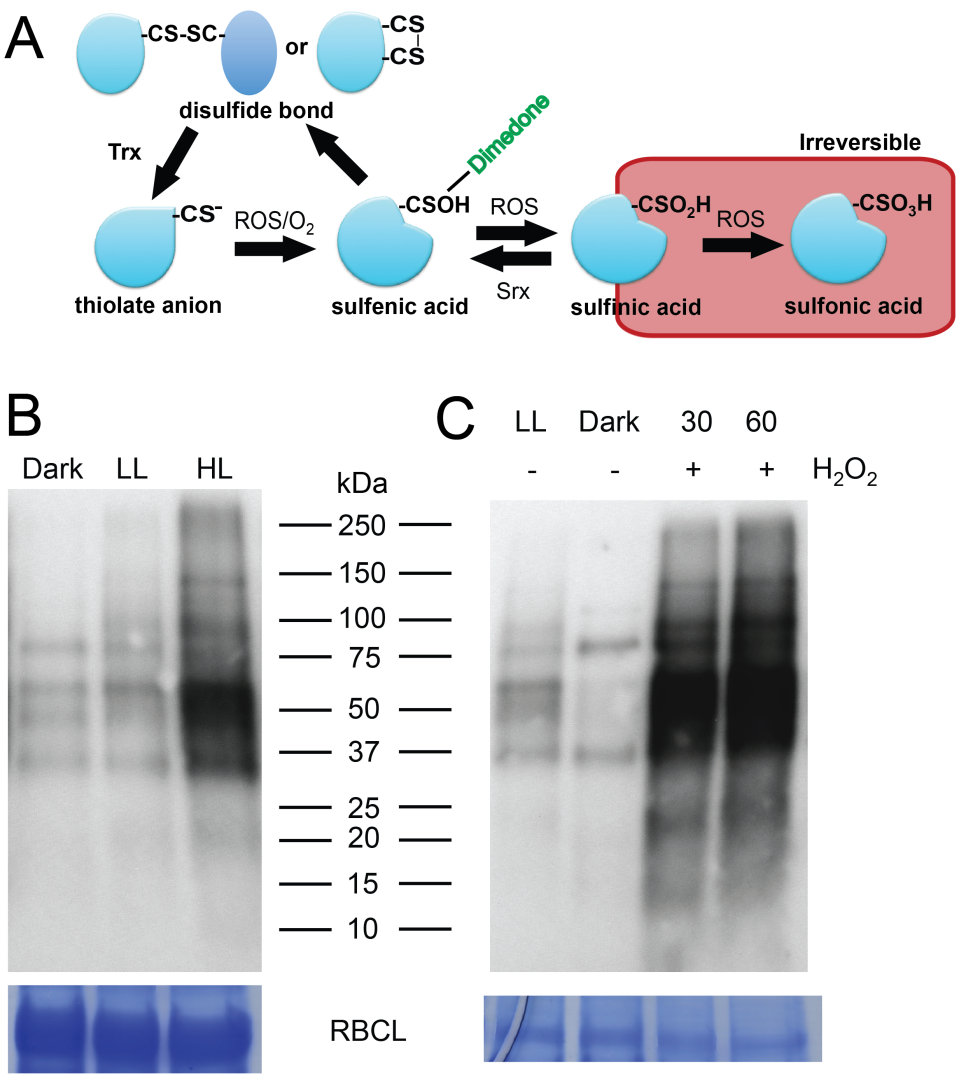

Figure 2.1: Schematic of cysteine posttranslational modifications and immunoblots of dimedone labeling.

A. Cysteine thiolate anion (-CS^-) can be oxidized to the sulfenic acid state (-CSOH), which can then be further oxidized to the sulfinic (CSO_2H) and potentially irreversible sulfonic acids states (CSO_3H) or can react with a nearby cysteine to form disulfide bonds which can play a role in the reduction of the cysteine back to the thiolate state. **B.** Immunoblot with anti-dimedone antibody on total *N. oceanica* protein with 2 hour light treatments of low light grown cells, Dark= 0 µmol photons m-2 s-1, LL=low light (100 µmol photons m-2 s-1); HL=high light (350µmol photons m-2 s-1). **C.** Immunoblot with anti-dimedone antibody on total *N. oceanica* protein with dark acclimated samples treated with 10mM H2O2 for 30 (30m) and 60 minutes (60m). B. and C. normalized to total protein loaded as seen in the commassie stained gels below each blot. Each immunoblot was run 4-6 times showing similar results.

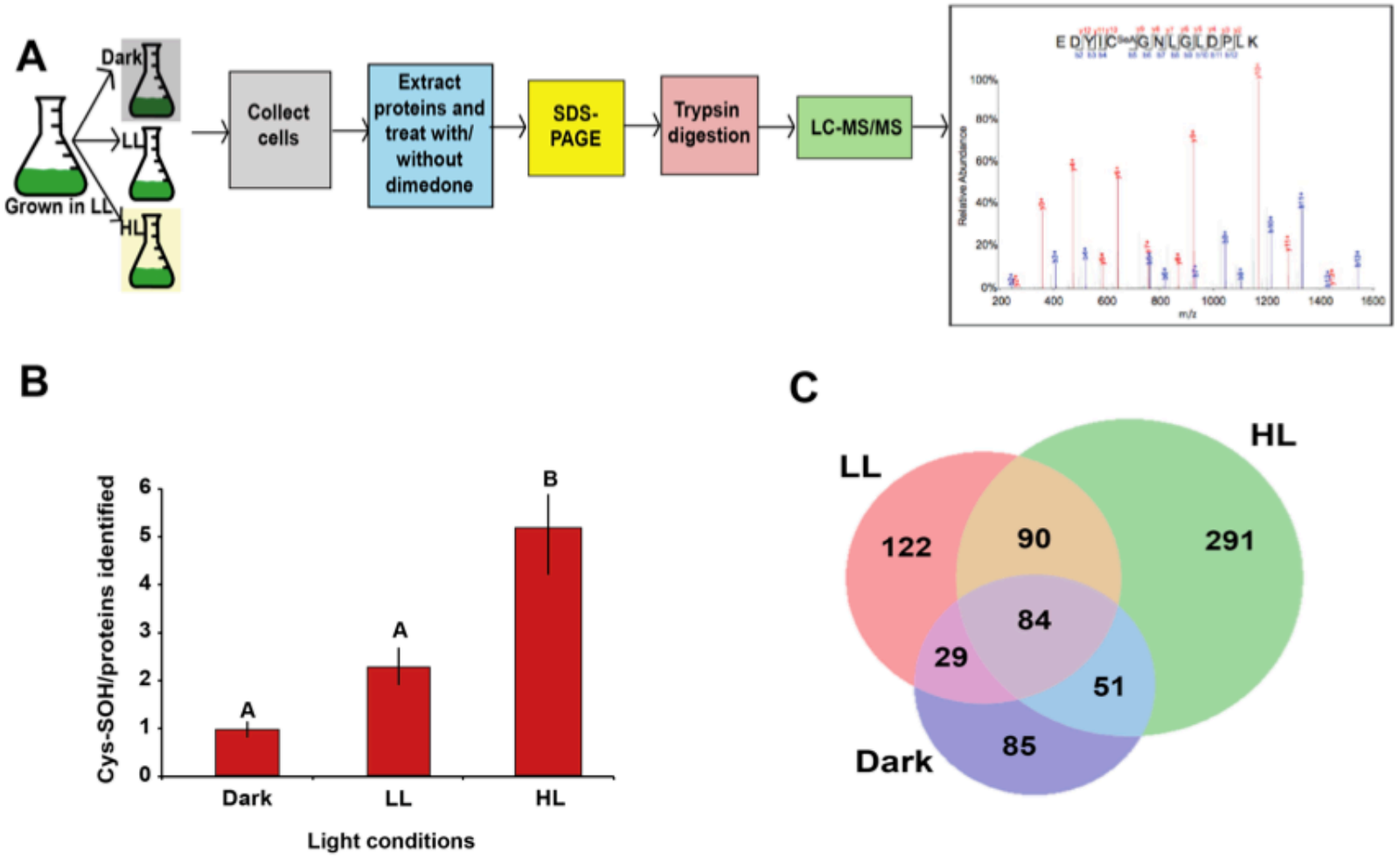

Figure 2.2: LC-MS/MS analysis to identify peptides with Cys-SOH modifications.
A. Scheme for LC-MS/MS analysis. MS spectra is for peptide in LHCX1 identifying the Cys-SOH adduction **B.** Total Cys-SOH identified by mass shifts relative to proteins identified in 3 light conditions, dark, Low light (LL) and High light (HL). Letters above the bars separate lines into groups by statistical significance values from one-way ANOVA with Tukey post-hoc test ($p<0.05$). **C**. Venn diagram of the total proteins identified with Cys-SOH in the 3 light conditions from totaling all proteins identified in 3 experiments.

modifications found in the LC-MS/MS results relative to the total number of proteins identified showed a significant increase in the HL-treated sample relative to both of the other samples (Fig. 2.2B; one-way ANOVA with Tukey test ($F(2,6)=10.518$, $p=0.011$)), and the total number of different sulfenylated proteins also increased with light intensity (Fig. 2.2C). Although many sulfenylated proteins were detected in more than one light treatment, in HL the majority of proteins found with Cys-SOH modifications was unique to that condition.

This global proteomic analysis has provided a list of proteins and cysteine residues that are prone to oxidation to the Cys-SOH state under the conditions tested (Appendix A). This analysis identified oxidation of a total of 248 proteins for the dark sample, 326 proteins in LL, and 516 proteins in HL. Notable proteins on the list include transcription factors and other proteins involved in nuclear gene expression, chloroplast translation elongation factors, metabolic enzymes, and light-harvesting complex (LHC) proteins (Table 2.1). For example, one putative transcriptional regulator, a plant homeodomain protein (PHD), was identified with eight separate Cys-SOH modification sites after the HL treatment (Appendix A). Proteins with similarity to nuclear subunits of RNA polymerase, a histone methyltransferase, chromatin remodeling proteins, and splice factors were also identified, suggesting molecular events that might be involved in altering the gene expression profile of the cell for acclimation to photo-oxidative stress. The identification of oxidation sites on chloroplast elongation factors in this study adds credence to this idea, because inactivation of EF-Tu by cysteine oxidation has already been shown in cyanobacteria (Yutthanasirikul et al., 2016). In addition, proteins with sequence similarity to the mitochondrial proteins citrate synthase, NADH dehydrogenase, and ATP synthase β subunit were identified.

Cys-SOH modification of LHCX1 increases the slowly reversible qZ component of NPQ without affecting cellular zeaxanthin content

Among the sulfenylated proteins detected in the LC-MS/MS analysis, we focused on LHCX1, a homolog of the stress-related LHC protein (LHCSR) in green algae (Peers et al., 2009), which is involved in qE. *N. oceanica* mutants that lack LHCX1 have a very strong qE deficiency phenotype (Lyska et al., 2018), and LHCX1 has a single cysteine (C162), which was detected in the Cys-SOH state in LL and HL (Table 2.1).

To investigate the possible effects of Cys-SOH modification of C162 on LHCX1 function, we expressed cysteine-to-alanine (C162A) and cysteine-to-serine (C162S) versions of the protein in an *lhcx1* knockout mutant (Lyska et al, 2018) to mimic the reduced and Cys-SOH states of the protein, respectively. In addition, we expressed the wild-type (WT) protein as a control. Immunoblot analysis showed various levels of the LHCX1 protein in different complemented lines (Fig. 2.3A), which correlated with the level of qE (Fig. 2.4-2.6). The mRNA expression levels of each version of the *LHCX1* gene correlated with the level of protein accumulation (data not shown). Lines with similar levels of LHCX1 protein accumulation (approximately 50% higher than the untransformed NoWT) were selected for further analysis.

Measurements of NPQ revealed differences between the LHCX1 mutants. As expected, the *lhcx1*+WT line showed higher NPQ than WT, and most of the NPQ was rapidly reversible qE (Fig. 2.3B), consistent with the ~50% higher LHCX1 content (Fig.

Table 2.1: Some photosynthesis proteins found by LC-MS/MS with Cys-SOH modification

Homology	Locus[a]	Cys-SOH	Peptide	D	LL	HL
LHCX1	**^_4201**	**162**	K.EDYIC*GNLGLDPLK.I	-	+	+
violaxanthin de-epoxidase	**^_11475**	**109**	K.ADEVGCQIGCGDLFENEVVGQFNACALSKKQC*VPR.K	-	+	-
zeaxanthin epoxidase	**^_6822**	**97**	K.WYC*QFDTGAPAQKRGLPLTR.V	-	+	+
LHC protein	**^_11954**	**71**	K.YREC*ELK.H	-	-	+
PEP carboxylase	**^_3970**	**361**	K.MVLSSTKC*SEELR.M	-	-	+
fructose-1,6-bisphosphatase	**^_4980**	**949**	K.TISSLVNRAC*ITKMTGYQDDGCSINVQGEQQ.K	-	-	+
		1062	K.EC*LLDDEDLEGGAMDPESRAAK.C	-	+	+
		1083	R.AAKC*LMSTLQPGTNLVVR.I	+	+	+
α-carbonic anhydrase 4	**^_6698**	**47**	K.MESWSYVPNENSNAC*VGADAK.S	-	-	+
		57	K.SWGC*CGKPEDGKER.C	-	-	+
L-ascorbate peroxidase 6	**^_9742**	**67**	K.NNC*APILVRLAWHDAGTFNVANAGQPFPAR.G	-	+	-
		294	K.LDTDLC*IFGDEGFRPFALK.Y	-	-	+
FNR	**^_2084**	**499/504**	K.KGIC*SNFLC*DAK.P	+	+	+
Aldolase	**^_11417**	**174**	K.VDTGLQNMFGTDGETATQGLDGLGDRC*K.A	-	-	+
porphobilinogen deaminase	**^_8678**	**284**	R.SFLAELDGNC*KTPIAGQAK.V	-	-	+
D-3-PG dehydrogenase	**^_7696**	**38**	R.AHLHASRPTLAKILC*ADSIDPVCIQIFKER.G	+	-	+
protoporphyrinogen IX oxidase	**^_10542**	**286**	K.PPSGSLC*GVSGI.-	-	-	+
superoxide dismutase	**^_9291**	**35**	K.AAAC*SSTTCMAVTLPALPYADTALEPLISKR.T	-	+	+
cytochrome c6	**PetJ[+]**	**52**	R.IFSANCSAC*HAGGNNVIIPEKTLKK.D	+	-	+
NDH subunit B3	**^_9798**	**78**	K.RGRDGRGC*VLISAIQPGGNAEKAAGEEQK.I	-	-	+
2Fe-2S ferredoxin-like	**^_7881**	**89**	K.EWDVPC*SCRNGICTTCAGRIIAMPGS.K	-	+	-
ferredoxin-Trx reductase	**^_7460**	**129/131**	K.HKDELGAPLC*PC*R.H	-	-	+
VDE-like	**^_10228**	**36**	K.TEANTTCIATYCQEAALSC*VKDK.D	-	-	+
ruBisCO large subunit-β	**^_349**	**75**	R.KSC*GFLPVVPLAGLSGAPSARR.T	+	+	+
ruBisCO large subunit-α	**^_3819**	**168**	R.GIMHC*SKVLCDTIK.Q	+	+	+
geranylgeranyl diphosphate reductase	**^_5038**	**90**	K.PC*GGAIPLC*MVSEFDLPPEIIDR.K	-	+	+

[a] Locus annotation determined by Vieler et al., 2012; ^ = NannoCCMP1779; [+] from chloroplast genome (Wei, Xin et al., 2013); * denotes location of Cys-SOH in peptide.

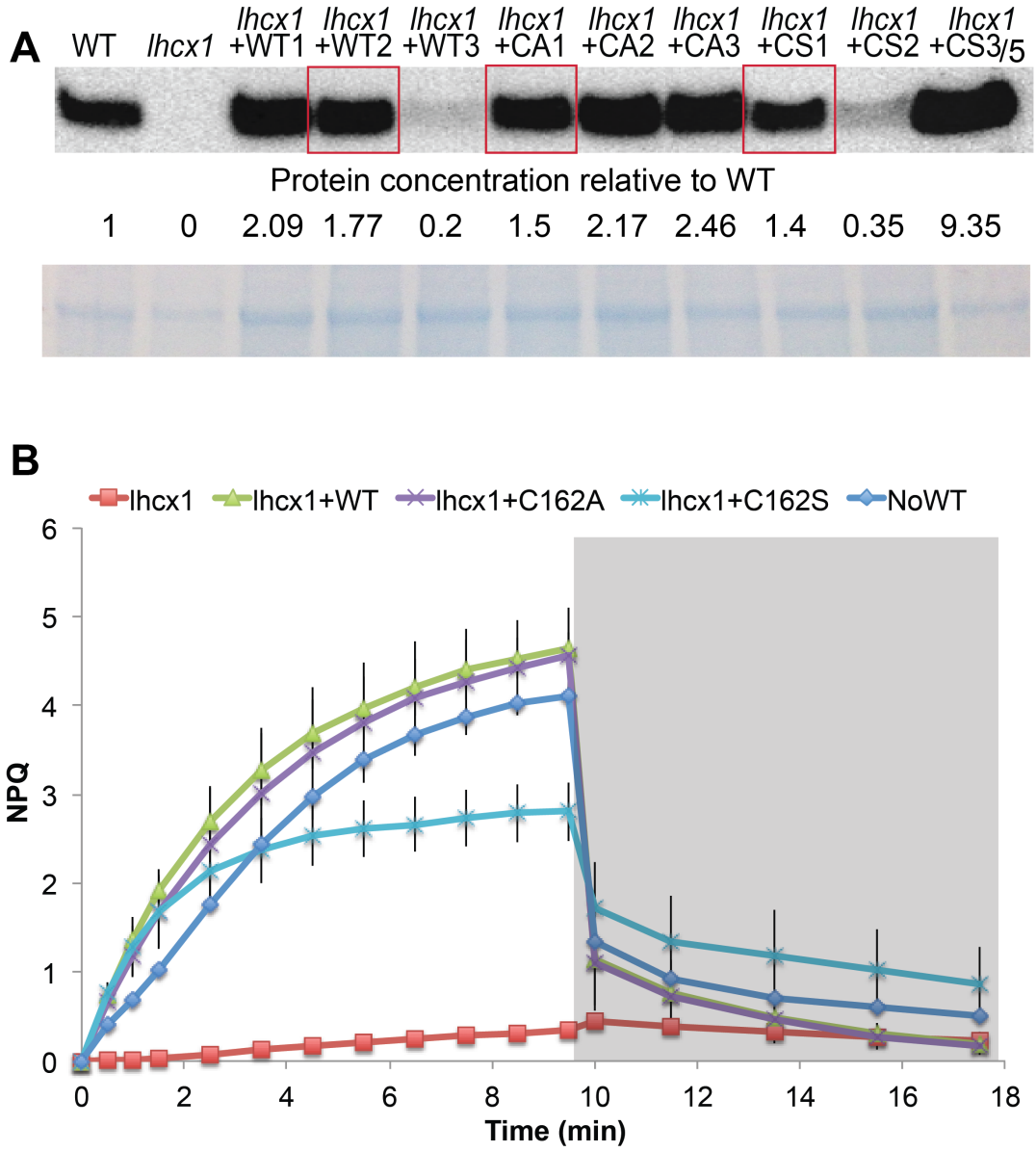

Figure 2.3: Complementation lines of *lhcx1*.

A. Immunoblot with anti-LHCX1 antibody. Loaded with 1µg Chl. Numbers under each lanes indicate protein amount of each line relative to WT protein level calculated by Image lab. It should be noted that the C162S-3 was loaded with 1/5 concentration as the level of over expression produced a signal so intense it prevented the detection of signal from the other lines. *lhcx1*+WT = WT complements, *lhcx1*+CA = *lhcx1*+C162A complements, and *lhcx1*+CS = *lhcx1*+C162S complements. **B.** NPQ traces of NoWT, *lhcx1* and mutant lines from panel A (highlighted by red boxes).

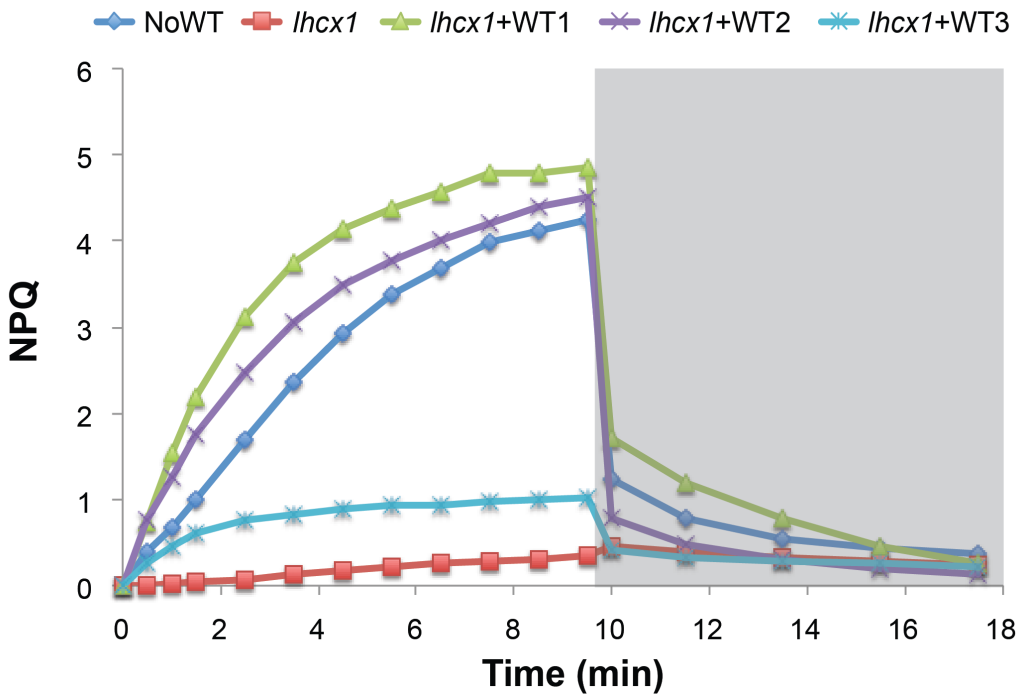

Figure 2.4: Representative NPQ trace of the 3 *lhcx1*+WT lines grown in LL.

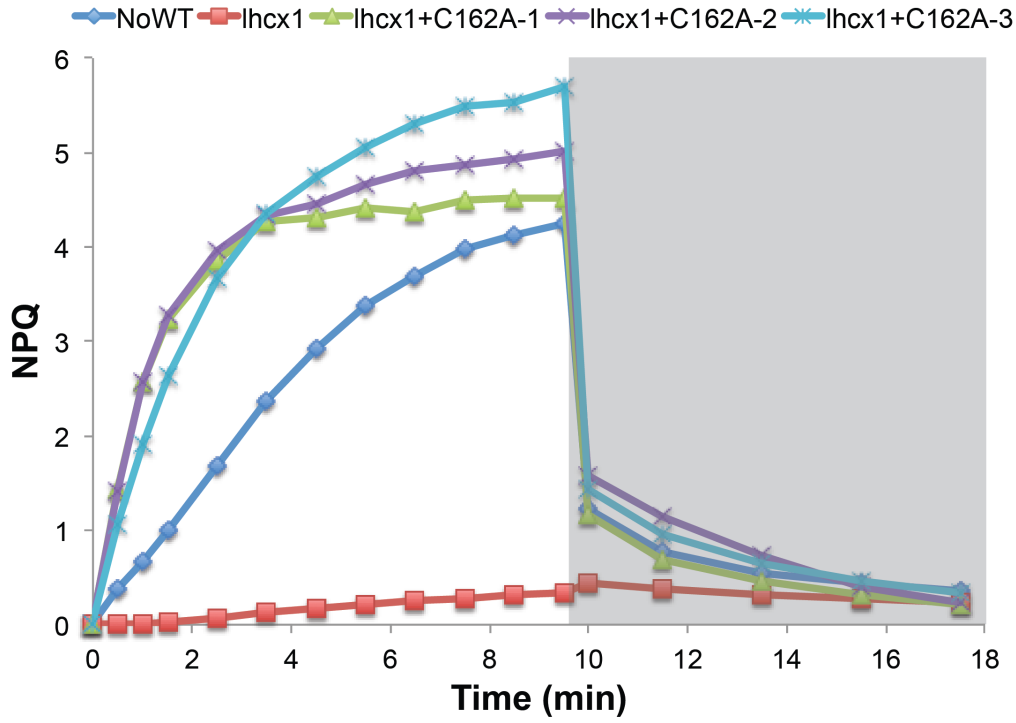

Figure 2.5: Representative NPQ trace of the 3 *lhcx1*+C162A lines grown in LL.

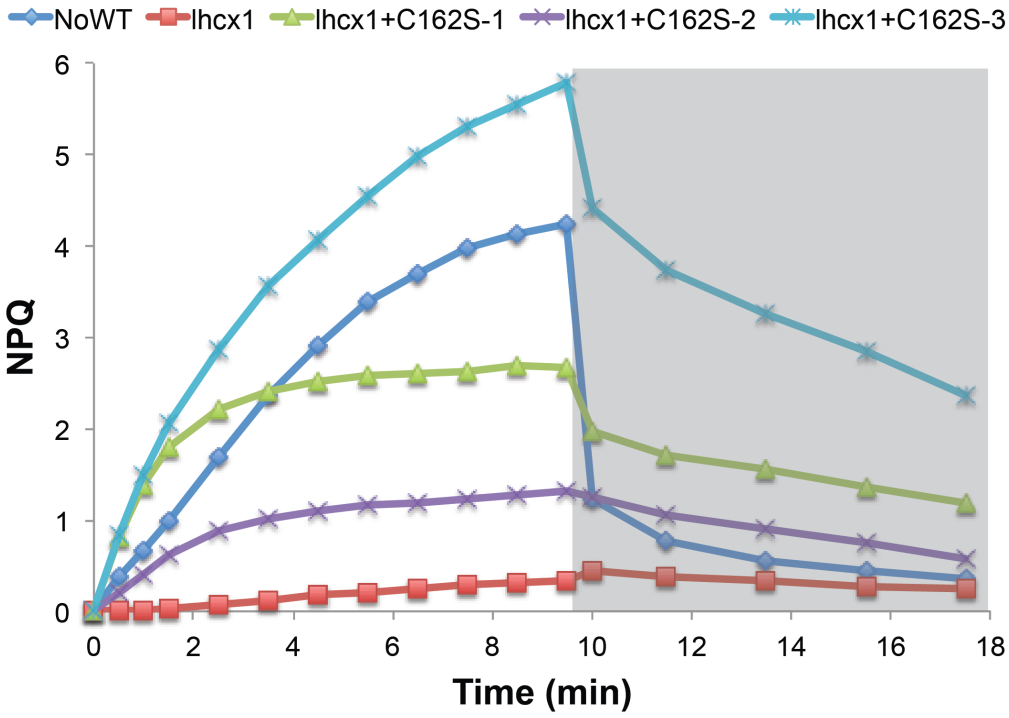

Figure 2.6: Representative NPQ trace of the 3 *lhcx1*+C162S lines grown in LL.

2.3A). The reduced mimic *lhcx1*+C162A line showed similarly increased levels of qE as the *lhcx1*+WT line (Fig. 2.3B). In contrast, the Cys-SOH mimic *lhcx1*+C162S line showed reduced NPQ with a notably slower relaxation in the dark compared to the other lines, including the untransformed NoWT (Fig. 2.3B). The *lhcx1* control line exhibited a nearly complete lack of qE, as previously reported (Lyska et al, 2018).

We then examined to what extent the slowly relaxing NPQ component, qZ, contributes to the total NPQ in the different lines during a series of HL-dark cycles. These repeated cycles resulted in saturation of the qE component of NPQ and buildup of the more slowly relaxing qZ during each consecutive cycle (Fig. 2.7A). An increase in the total NPQ was observed for all lines during the first two cycles, but then it decreased in the third and fourth cycles. The slowly relaxing qZ in the *lhcx1*+C162S line increased to a greater extent after each cycle relative to the other lines (Fig. 2.7A and B). The qZ reached ~50% of total NPQ in *lhcx1*+C162S after the fourth cycle, which is more than double the contribution of qZ in the *lhcx1*+WT and *lhcx1*+C162A lines (Fig. 2.7B). As expected, the *lhcx1* mutant had greatly reduced qE compared to the other lines, so the contribution of qZ to its total NPQ was much greater, 70-95% (not shown in Fig. 2.7B).

To test whether this increase in qZ in the *lhcx1*+C162S line was related to a higher de-epoxidation state of the xanthophyll cycle pool, pigments were analyzed at three time points along the four-cycle NPQ experiment (marked with arrows in Fig. 2.7A). As shown in Figure 2.7C, the de-epoxidation states of all the lines were very similar at each of the three time points. De-epoxidation states of the xanthophyll cycle pool have been shown to be tightly linked to qZ in WT *N. oceanica* (Lyska et al., 2018), and thus the observed uncoupling of qZ and xanthophyll de-epoxidation state in the *lhcx1*+C162S line implies a new mode of regulation of NPQ.

If the increase in qZ in the *lhcx1*+C162S line is attributable to mimicking the Cys-SOH state of LHCX1, then there should be conditions in which the *lhcx1*+WT line resembles *lhcx1*+C162S rather than *lhcx1*+C162A, perhaps when sulfenylation of LHCX1 increases. Although there was not a significant difference in NPQ between the *lhcx1*+WT and *lhcx1*+C162A lines within the time points of the NPQ experiments in Figures 2.3B and 2.7A, we observed that the *lhcx1*+WT line was beginning to show a small increase in qZ relative to the *lhcx1*+C162A line during the final HL cycle (Fig. 2.7A). This observation prompted us to measure NPQ upon illumination with a longer 20-min period of HL (Fig. 2.8A). Indeed, this experiment showed that the percentage of total NPQ represented by qZ in the *lhcx1*+WT line and the *lhcx1*+C162S line were similar (42% and 56% respectively), whereas qZ in the *lhcx1*+C162A line remained low (Fig. 2.8B). This result suggests that, during sustained HL stress, oxidation of the WT LHCX1 protein occurs that causes the *lhcx1*+WT line (and NoWT) to phenotypically resemble the *lhcx1*+C162S line that mimics the Cys-SOH state of LHCX1.

Protein modeling of LHCX1 shows position of C162 in a stromal loop with conformational changes induced by cysteine oxidation

To examine the structure of LHCX1, we generated an iterative model using Phyre2 (Fig. 2.9). This model shows the position of the C162 residue in the stromal loop between transmembrane helices 2 and 3. The model was overlaid with the structure of the LHCB2 protein from *A. thaliana* (PBD 3JCU chain G). The backbones of LHCX1 and

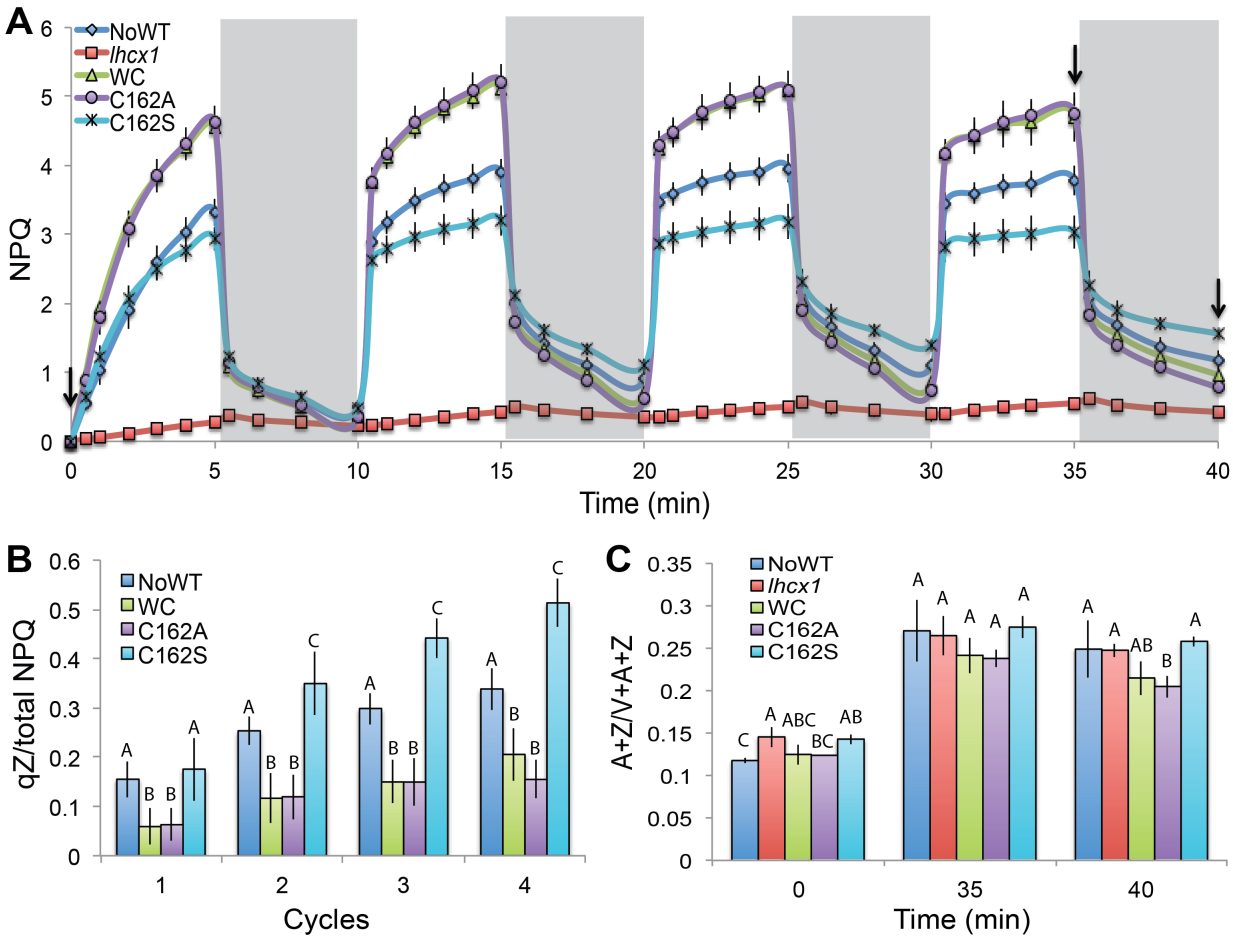

Figure 2.7: Induced qZ through four 5-minute light dark cycles.

A. PAM fluorometry reading of NPQ over the 4 cycles of light and dark. **B.** Bar graph highlighting the qZ component of each organism over the 4 cycles. There was a statistically significant difference between groups as determined by one-way ANOVA in each of the four cycles (1st cycle: $F(4,20)=241.23$, $p=<0.0001$; 2nd cycle: $F(4,20)=200.375$, $p=<0.0001$; 3rd cycle: $F(4,20)=153.838$, $p=<0.0001$; 4th cycle: $F(4,20)=79.344$, $p=<0.0001$). Letters above the bars separate lines into groups by statistical significance values from one-way ANOVA with Tukey post-hoc test ($p<0.05$). **C.** De-epoxidation state of the five lines from pigment analysis taken from 3 time points along the 4 cycle NPQ trace (0, 35 and 40 minute time points marked in A. by black arrows). There is a statistically significant difference between the lines by one-way ANOVA for the zero and forty minute time point readings ($F(4,10)=6.487$, $p=0.008$; $F(4,10)=6.069$, $p=0.01$). Through pairwise comparison there is significant differences between lhcx1 and NoWT, lhcx1 and C162A, and C162S and No WT in the dark adapted samples (zero); and between C162A and all except WC in the samples taken from after the last relaxation phase (40min).

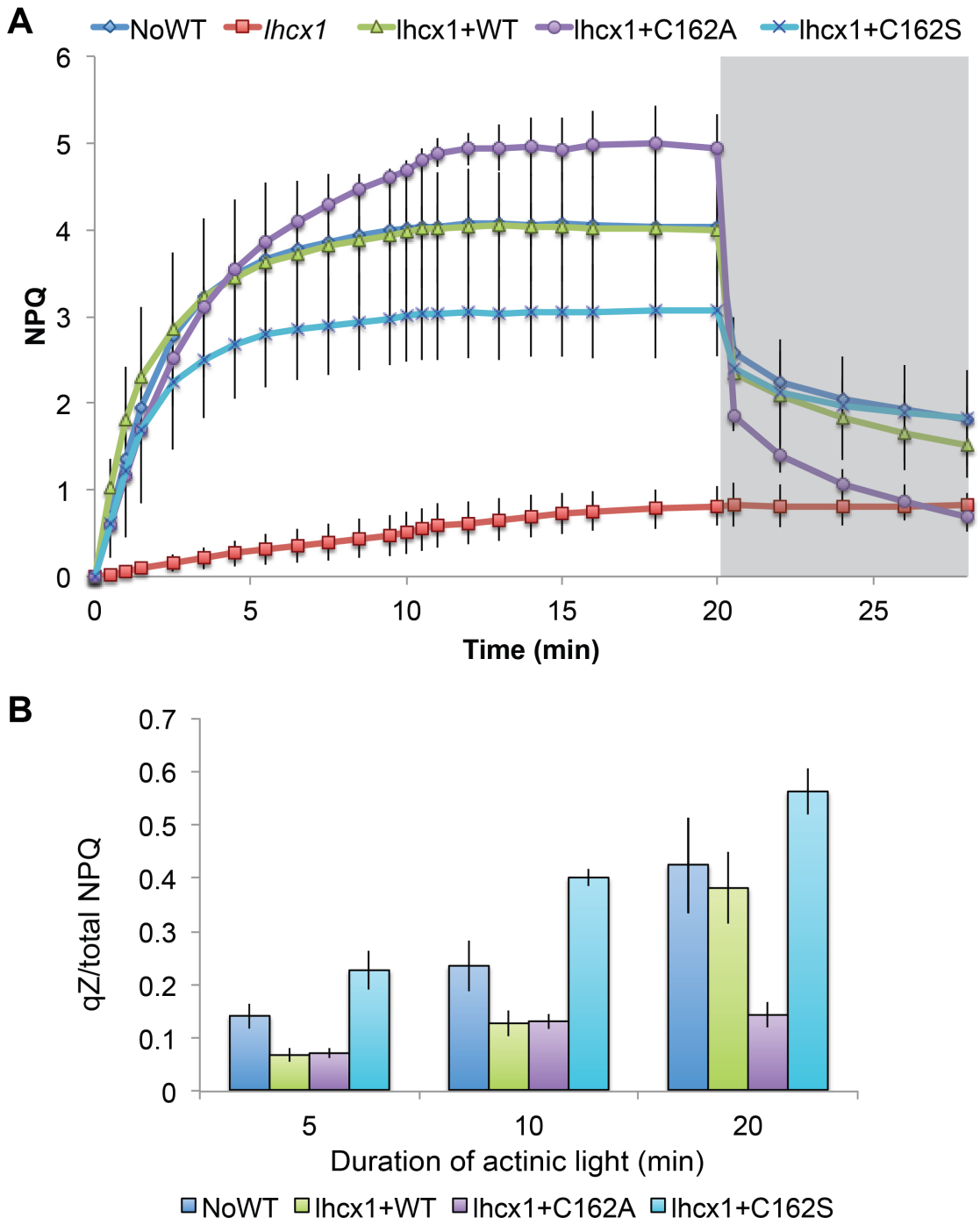

Figure 2.8: NPQ measurement with longer actinic which induces higher qZ.

A. NPQ trace of 20min actinic light NPQ induction curve. **B.** qZ of 5 lines over 3 separate actinic light durations; 5 minutes, 10 minutes and 20 minutes. Letters above the bars separate lines into groups by statistical significance values from one-way ANOVA ($F(4,10) = 85.365$, $p =< 0.0001$). On the Tukey pairwise comparison all lines showed significant differences compared to *lhcx1*+C162A (*lhcx1*+C162A: *lhcx1*+WT, p=0.001; *lhcx1*+C162A: *lhcx1*+C162S, p=<0.0001).

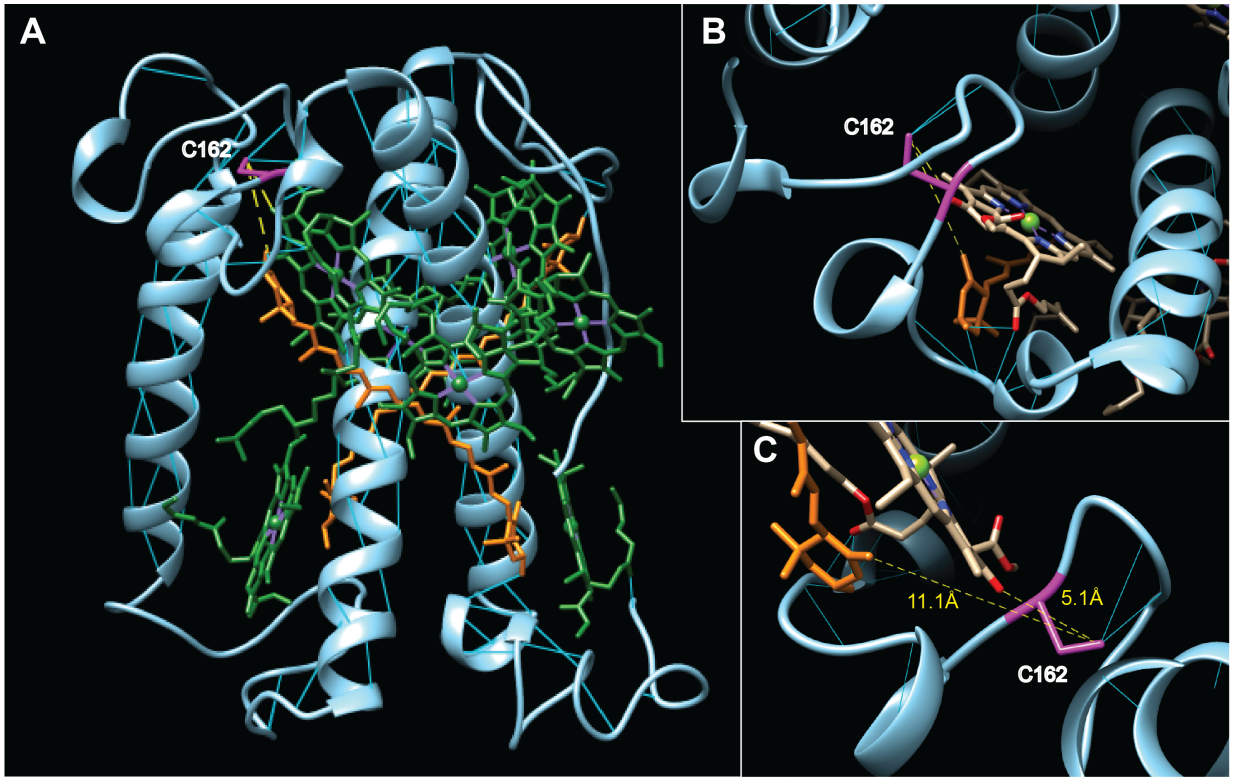

Figure 2.9: Chimera modeling of LHCX1 with carotenoids and Chlorophylls.

A. Iterative homology model of LHCX1 for Phyre2 overlaid with pigments (cross membrane carotenoids and chlorophyll A molecules with conserved binding sites) from *A. thaliana* LHCB2 (PBD 3JCU chain G) by Chimera structural similarity overlapping. **B.** Zoom in on top down view of stromal pocket focused on the cysteine close to the carotenoid and chlorophyll. **C.** Marked with atom distances from cysteine to carotenoid (11.1Å) and chlorophyll (5.1Å). Cysteine colored in purple, Carotenoids in orange and chlorophylls in green. Thin blue lines represent hydrogen bonding.

LHCB2 aligned very closely, which gave us high confidence in the predicted locations of bound chlorophylls and carotenoids in LHCX1. The C162 residue is in close proximity to a chlorophyll and a carotenoid. The distances from this cysteine residue and these pigments are 11.1 and 5.1 Å, respectively. Space-filling models show the predicted structural changes in the C162A and C162S versions of the protein (Fig. 2.10). A predicted structural change would restrict the access to the carotenoid-binding site site in the C162S protein, whereas this region of LHCX1 would have a more open structure in the C162A protein.

Discussion:

The role of Cys-SOH in oxidative stress-induced post-translational regulation of proteins has only recently become an area of active interest. Most of the previous work has focused on prokaryotic or mammalian systems with, even more recently, a few publications examining this topic in prokaryotic anoxygenic photoautotrophs. We were able to utilize tools developed in these other organisms to investigate if Cys-SOH could directly regulate proteins during oxidative stress conditions in eukaryotic photoautotrophs. It has been seen in photoautotrophs that oxidation of proteins as well as other cellular components does occur under HL stress conditions or with ectopic treatment of ROS (reviewed in Møller et al., 2007). Therefore it should not be surprising that protein oxidation can play a non-damaging direct role in the pathways that protect the cell from further oxidation, as seen here through the NPQ pathway associated with LHCX1.

From both the immunoblotting analysis after dimedone reaction and the MS data it is evident that there is a relationship between the light-induced oxidative stress and the number of Cys-SOH modifications throughout the total proteome of *N. oceanica*. Semi-quantitative analyses comparing total Cys-SOH identified relative to the total proteins identified supports the hypothesis that increases in light level are associated with increases in the number of Cys-SOH residues, showing a link between physiological conditions and direct oxidation states of proteins (Fig. 2.2B). The comparison of photosynthetic proteins identified in this analysis shows that some proteins are preferentially oxidized in one light condition over another, and even different cysteines on the same protein can be differentially oxidized between the light conditions (Table 2.1). An interesting example, which has eight different Cys-SOH sites, is PHD, a transcriptional regulator found on the chloroplast envelope that translocates into the nucleus during oxidative stress conditions in *A. thaliana* (Sun et al, 2011). The sheer number of Cys-SOH sites may impart a threshold response to oxidation, such that a certain number of Cys-SOH are needed to induce the transmembrane domain cleavage and translocation of the transcription factor domain, or this could be simply an indication of this protein's overall susceptibility to oxidation. Our screen also identified EF-Tu, a protein that is inactivated by cysteine oxidative in cyanobacteria (Yutthanasirikul et al, 2016).

From this vast number of proteins, a subset of targets was selected for a reverse genetic screen to examine photosynthetic phenotypes of mutant lines. Of the mutants generated, *lhcx1* had the strongest phenotype, with its complete loss of qE, its single cysteine in what appears to be a stromal-facing pocket of the protein that would be ideal

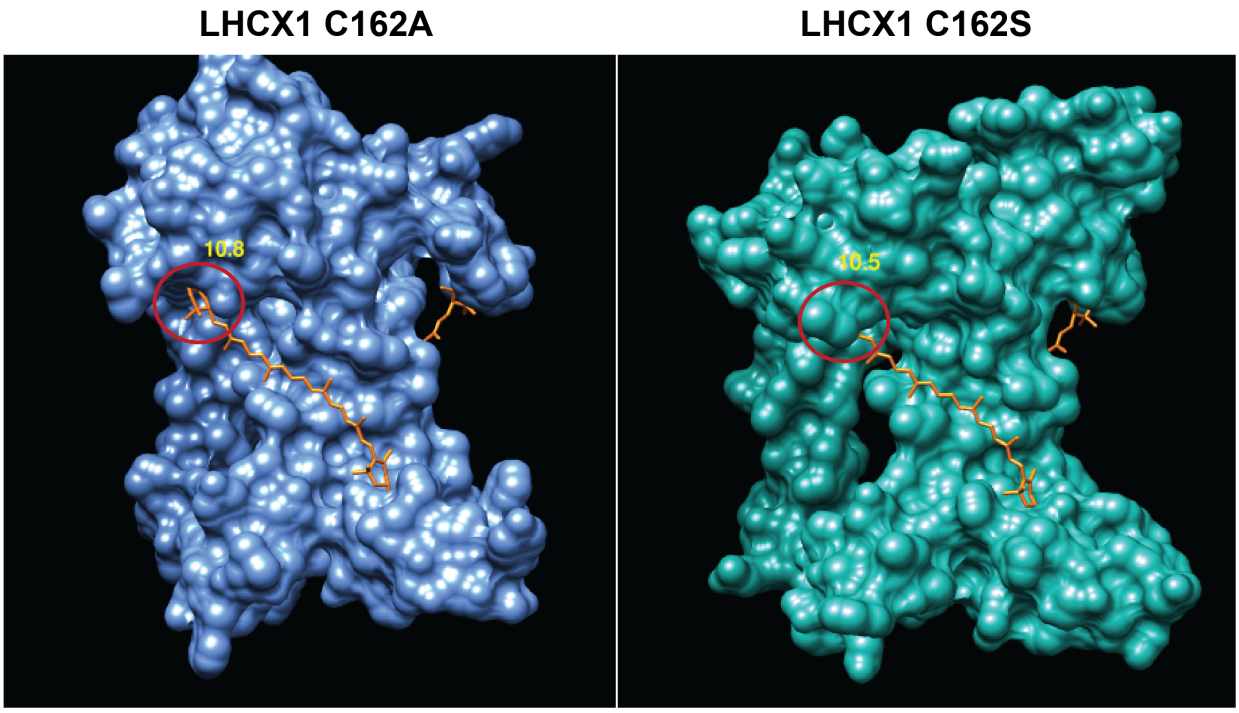

Figure 2.10: Space filling model of LHCX1 C162A and C162S modified proteins.

Red circle highlights the region where carotenoid is bound more tightly in C162S. Yellow number above circle is the Å distance from the alanine and serine, respectively, to the end of the carotenoid.

for stability of the Cys-SOH (Fig. 2.9), and the close proximity of this cysteine to predicted binding sites for a carotenoid and a chlorophyll. The NPQ analysis of the *lhcx1*+C162A and *lhcx1*+C162S lines indicated that C162 could have some role in the switch between a qE (rapid quenching) and qZ (sustained quenching) state (Fig. 2.7). During our analysis, the greatest difference between the lines was after four HL/dark cycles, with *lhcx1*+C162A having only half of the qZ of *lhcx1*+C162S (Fig. 2.8). The lack of higher qZ in the *lhcx1*+WT line could be due to the periods of dark, which would prevent a high accumulation of oxidative stress over the course of the experiment. The level of qZ in *lhcx1*+WT did increase and approach that of *lhcx1*+C162S when HL exposure was increased to 20 min, likely due to an increased oxidation at C162, while qZ of *lhcx1*+C162A stayed low. Higher qZ in C162S did not correlate with a higher xanthophyll de-epoxidation state, ratio of antheraxanthin and zeaxanthin to violaxanthin, indicating a different mechanism for the change in qZ caused by the oxidation of C162.

To determine if the *lhcx1*+WT's NPQ could further increase toward the C162S state, we examined the NPQ after an hour of HL followed by 20-min dark adaptation, to relax the qE. In this experiment *lhcx1*+C162A and the *lhcx1*+WT lines retained lower levels of qZ similar to the LL readings done previously (Fig. 2.11). This high qE and low qZ after 20-min dark adaptation in *lhcx1*+WT could be associated with the reduction of Cys-SOH on LHCX1. This also correlates well with the average stable Cys-SOH lifetimes calculated to be ~12 min (Gupta & Carroll, 2014). The fact that *lhcx1*+WT never reaches the level of qZ as *lhcx1*+C162S is not surprising, as even during the 20-min actinic light period the oxidation could be continuously reversed back to the thiolate species. Additional evidence for the reversibility of this modification of LHCX1 comes from LC/MS-MS, which shows in LL there was an 5.5:1 reduced to Cys-SOH identified peptide ratio and in HL there is a 2:1 Cys-SOH to reduced ratio, a shift from 18% up to 67% oxidation. The oxidation of this cysteine seems to occur at all points when the light is on; it was never identified in the dark, but with higher light the oxidation outcompetes the relaxation of the cysteine though never completely, indicating the possibility of a fairly robust reduction pathway.

We hypothesize that in the native LHCX1 protein the oxidation of C162 changes the conformation of the stromal loop (Fig. 2.9; Fig. 2.10) thereby lowering the zeaxanthin binding affinity at the X2 site, redirecting those pigments to qZ sites that are most likely found in other LHC proteins. In our current mechanistic model (Fig. 2.12), oxidation of LHCX1 is low in LL, and a potential violaxanthin in the X2 site could be exchanged with a zeaxanthin to fully activate the qE mechanism directed by LHCX1. In HL, the greater oxidative stress would lead to sulfenylation of C162, resulting in a conformational change around the carotenoid, decreasing the binding affinity to the X2 site (Fig. 2.10) and redirecting zeaxanthin molecules to qZ binding sites with higher affinity. In *lhcx1*+C162S, the predicted protein region appears to overlap the proximal end of the carotenoid, whereas in the *lhcx1*+C162A predicted structure the carotenoid is much more exposed to what would be the surrounding membrane, possibly allowing for easier pigment exchange. The affinity of the qZ sites for zeaxanthin is thought to be lower, with a lower dissociation constant, than the qE sites (Nilkens et al., 2010), so once the zeaxanthin is bound it would be more difficult to release, thereby increasing the time needed to relax NPQ. The location of the cysteine in LHCX1 would also be important for the reversibility of Cys-SOH back to the thiol state, which is likely mediated

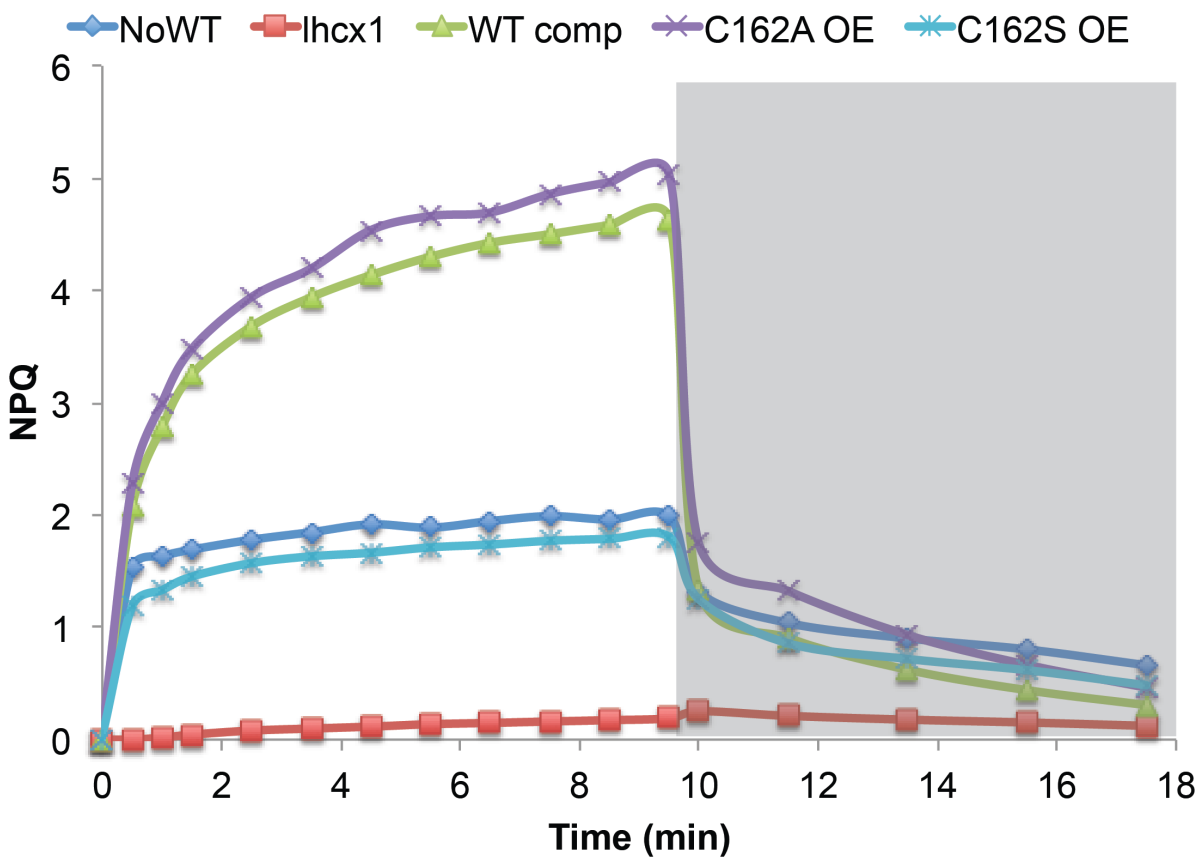

Figure 2.11: Representative NPQ trace of HL treated LHCX1 mutants.

1-h HL (350µmol photons m-2 s-1) treated samples were dark adapted for 20min prior to 10 min actinic light NPQ trace.

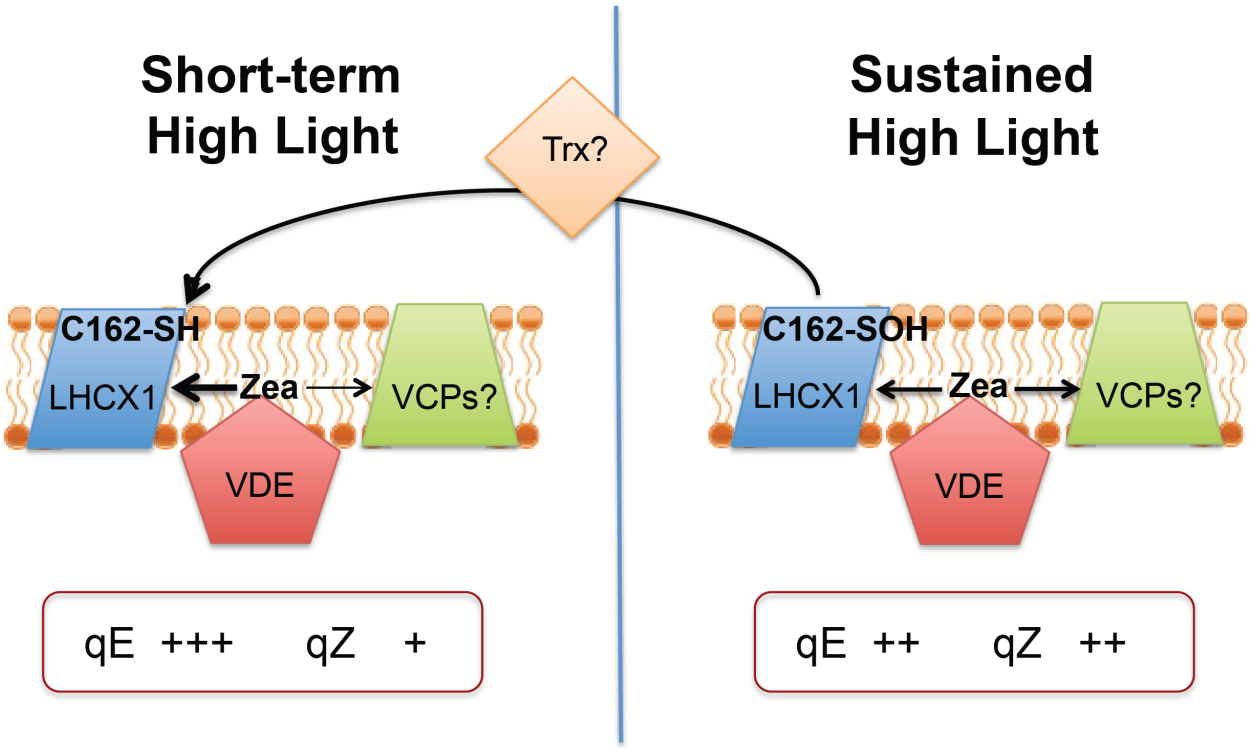

Figure 2.12: Model of potential mechanism of NPQ function around LHCX1 oxidation.

During short periods of HL zeaxanthin (Zea), produced by violaxanthin de-epoxidase (VDE) preferentially binds to LHCX1 and qE will be higher than qZ. During longer periods of HL, LHCX1 is oxidized at C162 to Cys-SOH reducing binding of Zea to LHCX1 and increasing binding to qZ site(s) possibly located on violaxanthin chlorophyll a binding proteins (VCPs) increasing qZ type quenching. This oxidation could be reversed by an unknown thioredoxin (Trx).

by a thioredoxin domain protein. Further work will be needed to determine what protein, if any, is involved in the reduction of this Cys-SOH, if the affinity of the carotenoid site is actually changed by its oxidation state, and if ROS are required to mediate this oxidative change.

Our results show that the oxidation of LHCX1 at C162 changes the relaxation dynamics of NPQ. The rapid reversibility of this modification would be necessary to allow for *N. oceanica* to quickly reset its NPQ as it moves from a HL to LL state in fluctuating conditions of the ocean or a dense culture. This would allow each cell to tune its NPQ relative to the incident light at any moment during its movement within the water column. Blocking of the cysteine oxidation in the C162A mutant caused a decrease in the overall qZ during longer periods of HL. This lack of qZ may be disadvantageous to survival in conditions with long periods of high irradiance but may conversely be beneficial in cultures grown under rapid fluctuating light, such as in bioreactors. The LHCX1-C162A and the wild-type over-expresser lines accelerate NPQ relaxation after periods of HL, thereby increasing the light utilization in periods of optimal light, which could increase the overall biomass yields. This would be similar to the results shown in a model crop where overexpression of qE and xanthophyll cycle genes increased biomass productivity by up to 20% (Kromdijk et al., 2016).

Materials and methods:

***N. oceanica* growth**

Nannochloropsis oceanica CCMP1779 was grown in an F2N media at 100µmol photons m^{-2} s^{-1} under continuous light in a Percival growth chamber. Media was supplemented with 5mM ammonium chloride as nitrogen source similar to Killian et al., 2012. Cultures were grown to mid log phase for all experiments (~5x10^6cell ml^{-1}).

Protein extraction and Immunoblot analysis of sulfenic acid containing proteins

5x10^8 total *N. oceanica* cells were collected in a 50ml falcon tube. Cells were centrifuged at 4000g in tabletop centrifuge for 10min. Supernatant was discarded and cell pellet was resuspended in 1ml of water. Resupended cells were transferred to a 2.0ml Lysing Matrix tube with size D glass bead. This tube was centrifuged at 8000g for 5 mins. Supernatant was removed and tubes were vortexed to coat the glass beads with cell suspension. Tubes were then flash frozen in liquid nitrogen. Tubes were vortexed to break up the frozen beads, since they are liable to freeze together. Samples were beaten in a bead beater (Millipore 116004500) at setting 6.5 for 60sec with dry ice in the reservoir to keep cells frozen. Resuspend cells off of beads with solubilization buffer (50 mM HEPES, 150 mM NaCl, 1% (vol/vol) Igepal CA-40 and 0.4% SDS with 10mM dimedone, protease inhibitors, catalase and ETDA were added to limited post-lysis oxidation and iodoacetamide was used to block cysteine thiols) and vortex for 15sec. The sample was spun at 10,000g for 5min and supernatant was transferred to fresh 1.5ml microfuge tube. The protein concentration was measured using DC protein assay kit (Bio-Rad #500-0120; Lowry et al., 1951) according to manufacture instructions. 25-40ug protein of each sample was supplememnted with 5x Laemmli buffer (supplemented with 0.1% β-DM and 0.1M urea) to final concentration of 1x. Samples were heated to 55°C for 15min, loaded onto mini-protean TGX gel (Bio-Rad

cat#456-9035) and run at 100V for 60-90 minutes until dye front reaches bottom of gel. Proteins were either stained with Coomassie brilliant blue or transferred to .2µm polyvinyl difluoride (PVDF) using Trans-Blot Turbo system (Bio-Rad cat#1704150). Immunoblot was run using α-dimedone antibody as primary and α-rabbit donkey IgG-HRP as secondary. Probe analysis was done using SuperSignal West Femto chemiluminescent substrate (Thermo Scientific). Visualization was done in the Bio-Rad Gel Doc XR+ system (#1708195).

LC-MS/MS

Total proteins from N. oceanica cells from three light conditions, dark, low light (100 µmol photons $m^{-2}s^{-1}$) and high light (600 µmol photons $m^{-2}s^{-1}$), were extracted for LC-MS/MS as above either with or without dimedone, as the 16 dalton increase due to oxygenation of a cysteine could be detected in the mass spectrometer. Proteins from both the treated and untreated samples were used for further analysis. All mass spectrum analysis done with Thermo Electron LTQ-Orbitrap XL Hybrid MS with high performance liquid chromatography. Proteins with this mass increase were identified from the dataset mapped to the base proteome from Vieler et al., 2012. From the total protein data provided by the Vincent J. proteomics laboratory we were able the extract just those proteins with the Cys-SOH modification by a simple Python script, which also blasted each protein against the NCBI database to give a potential homology.

PTM analysis

A python script was designed to extract the modified peptide sequences from the MS data sets and analyze those peptides for homology. The peptides were used to find the full protein sequence from the base proteome (Vieler et al, 2012) and this full protein sequence was then blasted against the nr database on NCBI to determine the nearest homologs, which was then compiled with the protein ID, modified peptide sequence and Cys-SOH amino acid location. Blast2GO was then used to determine specific gene ontology (GO) terms in order to organize the full data set into categories, which is located in Appendix A.

CRISPR/Cas9-RNP mediated homologous recombination

CRISPR/Cas9-RNP mediated homologous recombination (HR) was performed as described in Lyska et al, 2018. Specific gRNA sequence used was CUUGGCUGAGAUCGAACUGG, which was synthesized by IDT with the linker sequence. Map of HR vector can be found in Appendix A. HR product was linearized using forward primer: AAAGCATGGCTTGGAGGACAA and reverse primer: CAACGCACACACGACACAAATC. Inserted product was 2000bps with hygromycin b resistance gene for selection. Presence of the insertion product in the mutant *N. oceanica* colonies was checked by PCR using primers: TTCCGCACCTTCGCACCTGG and GGGAAGGCGTGACGTACCGTG.

Site directed mutagenesis

Completed site directed mutagenesis on the complement vector following the protocol by Zheng et al., 2004.For the cysteine to alanine modification used primers:

GATTACATCgctGGCAACCTGGGCCTTGACC and CAGGTTGCCgcaGATGTA ATCCTCCTTCACGCCGG. For the cysteine to serine modification used primers: CGTGAAGGAGGATTACATCagtGGCAACCTGGGCCTTGACC and AAGGCCC AGGTTGCCactGATGTAATCCTCCTTCACGCCGG.

Lower case letters in the primers indicate the cysteine mutation site.

Phenotypic analysis PAM fluorometry

All PAM fluorometry was done using the FMS2 fluorometer (Hansatech). The general procedure was done as in Lyska et al., 2018 with minor modifications. Cells were at concentrated to $1x10^8$ for readings on a fiberglass pre-filter (Millipore Ref. AP2001300). Actinic light used to induce NPQ was ~800µmol photons m^{-2} s^{-1}.

Transformation and complementation of *N. oceanica*

For complementation of *lhcx1* a cDNA gene vector was created using Gibson assembly (Gibson et al., 2009), see NoEif3-Paro vector map in Genbank (need to submit the plasmid and sequence to Genbank). RNA extraction using plant RNAeasy kit (Qiagen Cat. 74903) and cDNA synthesized using Omniscript (Qiagen) with 2-3µg DNA free RNA per 20µl reaction. Primers used for LHCX1 cDNA amplification: FW-actacaca gaggtagcctttATGCGTGTCCTCTCTTTCCTCG, Rev- tccttgtaatcggcgcctttGAAGAAGAA GTTGTAGACATCAGAGAG. Lowercase letters are the Gibson assembly flanking arms.

Linear amplification construct for *N. oceanica* transformation done through PCR with primers: FW-CCTTCGCACCTGGAATTTTCCAAT, Rev- GAAGTTGTAGACATCAGA GAGGGCG. Transformation of *N. oceanica* done as in Killian et al., 2011.

Immunoblot for LHCX1 protein

Protein extraction done as previously described above except without adding dimedone to the solubilization buffer. Protein concentration measured as above and gel electrophoresis and immunoblot run as above. Exception being that the primary antibody was α-LHCX1 (antibody from Tomas Morosinotto).

Pigment extraction/HPLC analysis

Pigments were extracted by bead beating cells in 100% acetone at highest setting for 60 sec. HPLC analysis of carotenoids and chlorophylls was done as previously described (Müller-Moulé et al., 2002). Average taken from a set of 3 cell cultures from each genetic line. Carotenoids were quantified relative to concentration of chlorophyll a, which was measured by standard curve of purified pigment (VKI).

Statistical analyses

XLSTAT plugin WAS USED for Microsoft Excel to preform all one-way ANOVA with Tukey pairwise statistical analyzes. P value cutoff was set to <0.05 for all with a tolerance of 0.0001 and a constraint of a1=0 using a least mean square.

Modeling of LHCX1

Developed the iterative model of LHCX1, and its modified versions, using the online Phyre2 modeling program as described in Kelly et al., 2015. Utilized the intensive setting to derive the best model from multiple structural sources and received a model with greater than 90% confidence over the entire structure. Used UCSF Chimera (Pettersen et al., 2004) to overlay the LHCX1 model with the PSII super complex crystal (PDB 3JCU) using the matchmaker function and removing all proteins except the one that match, chain G. Took the pigments that matched the binding sites in both proteins and removed the rest as well as the chain G backbone to end up with a LHCX1 protein with pigments attached. Utilized Chimera to look at pigment distances as well as the space filling model structure.

Acknowledgements:

This work was supported by the U.S. Department of Energy, Office of Science, Basic Energy Sciences, Chemical Sciences, Geosciences, and Biosciences Division under field work proposal 449B. Thanks to Tomas Morosinotto for providing the LHCX antibody we used for immunoblot analysis. This work used the Vincent J. Proteomics/Mass Spectrometry Laboratory at UC Berkeley, supported in part by NIH S10 Instrumentation Grant S10RR025622.

References:

Babuskin, SR, Krishnan KD, Babu PAS, Sivarajan M, Sukumar M. 2014. Functional foods enriched with marine microalga *Nannochloropsis oculata* as a source of omega-3 fatty acids. *Food Technol. Biotechnology* 53: 292-299.

Bailleul B., Cardol P., Breyton C. & Finazzi G. 2010. Electrochromism: a useful probe to study algal photosynthesis. Photosynthesis Research 106, 179–189.

Ballottari M, Truong TB, De Re E, Erickson E, Stella GR, Fleming GR, Bassi R & Niyogi KK. 2016. Identification of pH-sensing Sites in the Light Harvesting Complex Stress-related 3 Protein Essential for Triggering Non-photochemical Quenching in Chlamydomonas reinhardtii. J Biol Chem, 291(14):7334-46.

Bellafiore, S., Barneche, F., Peltier, G. and Rochaix, J.D. 2005. State transitions and light adaptation require chloroplast thyla- koid protein kinase STN7. Nature 433, 892–895.

Benitez, L. V., & Allison, W. S. 1974. The inactivation of the acyl phosphatase activity catalyzed by the sulfenic acid form of glyceraldehyde 3-phosphate dehydrogenase by dimedone and olefins. *The Journal of Biological Chemistry*, *249*(19), 6234–6243.

Brooks MD, Niyogi KK. 2011. Use of a pulse-amplitude modulated chlorophyll fluorometer to study the efficiency of photosynthesis in *Arabidopsis* plants. *Meth Mol Bio* 775: 299-310.

Buchanan B, Kalberer P, Arnon D. 1967. Ferredoxin-activated fructose diphosphatase in isolated chloroplasts. *Biochem Biophys Res Comm* 29: 74–9.

Cheng Z, Wu J, Setterdahl A, Reddie K, Carroll K, Hammad LA, et al. 2012. Activity of the tetrapyrrole regulator CrtJ is controlled by oxidation of a redox active cysteine located in the DNA binding domain. Molecular Microbiology, 85(4), 734–746.

Chiang BY, Chen TC, Pai CH, Chou CC, Chen HH, Ko TP, Hsu WH, Chang CY, Wu WF, Wang AH, Lin CH. 2010. Protein S-thiolation by glutathionylspermidine (Gsp): The role of *Escherichia coli* Gsp synthetase/amidase in redox regulation. *J Biol Chem 285*: 25345–25353.

Chukhutsina VU, Fristedt R, Morosinotto T & Croce R. 2017. Photoprotection strategies of the alga Nannochloropsis gaditana. BBA, 1858 (7), 544-552.

Couturier J, Chibani K, Jacquot JP, & Rouhier N. 2013. Cysteine-based redox regulation and signaling in plants. *Frontiers in Plant Science*, *4*, 105–105.

Liguori N, Roy LM, Opacic M, Durand G, & Croce R. 2013. Regulation of Light Harvesting in the Green Alga Chlamydomonas reinhardtii: The C-Terminus of LHCSR Is the Knob of a Dimmer Switch. J. Am. Chem. Soc., 135 (49), 18339–18342.

Dall'Osto L, Caffarri S, and Bassi R. 2005. A mechanism of nonphotochemical energy dissipation, independent from PsbS, revealed by a conformational change in the antenna protein CP26. Plant Cell 17: 1217–1232.

Demmig-Adams B. 1990. Carotenoids and photoprotection in plants: A role for the xanthophyll zeaxanthin. BBA - Bioenergetics, 1020 (1), 1-24.

Demmig-Adams B, Garab G, Adams WW III, Govindjee. 2014. Non-Photochemical Quenching and Energy Dissipation in Plants, Algae and Cyanobacteria. Springer.

Depège N, Bellafiore S and Rochaix JD. 2002. Role of chloroplast protein kinase Stt7 in LHCII phosphorylation and state transition in Chlamydomonas. Science 299, 1572–1575.
Eberhard S, Finazzi G, Wollman FA. 2008. The dynamics of photosynthesis. *Ann review gene*, 42: 463-515.
Foyer CH, Noctor G. 2009. Redox regulation in photosynthetic organisms: signaling, acclimation, and practical implications. Antioxid Redox Signal 11: 861–905
Foyer CH, & Shigeoka S. 2011. Understanding oxidative stress and antioxidant functions to enhance photosynthesis. *Plant Phys*, *155*, 93–100.
Furdui CM and Poole LB. 2013. Chemical approaches to detect and analyze protein sulfenic acids. *Mass Spectrom Rev.* 33:126-46.
Gibson DG, Young L, Chuang RY, Venter JC, Hutchison CA 3rd & Smith HO. (2009) Enzymatic assembly of DNA molecules up to several hundred kilobases. Nature methods, 6, 343-345.
Gupta V & Carroll KS. 2014. Sulfenic acid chemistry, detection and cellular lifetime. BBA. 1840 (2), 847-875.
Jones DP. 2006. Redefining oxidative stress. Antioxid Redox Signal 8: 1865–1879.
Kelley LA, Mezulis S, Yates CM, Wass MN & Sternberg MJE. 2015. The Phyre2 web portal for protein modeling, prediction and analysis. Nature Protocols, 10, 845-858.
Killian O, Benemann CSE, Niyogi KK, & Vick B. 2011. High-efficiency homologous recombination in the oil-producing alga *Nannochloropsis sp*. *PNAS*, *108*, 21265–21269.
Krause G, Vernotte C, and Briantais JM. 1982. Photoinduced quenching of chlorophyll fluorescence in intact chloroplasts and algae. Resolution into two components. Biochim. Biophys. Acta 679: 116–124.
Kromdijk J, Glowacka K, Leonelli L, Gabilly ST, Iwai M, Niyogi KK, & Long SP. 2016. Improving photosynthesis and crop productivity by accelerating recovery from photoprotection. *Science*, *354*(6314), 857–861.
Lavaud J, Materna AC, Sturm S, Vugrinec S & Kroth PG. 2012. Silencing of the Violaxanthin De-Epoxidase Gene in the Diatom Phaeodactylum tricornutum Reduces Diatoxanthin Synthesis and Non-Photochemical Quenching. PLoS ONE, 7(5): e36806.
Leonard SE, & Carroll KS. 2011. Chemical “omics” approaches for understanding protein cysteine oxidation in biology. *Cur Opin Chem Bio*, *15*, 88–102.
Li XP, Björkman O, Shih C, Grossman AR, Rosenquist M, Jansson S & Niyogi KK. 2000. A pigment-binding protein essential for regulation of photosynthetic light harvesting. *Nature* 403, 391-395.
Maller C, Schröder E, & Eaton P. 2011. Glyceraldehyde 3-phosphate dehydrogenase is unlikely to mediate hydrogen peroxide signaling: studies with a novel anti-dimedone sulfenic acid antibody. *Antioxidants and Redox Signaling*, *14*(1), 49–60.
Malnoë A, Schultink A, Shahrasbi S, Rumeau D, Havaux M, & Niyogi, KK. 2018. The Plastid Lipocalin LCNP Is Required for Sustained Photoprotective Energy Dissipation in Arabidopsis. *The Plant Cell online*, *30*(1), 196–208.
Møller IM, Jensen PE, & Hansson A. 2007. Oxidative Modifications to Cellular Components in Plants. *Annual Review of Plant Biology*, *58*(1), 459–481.

Montrichard F, Alkhalfioui F, Yano H, Vensel WH, Hurkman WJ, & Buchanan BB. 2009. Thioredoxin targets in plants: the first 30 years. *J. Proteomics* 72, 452–474.
Müller P, Li XP, & Niyogi KK. 2001. Non-photochemical quenching. A response to excess light energy. *Plant Phys*, *125*, 1558–1566.
Müller-Moulé P, Conklin PL & Niyogi KK. 2002. Ascorbate deficiency can limit violaxanthin de-epoxidase activity in vivo. Plant Physiol. 128 970–977.
Mullineaux PM, Exposito-Rodriguez M, Laissue PP, & Smirnoff N. 2018. ROS-dependent signalling pathways in plants and algae exposed to high light: Comparisons with other eukaryotes. *Free Radical Biology and Medicine*.
Niedzwiedzki DM, & Blankenship RE. 2010. Singlet and triplet excited state properties of natural chlorophylls and bacteriochlorophylls. *Photosynthesis Research*, *106*(3), 227–238.
Nilkens M, Kress E, Lambrev P, Miloslavina Y, Müller M, Holzwarth AR, and Jahns P. 2010. Identification of a slowly inducible zeaxanthin- dependent component of non-photochemical quenching of chlorophyll fluorescence generated under steady-state conditions in Arabidopsis. Biochim. Biophys. Acta 1797: 466–475.
Niyogi KK, Grossman AR & Björkman O. 1998. Arabidopsis Mutants Define a Central Role for the Xanthophyll Cycle in the Regulation of Photosynthetic Energy Conversion. The Plant Cell, 10 (7), 1121-1134.
Noctor G, Rees D, Young A, Horton P. 1991. The relationship between zeaxanthin, energy-dependent quenching of chlorophyll fluorescence and the trans-thylakoid pH-gradient in isolated chloroplasts. Biochim. Biophys. Acta 1057: 320– 30
Peers G, Truong TB, Ostendorf E, Busch A, Elrad D, Grossman AR, et al. 2009. An ancient light-harvesting protein is critical for the regulation of algal photosynthesis. *Nature*, *462*(7272), 518–521.
Pettersen EF, Goddard TD, Huang CC, Couch GS, Greenblatt DM, Meng EC, Ferrin TE. 2004. UCSF Chimera--a visualization system for exploratory research and analysis. J Comput Chem. Oct, 25(13), 1605-12.
Poliner E, Farré EM & Benning C. 2018. Advanced genetic tools enable synthetic biology in the oleaginous microalgae Nannochloropsis sp. Plant Cell Rep Online. https://doi.org/10.1007/s00299-018-2270-0
Rey P, Becuwe N, Barrault MB, Rumeau D, Havaux M, Biteau B, et al. 2007. The *Arabidopsis thaliana* sulfiredoxin is a plastidic cysteine- sulfinic acid reductase involved in the photooxidative stress response. *Plant J.* 49, 505–514.
Stöcker S, Maurer M, Ruppert T, & Dick TP. 2018. A role for 2-Cys peroxiredoxins in facilitating cytosolic protein thiol oxidation. *Nature Chemical Biology*, *14*(2), 148–155.
Sun X, Feng P, Xu X, Guo H, Ma J, Chi W, et al. 2011. A chloroplast envelope-bound PHD transcription factor mediates chloroplast signals to the nucleus. *Nature Communications*, *2*, 477.
Van Montfort RL, Congreve M, Tisi D, Carr R, Jhoti H. 2003. Oxidation state of the active-site cysteine in protein tyrosine phosphatase 1B. *Nature 423*:773–777.
Vieler A, Wu G, Tsai CH, Bullard B, Cornish AJ, Harvey C, et al. 2012. Genome, functional gene annotation, and nuclear transformation of the heterokont oleaginous alga *Nannochloropsis oceanica CCMP1779*. *PLoS Genetics*, *8*(11), e1003064.

Wang Q, Lu Y, Xin Y, Wei L, Huang S and Xu J. 2016. Genome editing of model oleaginous microalgae Nannochloropsis spp. by CRISPR/Cas9. Plant J, 88, 1071-1081.

Waszczak C, Akter S, Eeckhout D, Persiau G, Wahni K, Bodra N, et al. 2014. Sulfenome mining in Arabidopsis thaliana. *Proceedings of the National Academy of Sciences of the United States of America*, *111*(31), 11545–11550.

Wei L, Xin Y, Wang D, Jing X, Zhou Q, Su X, Jia J, Ning K, Chen F, Hu Q, Xu J. 2013. Nannochloropsis plastid and mitochondrial phylogenomes reveal organelle diversification mechanism and intragenus phylotyping strategy in microalgae. BMC Genomics, 14, 534.

Wu J, Cheng Z, Reddie K, Carroll K, Hammad LA, Karty JA, & Bauer CE. 2013. RegB Kinase Activity Is Repressed by Oxidative Formation of Cysteine Sulfenic Acid. Journal of Biological Chemistry, 288(7), 4755–4762.

Yutthanasirikul R, Nagano T, Jimbo H, Hihara Y, Kanamori T, Ueda T, et al. 2016. Oxidation of a Cysteine Residue in Elongation Factor EF-Tu Reversibly Inhibits Translation in the Cyanobacterium Synechocystis sp. PCC 6803. *Journal of Biological Chemistry*, *291*(11), 5860–5870.

Zheng, L., U. Baumann, and Jean-Louis Reymond. 2004. An efficient one-step site-directed and site-saturation mutagenesis protocol. Nucleic Acids Res. 2004; 32(14): e115.

Zhu XG, Ort DR, Whitmarsh J, & Long SP. 2004. The slow reversibility of photosystem II thermal energy dissipation on transfer from high to low light may cause large losses in carbon gain by crop canopies: a theoretical analysis. *Journal of Experimental Botany*, *55*(400), 1167–1175.

Chapter 3

CYSTEINE SULFENIC ACID MODIFICATION OF LHCA6 HAS A POTENTIAL REGULATORY ROLE IN *ARABIDOPSIS THALIANA* PHOTOSYNTHESIS

Abstract:

Oxidation of cysteine residues to the sulfenic acid state (Cys-SOH) has been shown to play an important role in protein regulation and function. However, very little is known about the roles of stable Cys-SOH residues in the chloroplast. *Arabidopsis thaliana* plants treated with high light (HL) or hydrogen peroxide showed increased chloroplast protein oxidation. LC-MS/MS analysis identified the specific sites of cysteine oxidation in 303 proteins. Based on this chloroplast sulfenome, T-DNA insertion lines affecting several sulfenylated proteins were examined for growth and photosynthesis-related phenotypes. From this analysis, an *lhca6* T-DNA line showed a higher level of non-photochemical quenching (NPQ) in both the low-light-grown plants and HL-treated plants. As expected for an *lhca6* mutant, the NDH-PSI supercomplex was reduced in this T-DNA insertion line. Vectors were developed for complementation of each of these lines with the corresponding wild-type gene, as well as cysteine-modified versions to mimic the constitutively reduced or oxidized Cys-SOH state. Thus, the *lhca6* mutant was transformed with the wild-type *LHCA6* gene (*lhca6*+WT), cysteine to alanine (*lhca6*+C58A), or cysteine to serine (*lhca6*+C58S) versions of the gene. NPQ recovered to wild-type levels only in the *lhca6*+WT and *lhca6*+C58A lines. In the *lhca6*+C58S lines, NPQ remained high and resembled the NPQ phenotype of the *lhca6* mutant. Further work is needed to check the presence of NDH-PSI supercomplex in these lines. This work suggests that oxidation of LHCA6 in wild-type chloroplasts may play a role in inactivation of this protein, which could regulate PSI cyclic electron flow.

Introduction:

Cysteine sulfenic acids (Cys-SOH) are one of the most essential protein modifications in biological redox regulation. As mentioned in the previous two chapters, the oxidation of proteins is not only a symptom of damage but is the linchpin in many signaling pathways in many cellular compartments. Cys-SOH is the primary oxidation of cysteine that occurs in the presence of a strong oxidant, e.g. reactive oxygen species (ROS). This oxidation is also dependent on the microenvironment around the cysteine, the pKa of the cysteine and the pH (Gupta & Carroll, 2014). These same factors dictate the stability of the Cys-SOH and can help to determine the specificity of both the oxidant that interacts with the protein and the further downstream modifications that can occur, if any. The best studied of these downstream modifications is the disulfide bond, which has been shown to be of paramount importance in both protein structure and in signaling. Disulfide bonds form when a Cys-SOH reacts with a cysteine thiol, either on the same protein or an adjacent one, to form a covalent bond between the two sulfur atoms, releasing a water molecule (Haber & Anfinsen, 1962).

For many decades sulfenic acids were thought to be too reactive to be stable, but recent evidence, in both chemistry and biology, shows that sulfenic acids can persist if

the conditions are right. Chemically, it was seen that Cys-SOH could be stabilized by both steric hindrance and hydrogen bonding (Goto et al. 1997; Tripolt et al., 1993). In biology these factors play a role, but it was also found that the cysteine must not be in proximity to any other cysteine, to prevent the spontaneous formation of disulfides (Miller & Claiborne, 1991). The discovery of hundreds of crystal structures with Cys-SOH modifications (reviewed in Furdui and Poole, 2013) has led a number of scientists to wonder if there might be some specific role of Cys-SOH that is distinct from its function as a redox intermediate.

CrtJ is one compelling example of a protein in which a stable sulfenic acid has functional importance (Cheng et al., 2012). CrtJ is a transcription factor in *Rhodobacter capsulatus*, an anaerobic phototrophic prokaryote, that is important in the repression of pigment biosynthetic pathways during oxidative stress conditions. In the presence of oxygen, CrtJ was seen to have a dramatic increase in DNA binding affinity to its target sequence compared to anoxic conditions. This binding affinity increase was shown to be caused by the oxidation of Cys420 to the Cys-SOH state by experiments in which that residue was changed to either an alanine (to mimic the reduced state) or serine (to mimic the Cys-SOH state). The C420A mutation had a phenotype similar to the CrtJ knockout (KO) line, but the C420S had a binding affinity even higher than the wild type (WT) in the presence of oxygen. The use of alanine and serine mimics was also well illustrated in the last chapter and will be employed again in this chapter.

Although there is strong evidence that Cys-SOH has important functions, so far all the work done on stable Cys-SOH regulation in biology has focused on prokaryotic, fungal, and mammalian cells. Considering that photosynthetic eukaryotes experience some of the greatest levels of oxidative stress of any organisms, it is likely that cysteine oxidation would play an important role in these organisms. This constant onslaught of stress, from the sun, drought, or pathogen attack, would require a very sophisticated redox regulatory system. Indeed, plants and algae have increased their total number of thioredoxins (Trx) and Trx targets compared to all other forms of life. Trx are essential proteins in the reduction of disulfide bonds and are important in the activation of many crucial proteins throughout the cell, such as fructose 1,6-bisphosphatase in the Calvin-Benson cycle (Buchanan et al., 1967). This led me to investigate if Cys-SOH could play an equally important role in plant redox homeostasis as a protein functional regulator in the model plant *Arabidopsis thaliana*. A previous study has identified a number of proteins that are susceptible to oxidation by H_2O_2 in the cytosol of *A. thaliana* (Waszczak et al., 2014). As I am most interesting in the effects of light-stress-induced oxidation on photosynthesis, I focused my analysis on the chloroplast proteome.

To determine what role light stress has on Cys-SOH modifications in the chloroplast of *A. thaliana*, I adapted protocols used in the previous chapter to examine the Cys-SOH modification profile of proteins in this compartment. Immunoblot and LC-MS/MS were used to identify which proteins were present with Cys-SOH modifications under different stress conditions. Mutants for seven target genes were acquired, and these mutants were phenotyped to determine if there were changes in growth or non-photochemical quenching (NPQ). The *cyp38* showed a growth phenotype, while *lhca6*, *prxq* and *atr2* mutants showed enhancement of NPQ. Complementation of *lhca6* with cysteine-modified versions of LHCA6 to mimic the constitutively reduced (C to A) or oxidized Cys-SOH state (C to S) showed a potential role of cysteine oxidation in the

inactivation of LHCA6. Unfortunately, the *lhca6* T-DNA line used in this work was only a knockdown, and therefore further analysis of a complete KO mutant would be needed to fully examine Cys-SOH's role in LHCA6 function.

Results:

Light stress and ROS induce Cys-SOH protein modifications

To determine the effect of light stress on the Cys-SOH profile in the chloroplast of *A. thaliana,* a set of WT plants were treated with either low light (LL) or high light (HL) for 30 or 60 min after overnight dark acclimation of LL-grown plants. Subsequently, the chloroplasts were isolated and chemically treated with dimedone, which specifically labels the Cys-SOH-modified proteins. These pools of proteins were then analyzed by immunoblotting with an antibody that recognizes dimedone-labeled cysteines. As shown in Fig. 3.1A, there was an increase in the number and intensity of bands seen in the samples treated with HL for 30 min compared to the Dark and LL samples with a further increase after 60 min of HL.

Isolated chloroplasts were also treated with exogenous H_2O_2 to examine how this ROS would affect the chloroplast sulfenome. After 30 min, H_2O_2-treated chloroplasts showed a similar number and intensity of bands present in the 60-min HL sample (Fig. 3.1B), although the intensity of specifc bands differed between H_2O_2 and HL treatment (Fig. 3.1). Specifically, it should be noted that the intensity of the 25-kD band was lower in both H_2O_2-treated samples compared to HL treatment. When the H_2O_2 treatment was extended to 60 min there was only a slight increase in the band intensity compared to the 30-min sample, indicating a likely saturation of potential Cys-SOH in the proteome at 30 min.

LC-MS/MS identifies specific sites of Cys-SOH modification in the chloroplast proteome

Immunoblot analysis strongly indicated that there are protein sulfenylation events occurring in the chloroplast during light stress conditions, but what are the specific proteins being oxidized? Chloroplast proteins from the dark, LL and HL (60 min) samples were subjected to LC-MS/MS to identify the proteins found in each condition. Samples treated with H_2O_2 were not analyzed by LC-MS/MS, because wanted to focus on the response to physiological light conditions. With this analysis we were able to identify specific proteins in the chloroplast with Cys-SOH modifications for each light condition, with only a minor contamination with vacuolar and mitochondrial proteins. Consistent with the immunoblot analysis of dimedone-labeled proteins, there was an increase in the total sulfenylated proteins in the HL-treated sample compared to both the LL-grown and dark-treated samples (Fig. 3.2a), with twice as many Cys-SOH proteins identified in HL compared to dark-treated plants. The distribution of these proteins showed some overlap between the light conditions, but the majority of proteins identified were unique to each light condition (Fig. 3.2b). Proteins involved in redox process, stress response, and photosynthesis were strongly represented in each light condition (LL and HL; Fig. 3.3) as determined by Blast2GO GO term enrichment

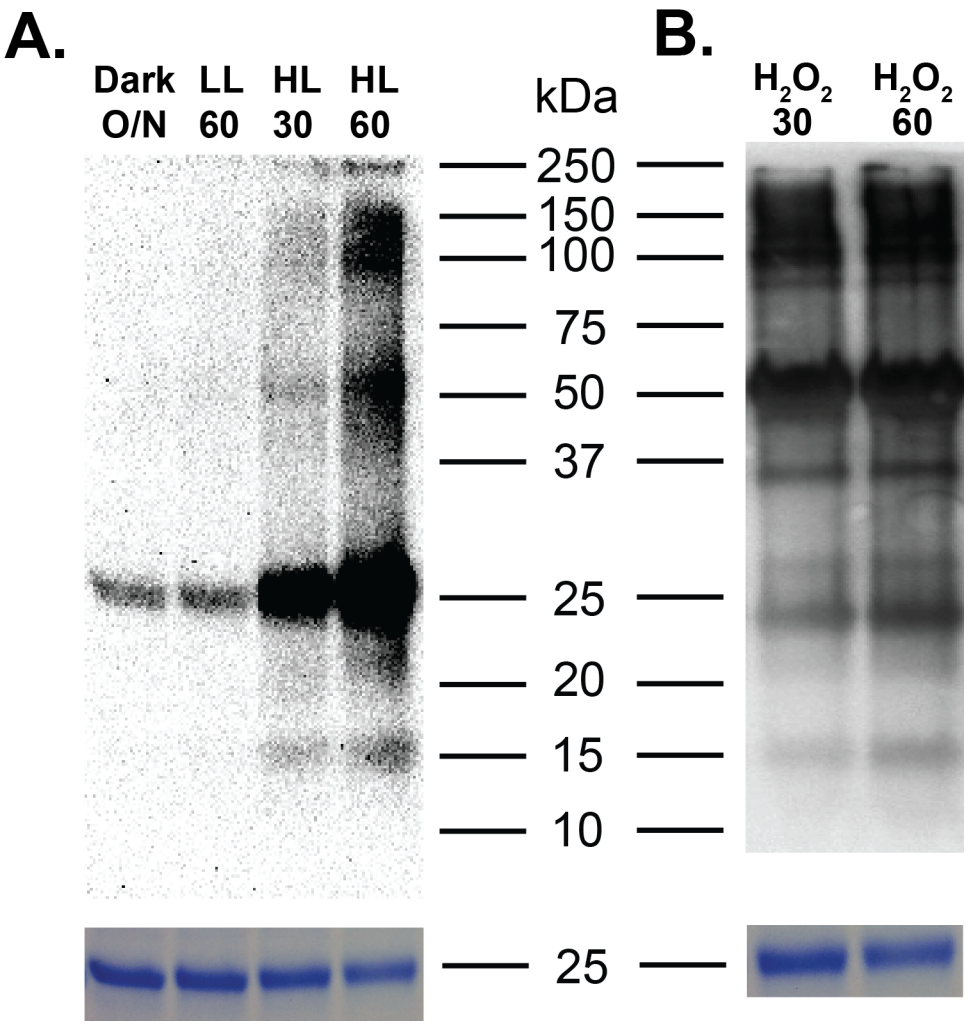

Figure 3.1: Immunoblot analysis of chloroplast proteins with an anti-dimedone antibody.

A. HL treatment of Col-0 plants. **B.** 10 mM H_2O_2 treatment of dark-acclimated chloroplasts. LL = 150 µmol photon m^{-2} sec^{-1}; HL = 600 µmol photon m^{-2} sec^{-1}. Gels were stained with Coomassie brilliant blue as a loading control. 1 µg of chlorophyll was loaded per lane.

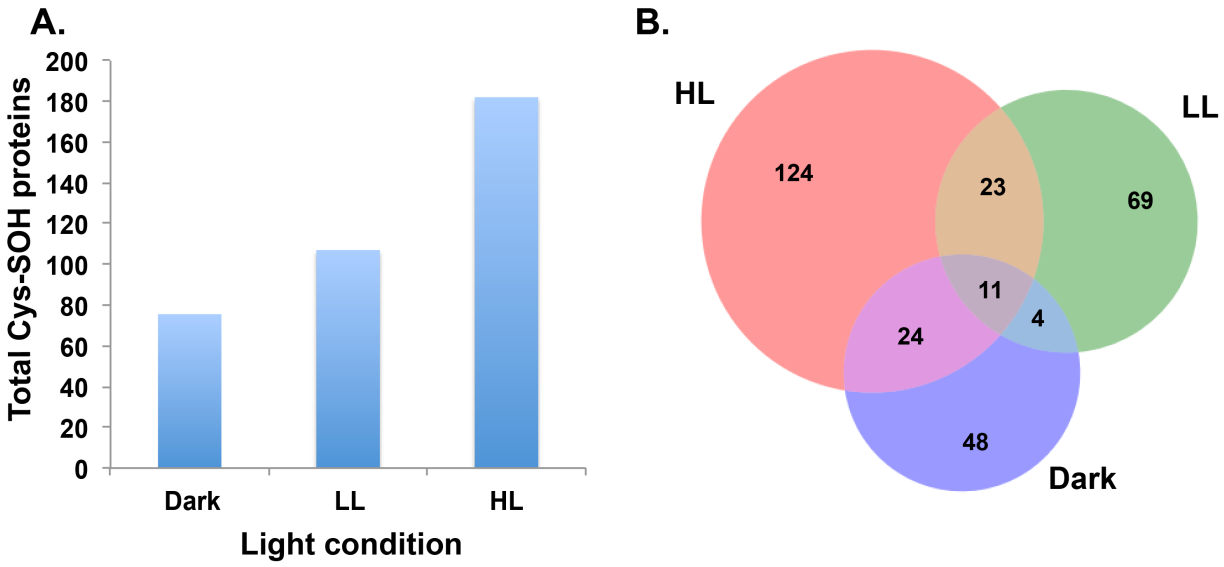

Figure 3.2: Summary of LC-MS/MS Cys-SOH analysis after different light conditions.

A. Bar graph of total Cys-SOH-modified protein identified by LC-MS/MS. **B.** Venn diagram of the distribution of the Cys-SOH-modified proteins.

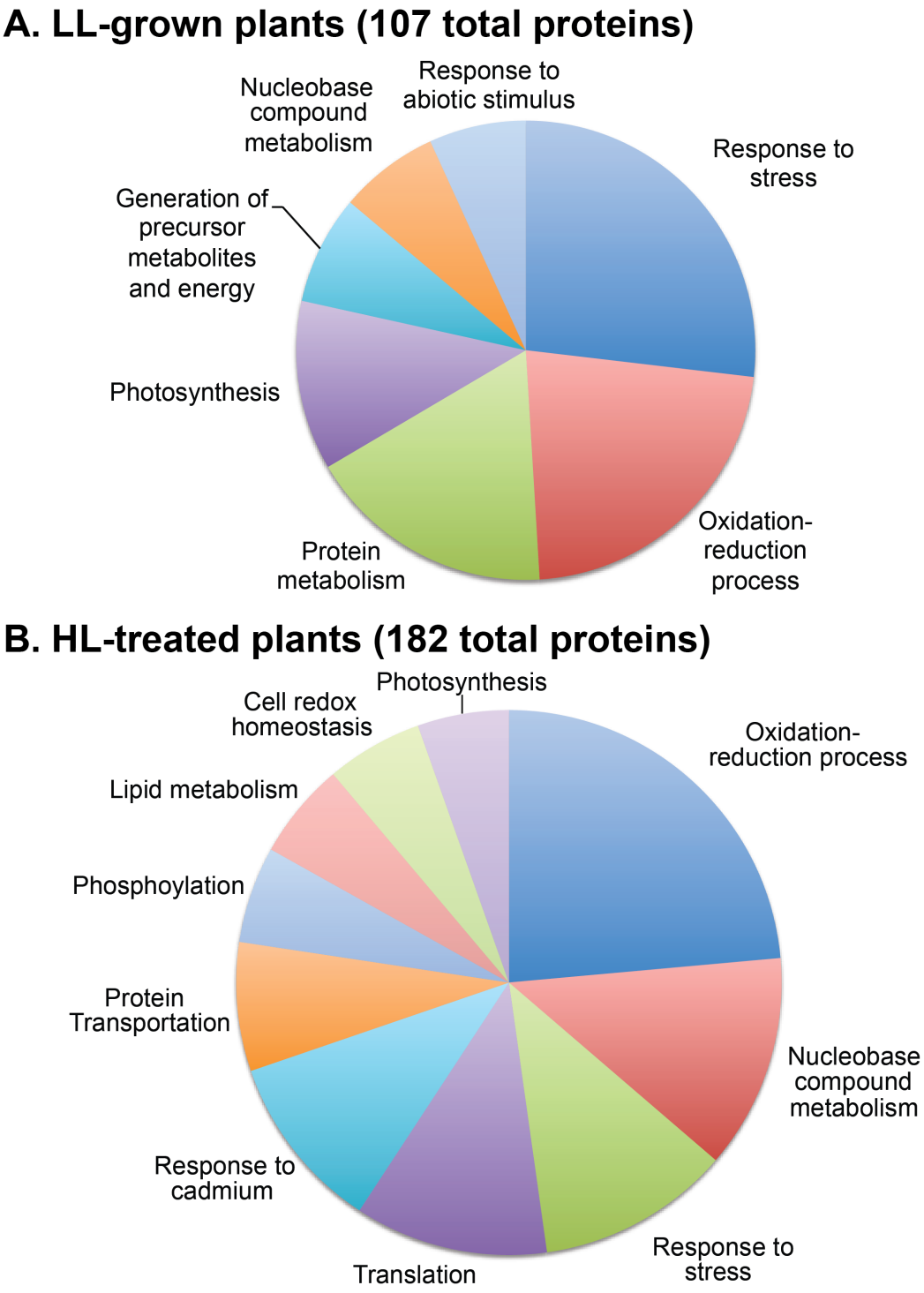

Figure 3.3: *Arabidopsis thaliana* GO enrichment analysis.

A. LL-grown plants. **B.** Plants treated with HL for 1 h. GO terms were limited to those with node scores greater than 15 and represented in more than 10% of the total sequences.

analysis tool. However, in HL-treated samples there was also enrichment for proteins involved in translation, protein transportation, and phosphorylation, based on Blast2GO analysis. A selection of proteins with known roles in photosynthesis is listed in Table 3.1. It is worth noting that no transcription factors were found, which would be expected since our analysis was limited to the chloroplast.

T-DNA lines of *lhca6*, *prxq,* and *atr2* all show enhancement of NPQ, while *cyp38* shows a growth defect

To determine if the Cys-SOH was important for the functional regulation of photosynthesis, a subset of target proteins were selected from the list in Table 3.1, and a set of T-DNA insertional knockout lines were acquired (Table 3.2). LHCA6 and PrxQ were chosen because of their published NPQ phenotypes (Peng et al., 2009; Petersson et al., 2006), CYP38 and PSB29 for their involvement in PSII assembly (Fu et al., 2007; Keren et al., 2005), and VIPP1 for its involvement in thylakoid biogenesis (Kroll et al., 2001). ATR2 was chosen because its function is less understood, although it is thought to be involved in redox signaling in the chloroplast (Jensen & Møller, 2010). COX6B is less studied but appears to be chloroplast localized and has homology to a mitochondrial cytochrome oxidase electron sink pathway and could have a role as an electron sink in chloroplasts. Each of these lines was tested by PCR for gene insertion to confirm correct identification of the mutants (data not shown). This analysis confirmed that 5 out of 7 lines were homozygous with proper insertion identification for all lines (Table 2). The two heterozygous lines, *psb29 and vipp1*, were selfed, but homozygous knockout lines could not be isolated. Gene expression was examined via qRT-PCR, and all lines had significant decreases in mRNA expression relative to WT by t-test analysis, although in some cases the reduction was less than half (Fig. 3.4). Interestingly, while the heterozygous *vipp1* shows a ~50% decrease in mRNA level as could be expected, the homozygous insertion line of *lhca6* also retained, on average, 50% expression of the gene.

Growth and NPQ phenotypes for each line were examined. The *cyp38* knockout had a dramatic growth defect relative to WT (Fig. 3.5), which caused difficulties due to very low seed production per plant. For each of the other T-DNA lines, I examined their NPQ phenotype in both LL growth conditions and after 1 h of HL treatment (Fig. 3.6 & 3.7). In the LL condition *lhca6, prxq,* and *atr2* all show an increased NPQ compared to WT after 10 min of actinic light. This increase was strongest in *lhca6*. Both *lhca6* and *prxq* also showed an increase in NPQ after the HL treatment, although it was reduced compared to the LL condition. The three other lines (*cox6b, psb29 and vipp1*) showed no change in NPQ or growth compared to WT.

NPQ of LHCA6 complement lines shows potential Cys-SOH regulation

To investigate possible Cys-SOH regulation of chloroplast protein function in *A. thaliana*, I developed complementation strategies for all 7 T-DNA lines. The summary of these complementation attempts is shown in Table 2. I was able to successfully produce the three expression vectors for all but two of the T-DNA lines, and from that I was able to generate T1 lines for all but *cyp38*, which did not produce enough seeds to

Table 3.1: Select photosynthesis proteins found by LC-MS/MS with Cys-SOH modification

Homology	Locus[a]	Cys-SOH	Peptide	D	LL	HL
Protochlorophyllide reductase	AT1G03630	280	K.VC*NMLTMQELHR.R	-	+	-
VDE	AT1G08550	120/127	K.TC*ACLLKGC*R.I	-	+	+
		159/163/178	R.PDETEC*QIKC*GDLFENSVVDEFNEC*AVSRKKCVPRK.S	-	+	+
		134/140	R.IELAKC*IANPAC*AANVACLQTCN.N	+	-	-
LHCA6	AT1G19150	58	K.EVSSVC*EPLPPDR.P	-	+	+
Geranylgeranyl diphosphate reductase	AT1G74470	415	K.VFYRSNPAREAFVEMC*NDEYVQKMTFDSYLYK.R	+	+	+
Carbonic anhydrase 1	AT3G01500	90	K.YMVFAC*SDSRVCPSHVLDFQPGDAFVVR.N	-	+	-
		203	K.SKVISELGDSAFEDQCGRC*ER.E	+	-	-
chlorophyll a-b binding protein 6	AT3G54890	91	K.ESELIHC*R.W	-	+	-
FNR	AT5G66190	178	K.GVC*SNFLCDLK.P	-	+	-
PSAC	ATCG01060	54	R.C*ESACPTDFLSVR.V	+	+	+
PGR5-like	AT4G22890	303	K.CTNC*GTAMVYDSGSR.L	-	+	-
Phytoene desaturase 3	AT4G14210	310	K.MAFLDGNPPERLC*MPVVDHIR.S	-	+	-
		500/503	K.TPRSVYKTIPNC*EPC*R.P	+	+	+
EF-Tu	AT1G07930	151	K.QMICC*NKMDATTPKYSK.A	-	-	+
PSB29	AT2G20890	284	K.C*LGDTLYNPSFLVER.K	-	-	+
PrxQ	AT3G26060	116	K.QAC*AFR.D	-	-	+
NDH-dependent CEF 1	AT1G64770	319	K.YGKQHYFVC*TGPTSMLVPVDVASGETWR.G	-	-	+
CYP38	AT3G01480	28	R.IGFSC*SKKPLEVR.C	-	-	+

[a] Accession number obtained from TAIR database. * denotes location of Cys-SOH in peptide

Table 3.2: T-DNA insertion lines and complementation progress

Gene Name	T-DNA line	Locus	Cys-SOH position	Confirmed homozygous	SDM		Transformants			Notes
					C->A	C->S	WT	C->A	C->S	
LHCA6	CS343795	AT1G19150	58	Yes	Yes	Yes	yes	yes	yes	Insertion only produces knockdown
PrxQ	CS803219	AT3G26060	116	Yes	Yes	Yes	yes	yes	yes	
Cox6B	Salk_040096C	AT1G22450	147	Yes	Yes	Yes	yes	yes	yes	
ATR2	Salk_152766C	AT4G30210	602	Yes	No	No	No	No	No	SDM issues prevented complementation
Cyp38	Salk_029448C	AT3G01480	28	Yes	Yes	Yes	No	No	No	Extreme growth phenotype
VIPP1	CS835706	AT1G65260	65	No	No	No	No	No	No	Could not clone gene
Psb29	Salk_094925	AT2G20890	284	No	Yes	Yes	yes	yes	yes	Double heterozygous

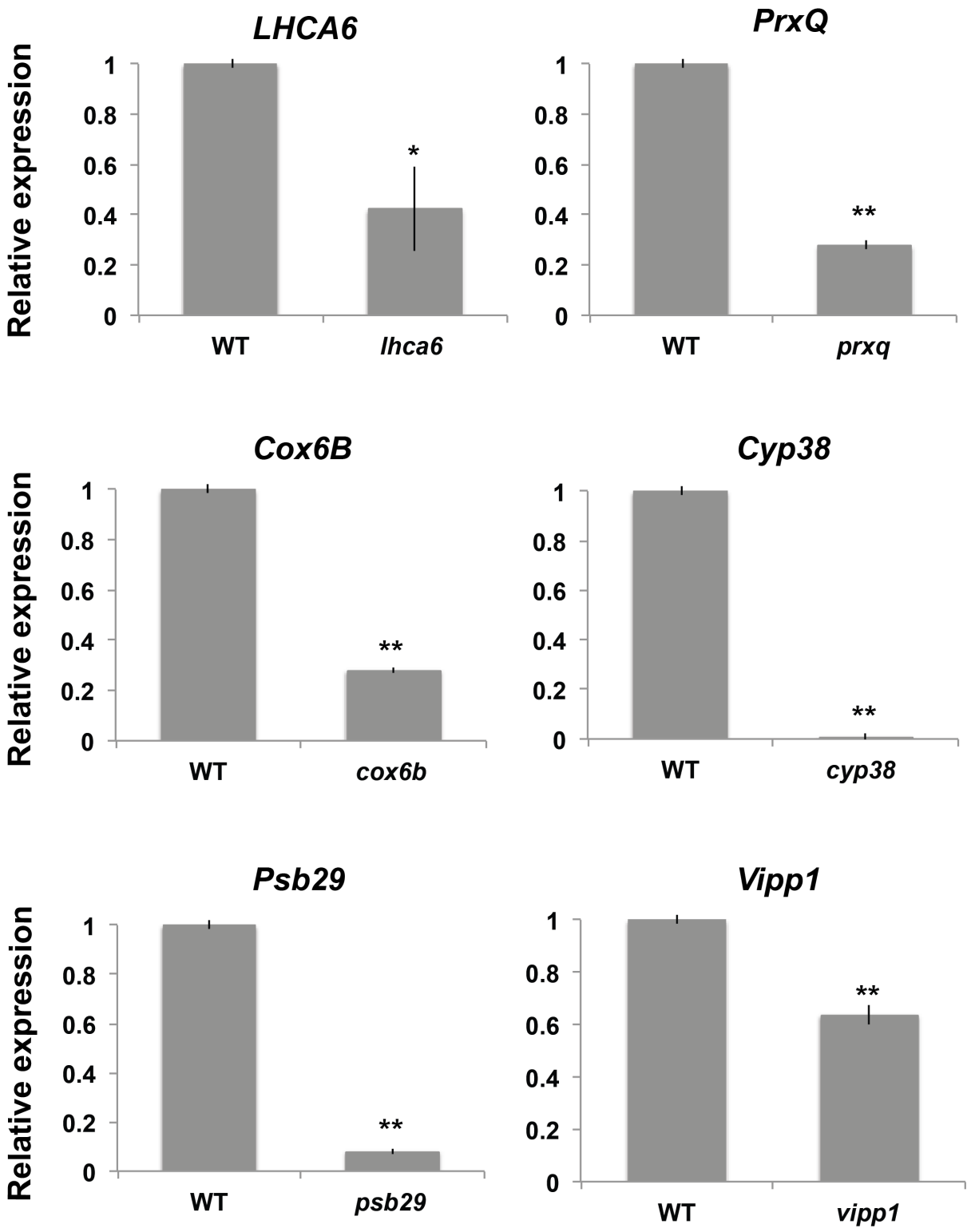

Figure 3.4: RNA expression levels in each T-DNA line relative to internal control.

Significance of expression change determined with student t-test (<0.05); * = p<0.05, ** = p<0.01.

Col-0

cyp38

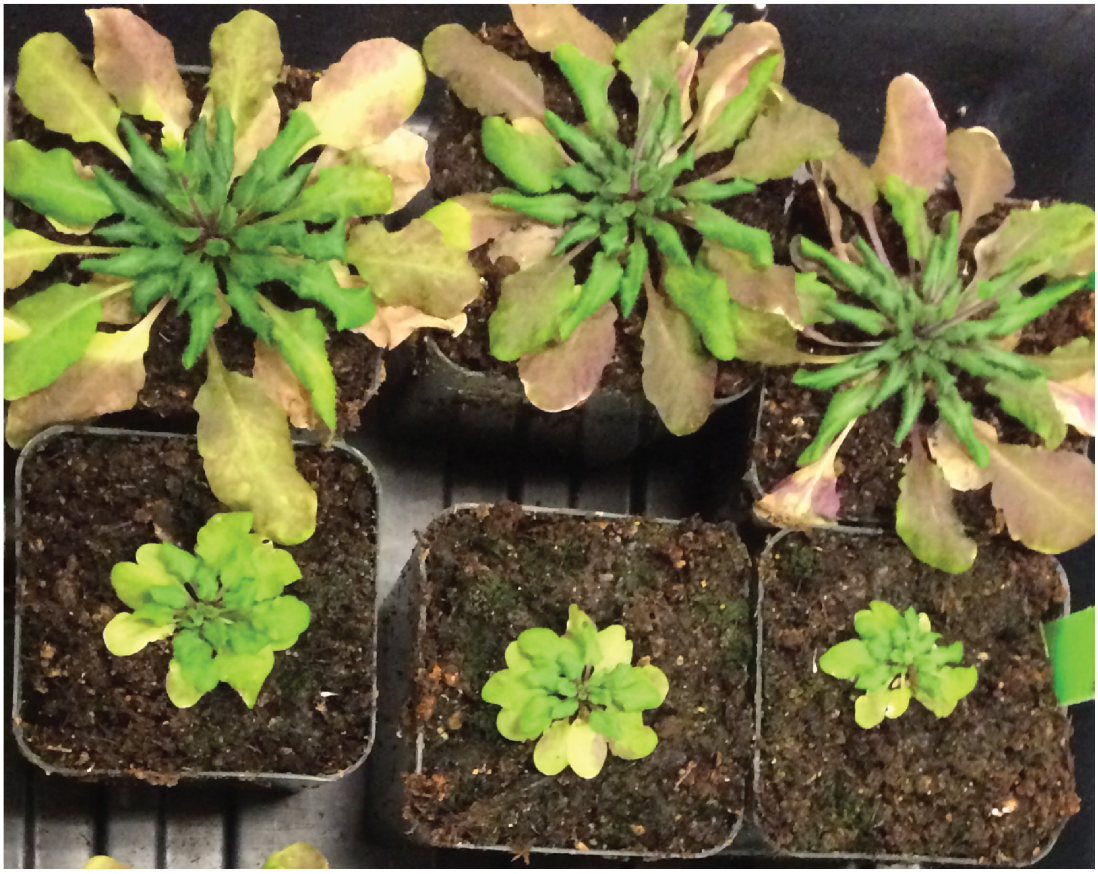

Figure 3.5: Growth phenotype of Col-0 and *cyp38* plants.

Image of eight-week old plants.

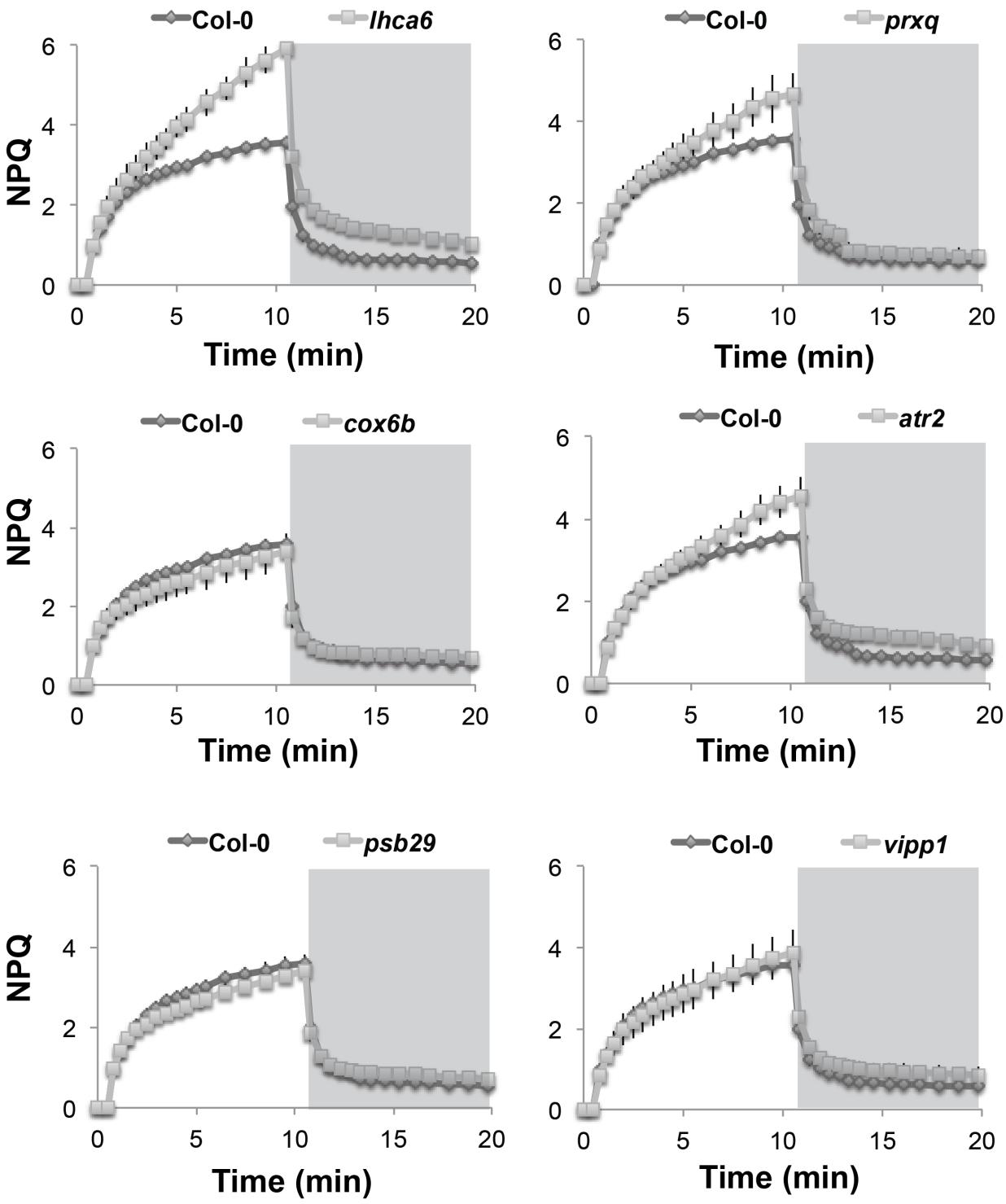

Figure 3.6: NPQ phenotypes of LL-grown T-DNA lines.

Shaded region denotes period of dark and unshaded region represents actinic light on.

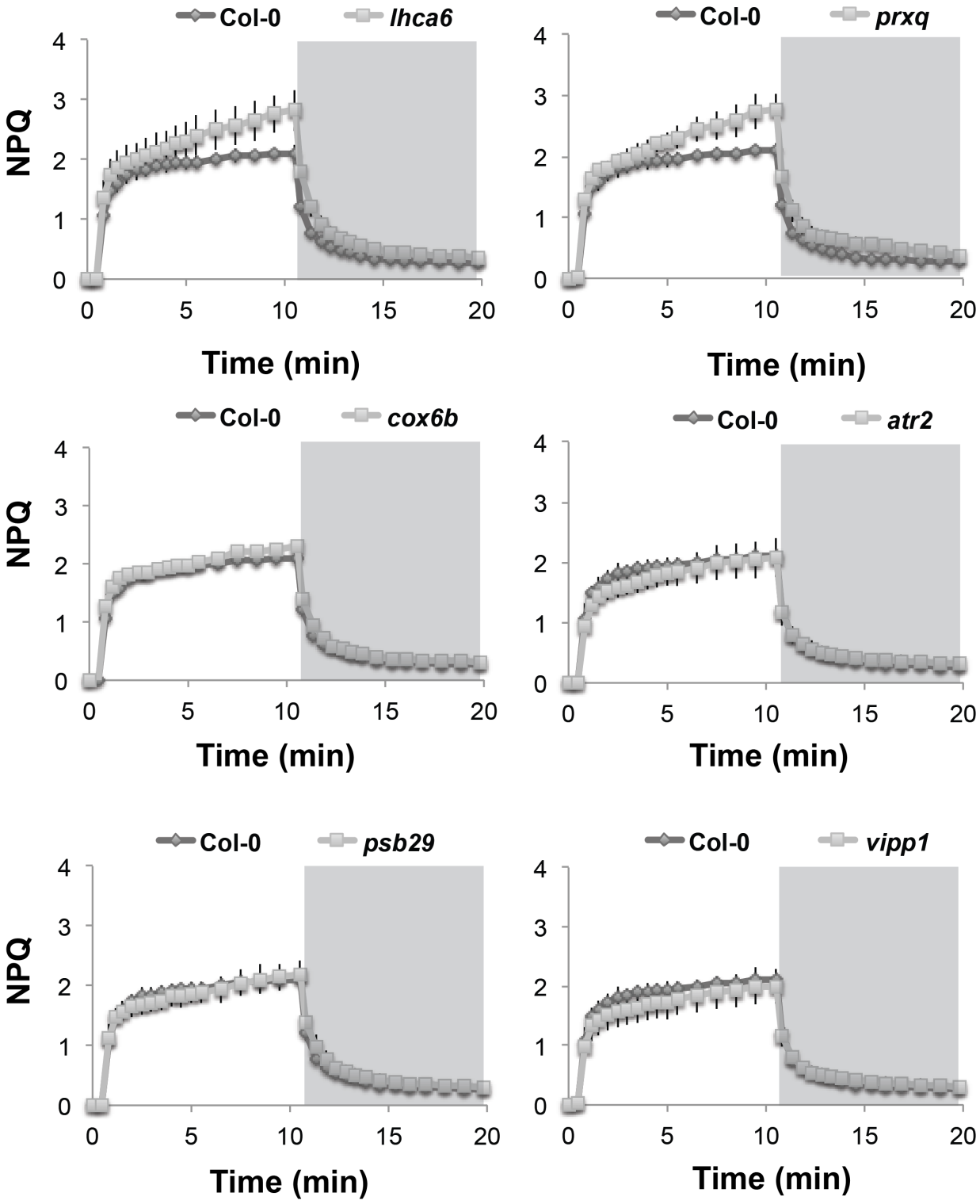

Figure 3.7: NPQ phenotypes of T-DNA lines treated with HL for 1 h.

Shaded region denotes period of dark and unshaded region represents actinic light on.

properly screen. The strong NPQ phenotype seen in *lhca6* made it a good candidate for complementation with the WT gene (*lhca6*+WT), and cysteine-modified mutants *lhca6*+C58A and *lhca6*+C58S.

The RNA expression levels of *LHCA6* in each of the transformed lines were examined and compared to WT levels to determine if there was a full recovery at the RNA level (Fig. 3.8a). In all independent insertions there was at least WT levels, and in a few cases much greater levels of RNA expression. The average NPQ of the *lhca6*+WT and *lhca6*+C58A lines showed similar NPQ levels as the WT plants (Fig. 3.8b). Interestingly, the *lhca6*+C58S line showed an average NPQ that is higher than all lines and resembles the NPQ of *lhca6* more so than WT. This separation of phenotype between the different modified versions of LHCA6 suggests that the oxidative state of this protein plays a role in protein regulation. It was previously shown that *lhca6* KO lines lose their largest NDH-PSI supercomplex so to confirm this in the T-DNA line, I looked at all native thylakoid membrane complexes of WT and the *lhca6* line, which showed a reduction in the NDH-PSI supercomplex band (Fig. 3.9). However, due to the incomplete loss of this band, blue native PAGE analysis of the other lines was not completed.

Discussion:

Cysteine oxidation to a stable Cys-SOH species has only very recently been shown to directly regulate protein function in a few instances, but the effect of this modification in chloroplasts of *A. thaliana* was unknown. To address this gap in knowledge, I undertook a proteomic screening of light-stress-induced protein oxidation in isolated chloroplasts to identify the proteins that are oxidized during these conditions. The reason I used only a maximum of 60 min for this study was to identify proteins that are involved in the early response to the light stress. Because my aim was to identify Cys-SOH regulatory modifications, I expected that these changes would occur within tens of minutes after light stress, when the level of oxidation would be sufficiently high. I found that protein sulfenylation in the chloroplast of *A. thaliana* increases with the increase of incident light intensity, as seen by both the immunoblotting and LC-MS/MS. The immunoblot analysis showed that chloroplast protein oxidation was very low in both the dark- and LL-treated plants, and only when the plants were treated with 30 min of HL was an appreciable difference in the number and intensity of the bands detected (Fig. 3.1A). Focusing on the band at 25 kD, which is present in all conditions, there was an increase in band intensity, by Image Lab analysis relative to the dark sample, of 20% percent in LL, ~200% after 30 min of HL and ~400% after 60 min of HL. While this rough quantitation is interesting, it is important to note that this band could represent a number of different proteins rather than the increased oxidation of a single target, because several LHC proteins are approximately 25 kD in size, examples from this analysis being LHCA1, 3, and 6.

Hydrogen peroxide reproduced the HL sulfenylation profile phenotype after 30 min, indicating that this level of ROS in the chloroplast causes similar protein oxidation during light stress conditions (Fig. 3.1). However, this result cannot rule out that the increase in molecular oxygen during higher light conditions also plays a role in direct protein oxidation. Also, it is interesting that the very intense 25 kD band in the HL

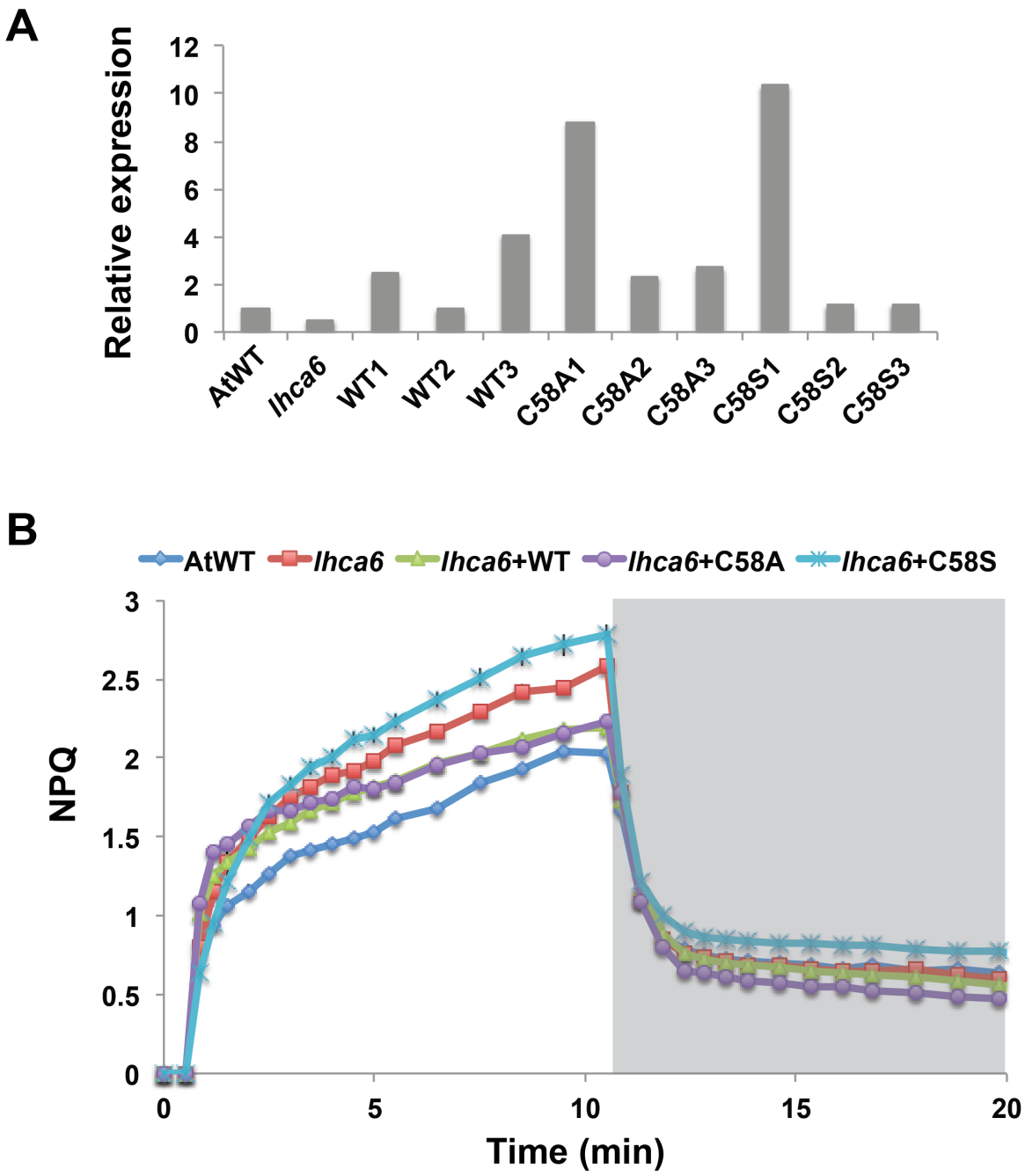

Figure 3.8: Analysis of LHCA6 lines.

A. Relative expression of *LHCA6* mRNA of three separate T1 plants of each construct.
B. NPQ induction and recovery (n = 7-10 plants with near WT levels of RNA).

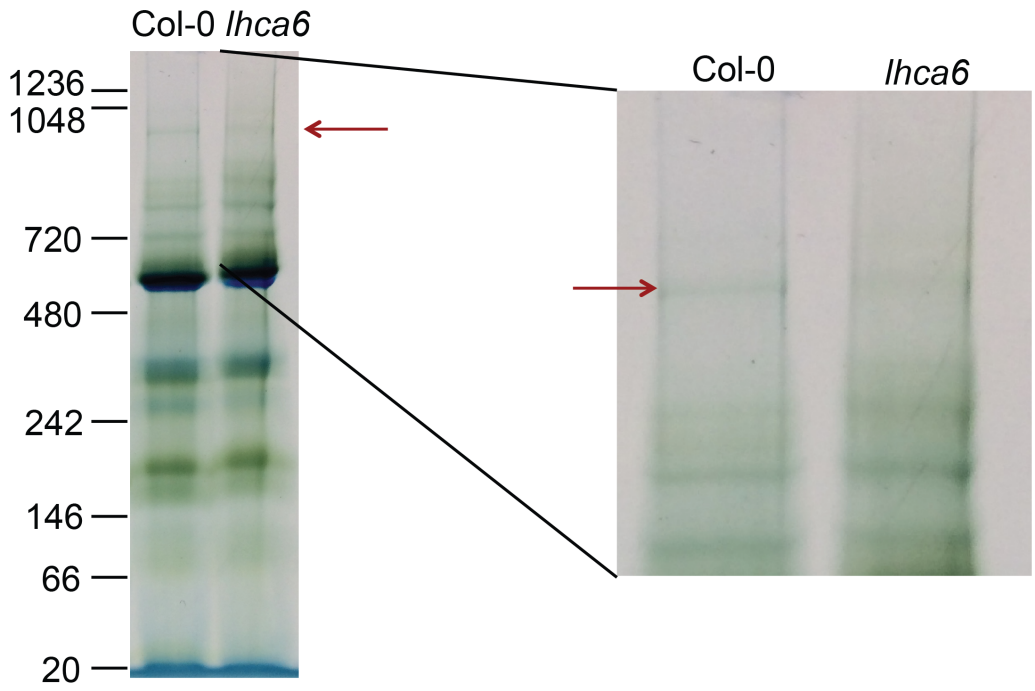

Figure 3.9: Blue native PAGE of WT and *lhca6*.

Red arrow indicates the location of the NDH-PSI supercomplex band. Inset is a closer look at the supercomplex region.

sample was less intense in the H_2O_2 treatment, indicating that there is something other than H_2O_2 triggering that protein oxidation in vivo. In the future, it would be worthwhile to examine these proteins in order to determine if there are differences in the protein oxidation response and to see how many proteins overlap with the HL treatment.

The LC-MS/MS sulfenome confirmed the pattern of increased sulfenylation with HL treatment (Fig. 3.2). The total number of sulfenylated proteins identified after HL treatment doubled when compared to the dark-acclimated sample, and the proteins identified in each condition appear to be mostly unique to that condition. There were 11 proteins that were oxidized in all conditions, which might represent oxidation-susceptible proteins possibly due to post-lysis oxidation during the protein extraction. GO term enrichment analysis showed that in both the LL and HL conditions a majority of the sulfenylated proteins are associated with stress response and redox reactions (Fig. 3.3), which would be expected since there is a lot of evidence that protein oxidation is paramount in both these processes, as discussed in greater detail in the previous chapters. Additionally, both conditions have enrichment in photosynthetic proteins, albeit smaller than some of the other categories. This enrichment may be smaller because of the many other regulatory factors, beyond Cys-SOH regulation, that control photosynthetic efficiency. After HL treatment there was an additional increase in the sulfenylation of proteins involved in protein transportation, phosphorylation, and translation. Each of these categories could play a role in signaling and development of both short term and a long-term light stress response. Regulation of phosphorylation could directly impact retrograde signaling as kinases play an important role in many signaling pathways, an example being the RegB Kinase in *Rhodobacter* (Wu et al., 2013). By changing the translation within the chloroplast, for example through EF-Tu sulfenylation and inactivation (Table 1; Yutthanasirikul et al., 2016), the protein homeostasis in the chloroplast would be changed.

From initial screening, *lhca6* appeared promising for further Cys-SOH regulatory analyses. It has previously been shown that LHCA6 is involved it the formation of the NDH-PSI supercomplex in *A. thaliana,* and it was noted that there was an increase in NPQ when this gene was knocked down by RNAi (Peng et al., 2009). This matches what I saw during my NPQ phenotyping. The NPQ results for the *lhca6* T-DNA line led me to hypothesize that sulfenylation of this protein could be important for its functional regulation. Peng et al. (2009) had shown that this mutant exhibits a reduction in the NDH-dependent chlorophyll fluorescence rebound in the dark, which occurs after a brief low level of illumination, and *lhca6* had an almost complete loss of the NDH-PSI complex band as seen by blue native PAGE. The *lhca6* T-DNA line had a variable amount of *LHCA6* mRNA, ranging from 20-60% of WT over three experiments (Fig. 3.3). Due to the incomplete KO of gene expression in *lhca6,* I analyzed the sequence at the insertion site and found that it occurs very close to the stop codon. This insertion point could allow for a residual level of functional protein to be produced, which would complicate the characterization of this mutant. I was unable reproduce the chlorophyll fluorescence rebound phenotype (data not shown). Peng et al. (2009) saw that there was still a substantial fluorescence rebound in immature leaves, so it is possible that the leaves that I tested were not at full maturity, or the limited and variable reduction in *LHCA6* expression in the T-DNA line might have allowed for formation of the NDH-PSI supercomplex. When I checked the native thylakoid protein complexes and their

abundance by blue native PAGE of WT and the *lhca6* T-DNA line, I did notice a decrease in the band associated with the NDH-PSI complex but not a complete loss (Fig. 3.9). Perhaps this reduction was not enough to completely disrupt the transient fluorescence rebound in the dark. Without an antibody for LHCA6, I was unable to test for protein concentration in *lhca6*. Each complemented line was FLAG-tagged, so an analysis of their protein levels could at least show if the complementation seen is due to the presence of the transgenic insertion, but this has not yet been done.

Despite the uncertainty of the *lhca6* T-DNA line, there is potential for Cys-SOH regulation of LHCA6 during light stress oxidation. There is an NPQ phenotype associated with the *lhca6* T-DNA line, and the recovery of that phenotype was only seen in the *lhca6*+WT and *lhca6*+C58A lines. *lhca6*+C58S showed an NPQ very similar to *lhca6*, even a little higher, which could indicate that the oxidation of this protein might inactivate it or cause the dissociation of the NDH-PSI supercomplex. It is possible then that the increase in NPQ in *lhca6* is due to the redirection of electrons into the PGR5 pathway, thereby increasing that type of PSI cyclic electron flow, which has been shown to increase ΔpH around the thylakoid and therefore increase NPQ (Joliot & Johnson, 2011).

The PrxQ T-DNA line is in a good position for further downstream analysis, because it has been complemented. The mutant affecting PrxQ, a chloroplast-localized peroxiredoxin, showed an increase in total NPQ during the 10-min actinic light test, and studies have shown that PrxQ is important in photosynthesis (Petersson et al., 2006). However, the Cys-SOH in PrxQ is one of the conserved pair that is required for the catalytic activity of this protein (Lamkemeyer et al., 2006). This confirms the importance of the Cys-SOH in this protein function, however the protein would be catalytically inactive if this reaction center cysteine was modified in any way.

Of the other lines only the *atr2* line showed an NPQ phenotype, which could be used to track the Cys-SOH mimic phenotype. Unfortunately this is a large protein with 711 amino acids, and that has made it difficult to complete the site-directed mutagenesis needed to modify the cysteine residue. This has prevented the complementation of that T-DNA insertion line from being completed. The substrate of ATR2 is not known, although it is known to be a CPR-type P450 reductase, of which there are only two identified in *A. thaliana.* This is much less than the 246 P450 reductases in the broader family (Jensen & Møller, 2010). These proteins are known to be involved in multistep electron transfer reactions from NADPH through an FAD and FMN domain in the CPR protein to an acceptor molecule (Munro et al., 2001). The Cys-SOH location is highly conserved and is not directly involved in FAD binding, making this an attractive candidate for further studies.

Finally, *cyp38* could also be an interesting target for future work due to its involvement in PSII assembly (Fu et al., 2007). It was shown that the growth phenotype of the T-DNA line is due to the decrease in the PSII supercomplexes as well as a change in the thylakoid membrane pigment and protein content. If CYP38 is involved in PSII assembly, the regulation of this protein by Cys-SOH modification could affect when this protein is active thereby controlling how much PSII is present during oxidative stress conditions. Unfortunately, the stunted growth phenotype also reduced the germination rate, even with sucrose supplementation, and the total number of inflorescences per plant, making it very difficult to produce sufficient T1 plants. In order

to complete this work many more *cyp38* plants would need to be transformed and screened for complementation. Then, phenotypic analysis of the different cysteine modifications could be examined.

Overall, this work has shown that there is an increase in the chloroplast Cys-SOH profile with increases in light stress, and these oxidized proteins seem to be mostly unique depending of the light condition. Of the selected candidate genes, LHCA6 appears to be a promising protein for further analysis because of the difference in phenotype of the *lhca6*+C58A and *lhca6*+C58S lines. The data suggest that there is some form of regulation occurring at this site, though more work is needed to confirm these results. On a whole this work has established a foundation of potential targets of redox regulation in the chloroplasts and could produce many more interesting results in the years to come.

Materials and methods:

Arabidopsis Growth Conditions

Col-0 *A. thaliana* plants and all T-DNA lines, which are derivatives of Col-0, were grown in a Percival chamber at 50% humidity in a 12/12 hour day/night cycle at 21°C under 100-150µmol photons m^{-2} sec^{-1}. Most T-DNA mutants were grown at 80µmol photons m^{-2} sec^{-1} due to light sensitivity and corresponding Col-0 control plants were grown at that level of light during those experiments. All experiments, except were stated, were done on four week old plants.

Chloroplast Isolation and Protein Extraction

Ten adult leaves, pooled from multiple 4-week-old plants, were cut off the plant, either right before dawn so that the plants would have had the entire night reduce all ROS or after the specified light treatment, and wash with cold water. These leaves were cut into strips and placed into a flacon tube and homogenized in 10ml of homogenizing buffer (0.4 M sorbitol, 5 mM EDTA, 5 mM MgCl2, 10 mM NaHCO3, 0.5% (w/v) BSA and 20 mM Tricine pH 8.4) set to 40% power with 20 0.5-second pulses. The supernatant was filtered through two layers of miracloth and set on ice in the dark. This cycle was repeated two more times. All collected supernatant was pooled and centrifuged at 2,600g for 3 minutes at 4°C. Supernatant was decanted and pellet was suspended into resuspension buffer (0.3 M sorbitol, 2.5 mM EDTA, 5 mM MgCl2, 10 mM NaHCO3, 0.5% (w/v) BSA, 20 mM HEPES pH 7.6) followed by 3 minute centrifugation at 2,600g to wash chloroplasts; wash was repeated 2 more times. 10mM H_2O_2 was added at this point, to the chloroplasts being treated, for the specified amount of time listed above then washed again before dimedone treatment. This washed pellet was resuspended in resuspension buffer with 50mM dimedone and left on ice in the dark for two hours. Chloroplasts were centrifuged at 2,600g for 3 minutes, super was removed and pellet was flash frozen in liquid nitrogen. Chloroplast proteins were solubilized in a lysis buffer (50 mM HEPES, 150 mM NaCl, 1% (vol/vol) Igepal CA-40 and 0.4% SDS) and vortexed for 5 minutes. Samples were centrifuged at max for 10 minutes to pellet unsuspended cell debris. Protease inhibitors, catalase and ETDA were added to all buffers to limit

post-lysis oxidation and iodoacetamide was used to block cysteine thiols. 10µl of sample were vortexed into 80% acetone to determine chlorophyll concentration in a spectrophotometer.

Immunoblot for Cys-SOH

1µg of chlorophyll for each sample was mixed with 5x Laemmli buffer (supplemented with 0.1% β-DM and 0.1M urea) to a final concentration of 1x. Samples were heated to 55°C for 15min. Separated by SDS-PAGE on Any-KD mini-protean TGX gel (Bio-Rad cat#456-9035) at 100V for 60-90 minutes until dye front reaches bottom of gel. Gels were either stained with Coomassie brilliant blue or transferred to .2µm polyvinyl difluoride (PVDF) using Trans-Blot Turbo system (Bio-Rad cat#1704150). 5% non-fat powder milk solution used for blocking and incubated with the following antibodies: α-dimedone antibody as primary and α-rabbit donkey IgG-HRP as secondary. Probe analysis done using SuperSignal West Femto chemiluminescent substrate (Thermo Scientific). Visualization was done in the Bio-Rad Gel Doc XR+ system (#1708195).

LC-MS/MS

Chloroplasts proteins from the three light conditions, dark, low light (100 µmol photons $m^{-2}s^{-1}$) and high light (600 µmol photons $m^{-2}s^{-1}$), were extracted for LC-MS/MS as above either with or without dimedone, as the 16 dalton increase due to oxygenation of a cysteine could be detected in the mass spectrometer. Proteins from both the treated and untreated samples were used for further analysis. All mass spectrum analysis done with Thermo Electron LTQ-Orbitrap XL Hybrid MS with high performance liquid chromatography. Proteins with this mass increase were identified from the dataset mapped to the base proteome from TAIR. Designed a Python script to identify the sulfenylated proteins from the data provided by the Vincent J. Coates proteomics laboratory. The script also blasted each protein against the TAIR *A. thaliana* database to give protein identifications.

The Blast2GO program was used to determine all GO terms for all proteins identified in MS analysis in order to classify the types of proteins enriched in each sample pool. The overall characterization of what biological processes were represented was done using the enrichment and chart builder tools, I set the cut off node values to a minimum of 25 sequences and a greater than 20 on the node distribution score to limit the results to a higher significance.

T-DNA Lines

All lines used in the study were obtained from Arabidopsis Biological Resource Center (ABRC). Seed stock and insertion locus can be found in table 3.2. Confirmation of insertion site done by PCR analysis using the primers in table 3.3.

Table 3.3: Primers used for T-DNA insertion genotyping.

Gene	Primers	
LHCA6	Fw	TACACGGAATCTGTCGCATTCG
	Rev	AGAAGAGTGAAGAGTGATCTTGTCCTT
	Gabi-Kat internal	8474
PrxQ	Fw	GTAGTCATGGAGAAGCACAAAAGC
	Rev	CCCAACTGTAGCAAACAATCTATCAATG
	Sail internal	LB2 short
p450 Reductase	Fw	GAAACTGGAGATCATGTTGGTGTAC
	Rev	CAGTTTTCACTCTTCTCGTAAGGCA
	Salk internal	LBb1.3
Cox6B	Fw	GAGGATCTGATTACACACGAATTAAGC
	Rev	CAAAAGTGGTAAAAGCAAAAGAAAGTCTC
	Salk internal	LBb1.3
Cyp38	Fw	GGATTTATCGATCCAAGCACAGAGA
	Rev	TGTTCTGTTTCCGCCGACAC
	Salk internal	LBb1.3
Psb29	Fw	CGAGTTGAATTCTGATGAATCTTGAGC
	Rev	CCATCTTCTGAGCATCAATTCTGTAC
	Salk internal	LBb1.3
VIPP1	Fw	TGATGGATGCGTCTGTGTTTGT
	Rev	TCTCAGCGCTCCACCTTGTAAAA
	Sail internal	LB2 short

Fluorescence Measurements

All pulse-amplitude-modulated (PAM) fluorometry was done with the Imaging-PAM M4 Maxi series (Walz, Germany) or the FMS2 (Hansatech, Germany) as described in Brooks & Niyogi (2011). Actinic light set to 1200µmol photons $m^{-2}s^{-1}$ to saturate all photosystems. For Imaging PAM, detached leaves were placed in a petri dish on a water soaked paper towel to prevent drying. Area of interest selected based on area of uniformity of each leaf. For FMS2, attached leaves were clipped into the holder. Saturating pulses set to 2500µmol photons $m^{-2}s^{-1}$ in both systems.

qRT-PCR

2-3 fully expanded leaves from 4-week-old Arabidopsis plants were flash frozen in liquid nitrogen then ground with a pellet pestle (Sigma Aldrich #Z359947) for 20 seconds. Total RNA was extracted from leaf material using the Plant RNeasy mini kit (Qiagen cat #74904). Two µg of total RNA was treated with DNAse, then cDNA was synthesized using Omniscript (Qiagen) in a 20µl reaction and diluted 1:5 with nuclease-free water. For selected genes, each sample was assayed in triplicate using 40 ng of cDNA, 500 nM of appropriate primers and iTaq Universal SYBR Green Supermix (Bio-Rad, cat# 1725124) in a 20-µL reaction, with Applied Biosystems 7500 Fast Real Time PCR

system. Gene expression was normalized to endogenous controls Actin 2 (At3g18780). Primers designed to span at least one intron to prevent amplification of genomic DNA. For list of primers used see table 3.4.

Table 3.4: qRT-PCR primers

Gene	Primers	
LHCA6	Fw	GGTTTCGATCCTCTCGGTTTAGGG
	Rev	ACCTAACCGCTCGAGACATTCTG
PrxQ	Fw	AGATGACTCTGCTTCTCACAAGGC
	Rev	TCCCTGGCAATGCTCCAAACAG
Cox6B	Fw	GGTGATGATGCTCCAGAATGCG
	Rev	TGCTCGTTCCACCTATCAACCC
Cyp38	Fw	ACAATGGCAATGGCAAGAGAAGAG
	Rev	AGACAGCGTAACGACCATCCAAG
Psb29	Fw	TCTTTGAATTCGCGTTCCACTTCG
	Rev	TCTGATACAGGAGGCACATCGG
VIPP1	Fw	TCTTGCACGTGAGGCCCTTAAAC
	Rev	TTCAAAGCAGTAGCGTTGTCAGC

Complement Vector and Site Directed Mutagenesis

Gateway cloning vector pEarlyGate 302 was used to produce the transformation vectors. After the BP vectors were cloned, site directed mutagenesis was done (Zheng et al., 2004) on each gene to produce the cysteine-modified versions (See table 3.5 for primers used). Each mutation was confirmed by sequencing, using M13F primer.

Table 3.5: Site-directed mutagenesis primers

Gene	Mod.	Primers	
LHCA6	C58A	F-	CTAGCGTCgccGAACCACTTCCTCCGGACCGTCC
		R-	GTGGTTCggcGACGCTAGAAACTTCTTTGCCGGCACGAAC
	C58S	F-	CTAGCGTCtccGAACCACTTCCTCCGGACCGTCC
		R-	GTGGTTCggaGACGCTAGAAACTTCTTTGCCGGCACGAAC
PrxQ	C116A	F-	GTGTACAACAGGCTgccGCTTTCAGAGACTCTTATGAG
		R-	GAAAGCggcAGCCTGTTGTACACAAGTAAAACCATTTACG
	C116S	F-	GTGTACAACAGGCTtccGCTTTCAGAGACTCTTATGAG
		R-	GAAAGCggaAGCCTGTTGTACACAAGTAAAACCATTTACG
ATR2	C602A	F-	CTTTGGAtgcAGAAACCGTAGAATGGTAATAAAGCC
		R-	GTTTCTgcaTCCAAAGAACAAAACTGATGGCCCAAG
	C602S	F-	CTTTGGAtgcAGAAACCGTAGAATGGTAATAAAGCC
		R-	GTTTCTgcaTCCAAAGAACAAAACTGATGGCCCAAG
Cox6B	C147A	F-	CAGAgccGTAGCTGCTAAGGGTGATGATGCTCCAG
		R-	GCAGCTACggcTCTGCATATTTGAAAACAATCAGAAAACTTAAC

	C147S	F-	CAGAtccGTAGCTGCTAAGGGTGATGATGCTCCAG
		R-	GCAGCTACggaTCTGCATATTTGAAAACAATCAGAAAACTTAAG
Cyp38	C28A	F-	GTTTTTCTgccTCCAAAAAGCCCCTCGAAGTTCGTTG
		R-	CTTTTTGGAggcAGAAAAACCGATTCTTCTTCTGGG
	C28S	F-	GTTTTTCTtccTCCAAAAAGCCCCTCGAAGTTCGTTG
		R-	CTTTTTGGAggaAGAAAAACCGATTCTTCTTCTGGG
Psb29	C284A	F-	CTCCAAGgccCTGGGAGATACTCTATATAACCCATCTTTC
		R-	CTCCCAGggcCTTGGAGATTGTTTCGTTAGCCTTC
	C284S	F-	CTCCAAGtccCTGGGAGATACTCTATATAACCCATCTTTC
		R-	CTCCCAGggaCTTGGAGATTGTTTCGTTAGCCTTC
VIPP1	C65A	F-	CTCAGGgccAATGGTCATGGTGCTACTATGAATC
		R-	GACCATTggcCCTGAGTCTATTATCACAAGCTAATCTC
	C65S	F-	CTCAGGtccAATGGTCATGGTGCTACTATGAATC
		R-	GACCATTggaCCTGAGTCTATTATCACAAGCTAATCTC

Lower case letters indicate codon modification site.

Transformation of *A. thaliana*

Primary inflorescence of each tDNA line were cut back just above the first node at least one time to increase floral branching before transformation. Floral dipping of developing buds was completed following the protocols in (Clough and Bent, 1998). T1 plants were selected on MS BASTA (10μM/ml) plates with 1% sucrose supplement.

Chlorophyll Fluorescent Rebound

Transient rebound of chlorophyll fluorescence done as in Shikanai et al., 1998 with minor modifications. I used the FMS2 system with white actinic light fiber optics and used an actinic light level of 50μmol photons $m^{-2}s^{-1}$.

Thylakoid Isolation and Blue Native PAGE

Thylakoid isolation and blue native PAGE was done as in Peng et al., 2009.

Acknowledgements:

This work was supported by the U.S. Department of Energy, Office of Science, Basic Energy Sciences, Chemical Sciences, Geosciences, and Biosciences Division under field work proposal 449B. This work used the Vincent J. Proteomics/Mass Spectrometry Laboratory at UC Berkeley, supported in part by NIH S10 Instrumentation Grant S10RR025622.

Reference:

Brooks, M.D., and Niyogi, K.K. (2011). Use of a pulse-amplitude modulated chlorophyll fluorometer to study the efficiency of photosynthesis in Arabidopsis plants. Methods Mol. Biol. 775, 299–310.

Buchanan B, Kalberer P, Arnon D. 1967. Ferredoxin-activated fructose diphosphatase in isolated chloroplasts. Biochem Biophys Res Comm 29: 74–9.

Cheng Z, Wu J, Setterdahl A, Reddie K, Carroll K, Hammad LA, et al. 2012. Activity of the tetrapyrrole regulator CrtJ is controlled by oxidation of a redox active cysteine located in the DNA binding domain. Molecular Microbiology, 85(4), 734–746.

Clough SJ & Bent AF. 1998. Floral dip: a simplified method for Agrobacterium-mediated transformation of Arabidopsis thaliana. The plant J, 16 (6), 735-743.

Fu A, He Z, Cho HS, Lima A, Buchanan BB & Luan S. 2007. A chloroplast cyclophilin functions in the assembly and maintenance of photosystem II in Arabidopsis thaliana. PNAS, 104(40), 15947-15952.

Furdui CM and Poole LB. 2013. Chemical approaches to detect and analyze protein sulfenic acids. *Mass Spectrom Rev.* 33:126-46.

Goto K, Holler M, Okazaki R. 1997. Synthesis, structure, and reactions of a sulfenic acid bearing a novel bowl-type substituent: the first synthesis of a stable sulfenic acid by direct oxidation of a thiol. J. Am. Chem. Soc. 119: 1460-1461

Gupta V & Carroll KS. 2014. Sulfenic acid chemistry, detection and cellular lifetime. BBA. 1840 (2), 847-875.

Haber E, Anfinsen CB. 1962. Side-chain interactions governing the pairing of half-cystine residues in ribonuclease. J Biol Chem., 237, 1839–1844.

Jensen K & Møller BL. 2010. Plant NADPH-cytochrome P450 oxidoreductases. Phytochemistry 71, 132–141.

Joliot P, & Johnson GN. 2011. Regulation of cyclic and linear electron flow in higher plants. Proceedings of the National Academy of Sciences of the United States of America, 108(32), 13317–13322.

Keren N, Ohkawa H, Welsh EA, Liberton M & Pakrasi HB. 2005. Psb29, a Conserved 22-kD Protein, Functions in the Biogenesis of Photosystem II Complexes in Synechocystis and Arabidopsis. The Plant Cell, 17 (10), 2768-2781.

Kroll D, Meierhoff K, Bechtold N, Kinoshita M, Westphal S, Vothknecht UC, Soll J & Westhoff P. 2001. VIPP1, a nuclear gene of Arabidopsis thaliana essential for thylakoid membrane formation. PNAS, 98 (7), 4238-4242.

Lamkemeyer P, Laxa M, Collin V, Li W, Finkemeier I, Schöttler MA, Holtkamp V, Tognetti VB, Issakidis-Bourguet E, Kandlbinder A, Weis E, Miginiac-Maslow M, & Dietz KJ. 2006. Peroxiredoxin Q of Arabidopsis thaliana is attached to the thylakoids and functions in context of photosynthesis. Plant J, 45, 968–981.

Miller H & Claiborne A. 1991. Peroxide modification of monoalkylated glutathione reductase. Stabilization of an active-site cysteine-sulfenic acid. J. Biol. Chem. 266, 19342-19350.

Munro AW, Noble MA, Robledo L, Daff SN & Chapman SK. 2001. Determination of the redox properties of human NADPH-cytochrome P450 reductase. Biochemistry, 40, 1956–1963.

Peng L, Fukao Y, Fujiwara M, Takami T, & Shikanai T. 2009. Efficient operation of NAD(P)H dehydrogenase requires supercomplex formation with photosystem I via minor LHCI in Arabidopsis. *The Plant Cell Online*, *21*(11), 3623–3640.

Petersson UA, Kieselbach T, García-Cerdán JG, & Schröder WP. 2006. The PrxQ protein of Arabidopsis thaliana is a member of the luminal chloroplast proteome. FEBS Lett, 580, 6055–6061.

Shikanai T, Endo T, Hashimoto T, Yamada Y, Asada K, & Yokota A. 1998. Directed disruption of the tobacco ndhB gene impairs cyclic electron flow around photosystem I. PNAS, 95(16), 9705–9709.

Tripolt R, Belaj F, Nachbaur E. 1993. Unexpectedly stable sulfenic acid—4,6-dimethoxy-1,3,5-triazine-2-sulfenic acid—synthesis, properties, molecular and crystal-structure. Z. Naturforsch., B: Chem. Sci. 48: 1212-22.

Waszczak C, Akter S, Eeckhout D, Persiau G, Wahni K, Bodra N, et al. 2014. Sulfenome mining in Arabidopsis thaliana. PNAS, 111(31), 11545–11550.

Yutthanasirikul R, Nagano T, Jimbo H, Hihara Y, Kanamori T, Ueda T, et al. 2016. Oxidation of a Cysteine Residue in Elongation Factor EF-Tu Reversibly Inhibits Translation in the Cyanobacterium Synechocystis sp. PCC 6803. *Journal of Biological Chemistry*, *291*(11), 5860–5870.

Zheng, L., U. Baumann, and Jean-Louis Reymond. 2004. An efficient one-step site-directed and site-saturation mutagenesis protocol. Nucleic Acids Res. 2004; 32(14): e115.

CHAPTER 4

CONCLUSIONS

Throughout any given day, plants and algae experience great fluctuations in irradiance as the sun rises higher into the sky, shadows move, clouds pass, or turbidity changes their position within the water column. For situations where light intensity increases above what can be used for photosynthesis, these organisms have evolved ways to dissipate excess absorbed light energy by non-photochemical quenching (NPQ) pathways (Müller et al., 2001). However, nothing in biology is perfect, and some of this excess energy ends up generating reactive oxygen species (ROS; Foyer and Shigeoka, 2011). ROS and the other reactive species discussed in Chapter 1, can oxidize many cellular components, causing oxidative damage (Villamena, 2017) or regulatory changes in proteins via the cysteine sulfenic acid (Cys-SOH) state. In Chapter 1, I discussed how this state can form and how it can act as an intermediate step in many redox reactions (reviewed in Yang, 2016) and how in a few examples a stable Cys-SOH was itself the end product in a regulatory pathway (Cheng et al., 2012; Wu et al., 2013). Although regulation involving stable Cys-SOH has been shown in bacteria, yeast, and mammals, it has not been well examined in eukaryotic photosynthetic organisms. This was the first time that a stable Cys-SOH was seen to have regulatory roles in a photosynthetic eukaryotic organism.

LHCX1 in *N. oceanica* is one of the primary proteins involved in qE, the rapidly reversible type of NPQ (Lyska et al., 2018). In conjunction with VDE, LHCX1 is responsible for essentially all of the qE in the cell and, based on the evidence detailed in Chapter 2, when absent or overexpressed it can change the dynamics of slowly reversible qZ as well. Thus, LHCX1 appears to be the switching box for *N. oceanica's* reaction to excess light, especially in the first tens of minutes. In Chapter 2, I showed that this switch box mechanism is regulated by the oxidation of a single cysteine (C162) located in the stromal loop of this protein, which I identified in a global proteomic analysis of Cys-SOH in *N. oceanica*. When this cysteine is modified to a serine (C162S) to mimic the Cys-SOH state, the NPQ response of the cell is shifted to the more slowly relaxing qZ type. In the wild type or a complemented *lhcx1* line (*lhcx1*+WT), this qZ type of quenching only begins to reach the level of C162S when the actinic high light period was extended to 20 min. This increase in light duration presumably allows for build up of oxidants that could then oxidize the C162 residue in LHCX1 to Cys-SOH. Based on protein structure modeling, I hypothesize that oxidation of C162 causes a change in the pigment binding affinity of LHCX1 that redirects zeaxanthin to qZ sites. When oxidation of this cysteine is blocked by mutation to alanine (C162A), the increase in qZ does not occur. Physiologically, oxidation of LHCX1, after a prolonged amount of time, could change the cellular NPQ response in order to protect the cell longer term. However, the relatively slow oxidation of LHCX1 and activation of qZ quenching could prevent this more slowly relaxing NPQ from building up when *N. oceanica* is only briefly exposed to excess light. Thus, this two-step NPQ regulation would help the organism respond appropriately to different light conditions.

In Chapter 3, the sulfenome of *A. thaliana* chloroplasts was analyzed to identify the Cys-SOH modifications that occur during a 1-h period of excess light. Similar to

what was seen in *N. oceanica*, overall protein sulfenylation increased with high light treatment. Also, the protein Cys-SOH profiles seemed to differ greatly between the three light conditions: dark, low light (LL) and high light (HL). As would be expected, proteins associated with photosynthesis, redox reactions, and stress response were enriched in both LL and HL samples. Interestingly, the HL sample had additional Cys-SOH enrichment in proteins involved in translation, protein transport, and phosphorylation, some of which might be involved in downstream longer term reactions to excess light.

The most promising candidate containing Cys-SOH was LHCA6. I analyzed a T-DNA knockdown line (*lhca6*) in which the insertion occurred in the 3' UTR of the gene. An almost complete knockdown of this protein has been shown previously to enhance the NPQ in *A. thaliana* as well as reduce the size of the NDH-PSI supercomplex (Peng et al., 2009). The NPQ phenotype of *lhca6* showed a similar increase in the total NPQ, and when the native complexes were examined it had a reduction, though not a complete loss, of the NDH-PSI supercomplex. Stable transgenic lines were made that express the wild-type *LHCA6* gene or either of two modified versions: cysteine to alanine (*lhca6*+C58A) and cysteine to serine (*lhca6*+C58S). Interestingly, there was a difference in rescue of the wild-type level of NPQ between the modified versions, which suggests oxidative regulation of LHCA6 by Cys-SOH. In the *lhca6*+C58A line there was a complete rescue to WT NPQ, but in the *lhca6*+C58S line there was an increased NPQ capacity, which resembled the *lhca6* NPQ. This could indicate that the oxidation at C58 inactivates the protein and that is why the Cys-SOH mimic, *lhca6*+C58S, acts like the knockdown line, whereas the *lhca6*+C58A line, in which LHCA6 cannot be oxidized, remains active. These experiments should be repeated with a confirmed knockout mutant of LHCA6. There are also other target protein KO lines, such as *atr2*, that were promising and could be pursued in the future. This leaves the question open of whether or not Cys-SOH can be a stable regulator of proteins in *A. thaliana*, although I think the work done here has gotten us closer to an answer.

Overall, the work detailed in this dissertation has expanded the knowledge of what proteins can be oxidized in excess light conditions in both *N. oceanica* and in *A. thaliana*. Additionally, I have shown that LHCX1 in *N. oceanica* is regulated by protein oxidation and that this oxidation changes the NPQ response of the cell, possibly through a change in pigment-binding affinity. As with most scientific experiments, answers to one question open the door to many more questions. Is the oxidation directed by ROS or some other oxidant? Is C162 oxidation reversible? If so, is it done through a Trx type mechanism? Does the pigment binding of the carotenoid associated with the cysteine undergo affinity changes? Despite the remaining questions, the work described here provides strong evidence of a stable Cys-SOH regulating protein function in a photosynthetic eukaryotic organism.

References

Cheng Z, Wu J, Setterdahl A, Reddie K, Carroll K, Hammad LA, et al. 2012. Activity of the tetrapyrrole regulator CrtJ is controlled by oxidation of a redox active cysteine located in the DNA binding domain. Molecular Microbiology, 85(4), 734–746.

Foyer CH, & Shigeoka S. 2011. Understanding oxidative stress and antioxidant functions to enhance photosynthesis. *Plant Phys*, *155*, 93–100.

Müller P, Li XP, & Niyogi KK. 2001. Non-photochemical quenching. A response to excess light energy. Plant Phys, 125(4), 1558–1566.

Peng L, Fukao Y, Fujiwara M, Takami T, & Shikanai T. 2009. Efficient operation of NAD(P)H dehydrogenase requires supercomplex formation with photosystem I via minor LHCI in Arabidopsis. The Plant Cell Online, 21(11), 3623–3640.

Villamena FA. 2017. Chapter 2- Chemistry of Reactive Species. Reactive species detection in biology, 12-64.

Wu J, Cheng Z, Reddie K, Carroll K, Hammad LA, Karty JA, & Bauer CE. 2013. RegB Kinase Activity Is Repressed by Oxidative Formation of Cysteine Sulfenic Acid. Journal of Biological Chemistry, 288(7), 4755–4762.

Yang Y. 2016. Chapter 9- peptide oxidation/reduction side reactions. Side reactions in peptide synthesis. Academic press. 217-233.

Appendix A

Full list of Cys-SOH modified proteins from *N. oceanica*

All repeat sequences were removed for clarity. This list is all of the proteins identified from at least one LC-MS/MS run, based on either the dimedone label or oxygen mass shift.

Table A1: Dark-treated cells

Protein ID	Description	Cys-SOH position(s)
Chloroplast - Photosynthesis		
gene_petJ	cytochrome c6, chloroplastic isoform X1	49
NannoCCMP1779_10579	diaminopimelate epimerase, chloroplastic	53
NannoCCMP1779_10595	heme-binding-like protein At3g10130, chloroplastic	15
NannoCCMP1779_11475	violaxanthin de-epoxidase, chloroplastic	58
NannoCCMP1779_2084	ferredoxin--NADP reductase, embryo isozyme, chloroplastic	135;499;640
NannoCCMP1779_2235	4-hydroxy-3-methylbut-2-en-1-yl diphosphate synthase (ferredoxin)	125;155
NannoCCMP1779_3236	glyceraldehyde-3-phosphate dehydrogenase	297
NannoCCMP1779_349	RuBisCO large subunit-binding protein subunit beta, chloroplastic	75
NannoCCMP1779_3819	RuBisCO large subunit-binding protein subunit alpha	168
NannoCCMP1779_440	divinyl chlorophyllide a 8-vinyl-reductase, chloroplastic	198
NannoCCMP1779_4980	fructose-1,6-bisphosphatase, chloroplastic	1083
NannoCCMP1779_501	zeta-carotene desaturase, chloroplastic/chromoplastic	235
NannoCCMP1779_5425	D-3-phosphoglycerate dehydrogenase 2, chloroplastic	38
NannoCCMP1779_6650	protochlorophyllide reductase-like	112
NannoCCMP1779_688	photosynthetic NDH subunit of subcomplex B 3, chloroplastic	110
NannoCCMP1779_7696	D-3-phosphoglycerate dehydrogenase 2, chloroplastic	38
NannoCCMP1779_8134	pheophorbide a oxygenase, chloroplastic	480
NannoCCMP1779_9007	geranylgeranyl diphosphate synthase	114
Chloroplast - Biosynthesis		
NannoCCMP1779_10581	6,7-dimethyl-8-ribityllumazine synthase, chloroplastic	64
NannoCCMP1779_1488	acetylornithine aminotransferase, chloroplastic/mitochondrial	27
NannoCCMP1779_4978	ferredoxin-dependent glutamate synthase, chloroplastic	136;992
NannoCCMP1779_5694	glutamate--glyoxylate aminotransferase 2	229
NannoCCMP1779_6045	glutamate--tRNA ligase, cytoplasmic-like	774
NannoCCMP1779_6382	dihydrolipoyl dehydrogenase 2, chloroplastic-like	104
NannoCCMP1779_6649	protein ABCI7, chloroplastic	441
NannoCCMP1779_7110	LL-diaminopimelate aminotransferase, chloroplastic isoform X2	628
NannoCCMP1779_7147	enolase	97
NannoCCMP1779_923	carbamoyl-phosphate synthase large chain, chloroplastic	787;1310

Chloroplast - Metabolism

NannoCCMP1779_10574	pyruvate dehydrogenase E1 component subunit alpha-3, chloroplastic	228
NannoCCMP1779_11838	ATP-dependent zinc metalloprotease FTSH, chloroplastic	355
NannoCCMP1779_2758	Double Clp-N motif- P-loop nucleoside triphosphate hydrolase	51
NannoCCMP1779_3874	ATP-dependent Clp protease proteolytic subunit-related protein 4	184
NannoCCMP1779_6032	pyruvate orthophosphate dikinase	95
NannoCCMP1779_6562	malonyl CoA-acyl carrier protein transacylase	334
NannoCCMP1779_6748	transketolase, chloroplastic	330

Chloroplast - Translation

gene_rpl18	50S ribosomal protein L18, chloroplastic-like	38
gene_rpl6	50S ribosomal protein L6, chloroplastic	40
gene_rps12	ribosomal protein S12 (chloroplast)	34
NannoCCMP1779_3281	30S ribosomal protein S1, chloroplastic	380
NannoCCMP1779_3598	60S ribosomal protein L10-like	48
NannoCCMP1779_5424	translation initiation factor IF-2, chloroplastic	338
NannoCCMP1779_5435	28 kDa ribonucleoprotein, chloroplastic	65
NannoCCMP1779_5596	Chaperone protein DnaJ	188
NannoCCMP1779_6381	elongation factor G-2, chloroplastic	195;266;458
NannoCCMP1779_7784	pentatricopeptide repeat-containing protein At2g31400, chloroplastic	256
NannoCCMP1779_7868	pentatricopeptide repeat-containing protein At4g19890	197

Chloroplast – Redox Reactions

NannoCCMP1779_11663	glutathione reductase, chloroplastic-like	111;185
NannoCCMP1779_11851	nicotinate phosphoribosyltransferase 2-like	1320
NannoCCMP1779_1998	plastidic ATP/ADP-transporter-like	49;371
NannoCCMP1779_2067	1-deoxy-D-xylulose 5-phosphate reductoisomerase, chloroplastic	72
NannoCCMP1779_344	pyridoxal reductase, chloroplastic	351
NannoCCMP1779_4766	glutathione reductase, chloroplastic	89
NannoCCMP1779_6931	peroxiredoxin-2E-2, chloroplastic	92
NannoCCMP1779_8455	Peroxiredoxin-2E-1, chloroplastic	108
NannoCCMP1779_8696	2-Cys peroxiredoxin BAS1, chloroplastic	284

Chloroplast - Other

NannoCCMP1779_10312	NAD(P)-binding rossmann-fold protein	120
NannoCCMP1779_10332	uncharacterized aarF domain-containing protein kinase	910
NannoCCMP1779_10827	short-chain dehydrogenase TIC 32, chloroplastic-like isoform X1	391
NannoCCMP1779_1808	phosphoglycerate kinase	78

NannoCCMP1779_1996	thylakoid membrane protein slr0575	72;104
NannoCCMP1779_3273	phosphoglycerate kinase, chloroplastic	77;367
NannoCCMP1779_6637	UDP-sulfoquinovose synthase, chloroplastic	125

Mitochondrion

NannoCCMP1779_10056	succinate dehydrogenase [ubiquinone] flavoprotein subunit, mitochondrial	184
NannoCCMP1779_11349	D-lactate dehydrogenase [cytochrome], mitochondrial isoform X2	262
NannoCCMP1779_11811	serine hydroxymethyltransferase 2, mitochondrial	99
NannoCCMP1779_1590	electron transfer flavoprotein subunit beta, mitochondrial	78
NannoCCMP1779_2497	NADH dehydrogenase [ubiquinone] 1 alpha subcomplex subunit 8-B-like	109
NannoCCMP1779_3052	succinate--CoA ligase [ADP-forming] subunit beta, mitochondrial	128
NannoCCMP1779_4346	aspartate aminotransferase, mitochondrial	351
NannoCCMP1779_4352	glycine--tRNA ligase, mitochondrial 1	528
NannoCCMP1779_4381	mitochondrial phosphate carrier protein 3, mitochondrial-like	5;74
NannoCCMP1779_4707	CLP protease regulatory subunit CLPX3, mitochondrial	127
NannoCCMP1779_4847	mitochondrial 28S ribosomal protein S29-related	507
NannoCCMP1779_6537	NADH dehydrogenase [ubiquinone] iron-sulfur protein 1, mitochondrial-like	584
NannoCCMP1779_6999	dihydrolipoyllysine-residue acetyltransferase of pyruvate dehydrogenase complex	59;636
NannoCCMP1779_7944	FUMARASE 2	185
NannoCCMP1779_7991	pentatricopeptide repeat-containing protein At2g15630, mitochondrial-like	266
NannoCCMP1779_8141	succinyl-CoA ligase [ADP-forming] subunit alpha-1, mitochondrial	165
NannoCCMP1779_8242	heat shock 70 kDa protein, mitochondrial	358
NannoCCMP1779_829	chaperonin CPN60-2, mitochondrial	125
NannoCCMP1779_9764	succinate dehydrogenase [ubiquinone] iron-sulfur subunit 1, mitochondrial-like	197;251
NannoCCMP1779_9984	ATP synthase subunit beta, mitochondrial	111

Transmembrane system

NannoCCMP1779_10128	Phosphatidylinositol:ceramide inositolphosphotransferase	136
NannoCCMP1779_10721	puromycin-sensitive aminopeptidase isoform X2	919
NannoCCMP1779_11004	lactoylglutathione lyase isoform X1	77
NannoCCMP1779_11360	ABC transporter E family member 2	31;48
NannoCCMP1779_11367	auxin efflux carrier family protein	425
NannoCCMP1779_11499	dnaJ protein ERDJ3B	183
NannoCCMP1779_11688	ABC transporter G family member 15-like	245
NannoCCMP1779_125	heme-binding protein 2	277
NannoCCMP1779_16	probable protein disulfide-isomerase A6	39;57
NannoCCMP1779_1655	signal recognition particle subunit SRP68	530
NannoCCMP1779_2320	vacuolar-sorting receptor 5	131

NannoCCMP1779_236	O-acyltransferase WSD1	221
NannoCCMP1779_2568	Tetratricopeptide repeat (TPR)-like superfamily protein	70
NannoCCMP1779_2640	---NA---	78
NannoCCMP1779_3187	phosphoinositide phosphatase SAC6	225
NannoCCMP1779_3350	ABC transporter C family member 2-like	646
NannoCCMP1779_3541	auxin transport protein BIG	471
NannoCCMP1779_356	---NA---	22
NannoCCMP1779_4091	calcium-transporting ATPase 4, endoplasmic reticulum-type	935
NannoCCMP1779_4499	---NA---	161;264;270
NannoCCMP1779_4689	squalene synthase-like	566;630
NannoCCMP1779_5740	S-adenosyl-L-methionine-dependent methyltransferase	13
NannoCCMP1779_6355	sphingosine-1-phosphate lyase	32;373
NannoCCMP1779_6395	6-phosphogluconate dehydrogenase, decarboxylating	413
NannoCCMP1779_6720	6-deoxyerythronolide-b synthase erya1, modules 1 and 2	353;359
NannoCCMP1779_7244	26S proteasome non-ATPase regulatory subunit 10	307
NannoCCMP1779_7486	calcium-transporting ATPase 4, endoplasmic reticulum-type-like	318;367
NannoCCMP1779_7589	putative acyltransferase	281
NannoCCMP1779_7851	plasma membrane atpase 1	48
NannoCCMP1779_7922	---NA---	342
NannoCCMP1779_7943	V-type proton ATPase subunit d2	135
NannoCCMP1779_7978	---NA---	34
NannoCCMP1779_8188	GTP-binding nuclear protein Ran-3	109
NannoCCMP1779_9051	---NA---	42
NannoCCMP1779_9383	endoplasmin homolog	55
NannoCCMP1779_9544	---NA---	1876

Nucleus

NannoCCMP1779_10260	actin-related protein 4	403
NannoCCMP1779_10745	DNA-directed RNA polymerase II subunit 1	125
NannoCCMP1779_10747	CCR4-NOT transcription complex subunit 3-like isoform X2	100
NannoCCMP1779_11356	splicing factor 3b subunit 1	1063
NannoCCMP1779_11494	transcription factor GTE12-like	345;443
NannoCCMP1779_11597	pre-mRNA-splicing factor ATP-dependent RNA helicase DEAH7	827
NannoCCMP1779_177	eukaryotic initiation factor 4A-15-like	165
NannoCCMP1779_2959	importin subunit alpha-1-like	134
NannoCCMP1779_34	lysine-specific demethylase rbr-2	1606;1648
NannoCCMP1779_3497	nuclear cap-binding protein subunit 2	75
NannoCCMP1779_35	DNA-directed RNA polymerase I subunit 1	10;498
NannoCCMP1779_444	protein CHROMATIN REMODELING 5	92
NannoCCMP1779_4642	Proteasome subunit alpha type-7	93
NannoCCMP1779_518	transformation/transcription domain-associated protein-like	2352;2354;2358

NannoCCMP1779_6242	Pre-mRNA-splicing factor SLU7-A	402
NannoCCMP1779_7040	30-kDa cleavage and polyadenylation specificity factor 30	4;97
NannoCCMP1779_7750	DNA polymerase epsilon catalytic subunit A-like	1520
NannoCCMP1779_8165	DNA-directed RNA polymerase II subunit RPB2	1074
NannoCCMP1779_817	UDP-glucose 6-dehydrogenase 1	10;110;113
NannoCCMP1779_8795	AMP-dependent synthetase/ligase	298
NannoCCMP1779_8806	Cell division control protein 48 homolog D	728
NannoCCMP1779_9716	transcription factor DIVARICATA-like	187

Cytosol - Biosynthesis

NannoCCMP1779_102	tryptophan synthase beta chain 1	681
NannoCCMP1779_10387	peptidyl-prolyl cis-trans isomerase	159
NannoCCMP1779_11453	S-adenosyl-l-homocysteine hydrolase A	30;249
NannoCCMP1779_11841	UDP-sugar pyrophosphorylase	381
NannoCCMP1779_11859	KH domain-containing protein At4g18375 isoform X2	235
NannoCCMP1779_1506	glutamate decarboxylase-like	184
NannoCCMP1779_1597	Dihydrolipoyllysine-residue succinyltransferase	309
NannoCCMP1779_1866	aminopeptidase M1-like	589
NannoCCMP1779_1978	long chain base biosynthesis protein 1	172
NannoCCMP1779_2450	rab family GTPase	26
NannoCCMP1779_274	bifunctional protein FolD 2	158
NannoCCMP1779_3124	UDP-sugar pyrophosphorylase	470
NannoCCMP1779_3241	alpha,alpha-trehalose-phosphate synthase [UDP-forming] 1-like	347
NannoCCMP1779_4001	long chain acyl-CoA synthetase 6, peroxisomal-like	177
NannoCCMP1779_5117	UDP-glucose 4-epimerase GEPI48	95
NannoCCMP1779_512	3-oxoacyl-[acyl-carrier-protein] reductase 4	63
NannoCCMP1779_5344	bifunctionalglutamate/aspartate-prephenate aminotransferase	195
NannoCCMP1779_5917	probable ribose-5-phosphate isomerase 2	161
NannoCCMP1779_6291	OTU domain-containing protein 5-B	6

Cytosol - Redox reactions

NannoCCMP1779_10922	probable aldehyde dehydrogenase isoform X2	25
NannoCCMP1779_1155	uncharacterized oxidoreductase At4g09670-like	98
NannoCCMP1779_11753	inosine-5'-monophosphate dehydrogenase 2	254
NannoCCMP1779_1473	---NA---	269
NannoCCMP1779_1692	probable mannitol dehydrogenase	99
NannoCCMP1779_2044	inosine-5'-monophosphate dehydrogenase 2	254
NannoCCMP1779_2814	---NA---	254
NannoCCMP1779_3107	oxidoreductase, putative	128
NannoCCMP1779_4405	peptide methionine sulfoxide reductase B5-like	185
NannoCCMP1779_4448	uncharacterized oxidoreductase At4g09670-like	220
NannoCCMP1779_6256	prostamide/prostaglandin F synthase	33

NannoCCMP1779_7921	alcohol dehydrogenase 1	426;616
NannoCCMP1779_8891	NADP-specific glutamate dehydrogenase-like isoform X1	193
NannoCCMP1779_9838	retinol dehydrogenase 11	184

Cytosol - Chaperones

NannoCCMP1779_10394	dnaJ protein homolog	242
NannoCCMP1779_11734	heat shock 70 kDa protein	105
NannoCCMP1779_1223	chaperone protein ClpB1	106
NannoCCMP1779_275	hsp70-Hsp90 organizing protein 3-like	452;499
NannoCCMP1779_3186	dnaJ homolog subfamily B member 13 isoform X2	327
NannoCCMP1779_5366	heat shock protein 83	339
NannoCCMP1779_7349	chaperone protein clpb1	355
NannoCCMP1779_7535	chaperone protein ClpB1	78
NannoCCMP1779_7880	heat shock protein 83	121

Cytosol - Phosphorylation

NannoCCMP1779_10476	ATP-dependent 6-phosphofructokinase 3 isoform X2	291
NannoCCMP1779_10959	calcium-dependent protein kinase 11	291
NannoCCMP1779_11308	calcium-dependent protein kinase 24-like	333
NannoCCMP1779_3202	eIF-2-alpha kinase activator GCN1	748
NannoCCMP1779_3263	serine/threonine-protein kinase Nek6-like	357
NannoCCMP1779_5795	nucleoside diphosphate kinase 1	60
NannoCCMP1779_6821	phosphoenolpyruvate carboxykinase [ATP]-like	139

Other

NannoCCMP1779_11340	polyadenylate-binding protein 4-like	136
NannoCCMP1779_11914	aspartate-semialdehyde dehydrogenase	9
NannoCCMP1779_1288	40S ribosomal protein S5	83
NannoCCMP1779_1599	Cullin-1	1094
NannoCCMP1779_207	proline--tRNA ligase, cytoplasmic	212
NannoCCMP1779_2194	60S ribosomal protein L7a-1	210
NannoCCMP1779_2255	H/ACA ribonucleoprotein complex subunit 4	125
NannoCCMP1779_3275	cysteine synthase	338
NannoCCMP1779_4039	alpha,alpha-trehalose-phosphate synthase [UDP-forming] 5	449
NannoCCMP1779_4343	probable nucleoredoxin 1	371
NannoCCMP1779_441	40S ribosomal protein S10-1	980
NannoCCMP1779_4637	DEAD-box ATP-dependent RNA helicase 51	445
NannoCCMP1779_4644	Phosphoglycerate kinase, cytosolic	172
NannoCCMP1779_4979	transmembrane 9 superfamily member 2-like	448
NannoCCMP1779_5187	T-complex protein 1 subunit delta	177
NannoCCMP1779_5939	galactokinase	46;91
NannoCCMP1779_6580	eukaryotic translation initiation factor 3 subunit a	89
NannoCCMP1779_668	leucine aminopeptidase 1-like	446

NannoCCMP1779_6818	eukaryotic translation initiation factor 2 subunit gamma-like	72;417
NannoCCMP1779_6819	glutamine synthetase	102;104;120
NannoCCMP1779_7085	serine--tRNA ligase-like	360
NannoCCMP1779_7263	60S ribosomal protein L28-1-like	9;15
NannoCCMP1779_7414	60s ribosomal protein l11	21
NannoCCMP1779_7418	putative transaldolase-like	249
NannoCCMP1779_7491	casein lytic proteinase B3	403
NannoCCMP1779_7580	formate--tetrahydrofolate ligase	387
NannoCCMP1779_8189	cytosolic Fe-S cluster assembly factor NBP35	35
NannoCCMP1779_8561	beta-adaptin-like protein B	307
NannoCCMP1779_8715	tubulin beta chain	234;313;315
NannoCCMP1779_8740	monothiol glutaredoxin-S17	297
NannoCCMP1779_9086	actin-1	278
NannoCCMP1779_937	eukaryotic translation initiation factor 5-like	121;130
NannoCCMP1779_9913	proteasome subunit alpha type-6-B	137

Hypothetical Proteins

NannoCCMP1779_10341	---NA---	68
NannoCCMP1779_10814	---NA---	136;312
NannoCCMP1779_10886	---NA---	545
NannoCCMP1779_11446	---NA---	337;362
NannoCCMP1779_199	carbon catabolite repressor protein 4 homolog 1-like isoform X1	90;96;99
NannoCCMP1779_2086	---NA---	317
NannoCCMP1779_2452	guanine nucleotide-binding protein subunit beta-like protein	148;192
NannoCCMP1779_2626	---NA---	382
NannoCCMP1779_3183	---NA---	46;75;78
NannoCCMP1779_3873	---NA---	134
NannoCCMP1779_4339	---NA---	189
NannoCCMP1779_5095	---NA---	239
NannoCCMP1779_541	---NA---	9
NannoCCMP1779_5550	---NA---	145
NannoCCMP1779_5637	---NA---	71
NannoCCMP1779_5830	---NA---	355
NannoCCMP1779_6459	---NA---	329
NannoCCMP1779_7022	---NA---	254
NannoCCMP1779_7489	---NA---	95
NannoCCMP1779_7541	---NA---	16
NannoCCMP1779_7934	---NA---	171;232
NannoCCMP1779_9314	---NA---	255
NannoCCMP1779_9351	---NA---	136
NannoCCMP1779_9385	---NA---	189
NannoCCMP1779_9705	---NA---	812

NannoCCMP1779_9993	---NA---	273

Table A2: Low-light-grown cells

Protein ID	Description	Cys-SOH position
Chloroplast - Photosynthesis		
gene_psaB	photosystem I P700 apoprotein A2 (chloroplast)	561
NannoCCMP1779_11475	violaxanthin de-epoxidase, chloroplastic	109
NannoCCMP1779_2084	ferredoxin--NADP reductase, chloroplastic	477
NannoCCMP1779_2947	sedoheptulose-1,7-bisphosphatase, chloroplastic	80
NannoCCMP1779_349	RuBisCO large subunit-binding protein subunit beta	75
NannoCCMP1779_3819	RuBisCO large subunit-binding protein subunit alpha	168
NannoCCMP1779_4201	chlorophyll a-b binding protein CP24 10A	132
NannoCCMP1779_4643	protochlorophyllide reductase	277
NannoCCMP1779_4980	fructose-1,6-bisphosphatase, chloroplastic	1062;1083
NannoCCMP1779_5038	geranylgeranyl diphosphate reductase, chloroplastic	90
NannoCCMP1779_5333	1Chain 1, Improved Model Of Plant Photosystem I	8
NannoCCMP1779_6822	zeaxanthin epoxidase	202
NannoCCMP1779_7881	2Fe-2S ferredoxin-like superfamily protein	13;89
NannoCCMP1779_8134	pheophorbide a oxygenase, chloroplastic	477;480;531
NannoCCMP1779_8458	photosynthetic NDH subunit of subcomplex B 3	126
Chloroplast - Biosynthesis		
NannoCCMP1779_102	tryptophan synthase beta chain 1	436;681
NannoCCMP1779_10446	bifunctional aspartokinase/homoserine dehydrogenase 1	892
NannoCCMP1779_10579	diaminopimelate epimerase, chloroplastic	53
NannoCCMP1779_11497	D-3-phosphoglycerate dehydrogenase 1, chloroplastic	250
NannoCCMP1779_11837	arogenate dehydrogenase 2, chloroplastic	559
NannoCCMP1779_11891	tetrapyrrole-binding protein, chloroplastic	133
NannoCCMP1779_1396	Aspartate carbamoyltransferase 1, chloroplastic	114
NannoCCMP1779_1932	histidinol-phosphate aminotransferase, chloroplastic	319
NannoCCMP1779_3408	methionine--tRNA ligase, chloroplastic/mitochondrial	374
NannoCCMP1779_4384	digalactosyldiacylglycerol synthase 1, chloroplastic	318
NannoCCMP1779_4513	3-dehydroquinate synthase, chloroplastic-like	510
NannoCCMP1779_5307	phosphomethylpyrimidine synthase, chloroplastic	130;609
NannoCCMP1779_5351	probable glucan 1,3-alpha-glucosidase	22
NannoCCMP1779_6047	aminomethyltransferase, mitochondrial	79
NannoCCMP1779_6341	nifU-like protein 1, chloroplastic	380; 383
NannoCCMP1779_6650	protochlorophyllide reductase	226;284
NannoCCMP1779_7110	LL-diaminopimelate aminotransferase, chloroplastic	628
NannoCCMP1779_734	glyoxylate/succinic semialdehyde reductase 2, chloroplastic	121

NannoCCMP1779_7616	asparagine--tRNA ligase, chloroplastic	650

Chloroplast - Metabolism

NannoCCMP1779_10879	formate dehydrogenase, chloroplastic/mitochondrial	68
NannoCCMP1779_1243	acetyl-coenzyme A synthetase, chloroplastic	174
NannoCCMP1779_1998	plastidic ATP/ADP-transporter	49;54
NannoCCMP1779_2822	glucose-6-phosphate 1-dehydrogenase, cytoplasmic	969
NannoCCMP1779_3273	phosphoglycerate kinase, chloroplastic	77
NannoCCMP1779_3814	proteasome subunit beta type-1	108
NannoCCMP1779_3874	ATP-dependent Clp protease subunit-related protein 4	132;184
NannoCCMP1779_4504	pyruvate carboxylase	633
NannoCCMP1779_567	fructose-bisphosphate aldolase cytoplasmic	144;260
NannoCCMP1779_5763	protease Do-like 1, chloroplastic	8
NannoCCMP1779_5917	probable ribose-5-phosphate isomerase 3, chloroplastic	35
NannoCCMP1779_6099	fatty-acid-binding protein 3, chloroplastic	8
NannoCCMP1779_6748	transketolase, chloroplastic	645
NannoCCMP1779_7147	enolase	97
NannoCCMP1779_8891	NADP-specific glutamate dehydrogenase isoform X2	193

Chloroplast - Translation

gene_rpl36	ribosomal protein L36 (plastid)	14
gene_rps12	ribosomal protein S12 (chloroplast)	34
NannoCCMP1779_2188	translation factor GUF1 homolog, chloroplastic	610
NannoCCMP1779_3598	60S ribosomal protein L10-1	8;105
NannoCCMP1779_6381	elongation factor G-2, chloroplastic	458
NannoCCMP1779_954	cell division protein FtsY homolog, chloroplastic	39

Chloroplast - Redox reactions

NannoCCMP1779_10662	NADP-dependent alkenal double bond reductase P2	184
NannoCCMP1779_2704	peptide methionine sulfoxide reductase	230
NannoCCMP1779_2758	Double Clp-N motif-containing P-loop hydrolase	157
NannoCCMP1779_344	pyridoxal reductase, chloroplastic	11;351
NannoCCMP1779_4338	thioredoxin Y2, chloroplastic	176
NannoCCMP1779_4766	glutathione reductase	89
NannoCCMP1779_6931	peroxiredoxin-2E-2, chloroplastic-like	119
NannoCCMP1779_6935	cytochrome P450 97B2, chloroplastic	299;300
NannoCCMP1779_8541	thioredoxin-like protein aaed1, chloroplastic	243
NannoCCMP1779_8696	2-Cys peroxiredoxin BAS1, chloroplastic	360
NannoCCMP1779_8740	monothiol glutaredoxin-S17	297
NannoCCMP1779_9291	superoxide dismutase [Fe], chloroplastic	35
NannoCCMP1779_9742	probable L-ascorbate peroxidase 6, chloroplastic	67

Chloroplast - Other

NannoCCMP1779_1593	hypothetical protein CICLE_v10009207mg	560
NannoCCMP1779_2011	S-adenosylmethionine carrier 1,	32
NannoCCMP1779_2371	thylakoid lumenal 15.0 kDa protein 2, chloroplastic	287
NannoCCMP1779_4392	pentatricopeptide repeat-containing protein	385
NannoCCMP1779_4672	plastidial lipoyltransferase 2-like	216
NannoCCMP1779_7780	Chaperone protein dnaJ A6 chloroplastic	284
NannoCCMP1779_7784	pentatricopeptide repeat-containing protein	663

Chloroplast - Phosphorylation

NannoCCMP1779_1873	uncharacterized aarF domain-containing protein kinase	1390
NannoCCMP1779_2768	phosphate dikinase chloroplastic-like	346
NannoCCMP1779_8530	adenylate kinase, chloroplastic	350

Mitochondrion

NannoCCMP1779_10056	succinate dehydrogenase [ubiquinone] flavoprotein subunit	184
NannoCCMP1779_10233	V-type proton ATPase catalytic subunit A	315
NannoCCMP1779_11349	D-lactate dehydrogenase [cytochrome], mitochondria	264;341
NannoCCMP1779_11453	S-adenosyl-l-homocysteine hydrolase A	249;736;745
NannoCCMP1779_11663	glutathione reductase	111;185
NannoCCMP1779_1382	putative oxidoreductase TDA3	325
NannoCCMP1779_1506	glutamate decarboxylase-like	184
NannoCCMP1779_1590	electron transfer flavoprotein subunit beta, mitochondrial	122
NannoCCMP1779_1681	Glycine--tRNA ligase mitochondrial 1	685
NannoCCMP1779_18	elongation factor G-2, mitochondrial	9
NannoCCMP1779_2192	methylcrotonoyl-CoA carboxylase beta chain, mitochondrial	314
NannoCCMP1779_2465	cysteine desulfurase, mitochondrial-like	205
NannoCCMP1779_2497	NADH dehydrogenase 1 alpha subcomplex subunit 8-B-like	109
NannoCCMP1779_3428	Molecular chaperone of the GrpE family	134;141
NannoCCMP1779_4352	glycine--tRNA ligase, mitochondrial 1	528
NannoCCMP1779_4381	mitochondrial phosphate carrier protein 3, mitochondrial-like	66;74
NannoCCMP1779_4405	peptide methionine sulfoxide reductase B5	152;182
NannoCCMP1779_4574	NADH dehydrogenase [ubiquinone] flavoprotein 1	153
NannoCCMP1779_4707	CLP protease regulatory subunit CLPX3, mitochondrial	127
NannoCCMP1779_5694	glutamate--glyoxylate aminotransferase 2	229;385
NannoCCMP1779_5740	S-adenosyl-L-methionine-dependent methyltransferase	13;15
NannoCCMP1779_6537	NADH dehydrogenase [ubiquinone] iron-sulfur protein 1	668
NannoCCMP1779_6999	dihydrolipoyllysine-residue acetyltransferase	636
NannoCCMP1779_7307	L-galactono-1,4-lactone dehydrogenase, mitochondrial	129
NannoCCMP1779_8242	heat shock 70 kDa protein, mitochondrial	361
NannoCCMP1779_826	2-oxoglutarate dehydrogenase, mitochondrial-like	793

NannoCCMP1779_829	chaperonin CPN60-2, mitochondrial	125
NannoCCMP1779_9186	putative aconitate hydratase, mitochondrial	494
NannoCCMP1779_9764	succinate dehydrogenase [ubiquinone] iron-sulfur subunit 1	251
NannoCCMP1779_9984	ATP synthase subunit beta, mitochondrial	111

Nucleus

NannoCCMP1779_10103	cell division cycle 5-like protein isoform X1	47
NannoCCMP1779_10256	CCR4-NOT transcription complex subunit 1-like	377
NannoCCMP1779_10293	DNA-directed RNA polymerase I subunit RPA2-like	355
NannoCCMP1779_10745	DNA-directed RNA polymerase II subunit 1	81;97
NannoCCMP1779_10882	pre-mRNA-processing factor 17-like isoform X1	377
NannoCCMP1779_11131	splicing factor U2af small subunit B-like	84;99
NannoCCMP1779_11597	pre-mRNA-splicing factor ATP-dependent RNA helicase DEAH7	827
NannoCCMP1779_1347	transducin/WD40 repeat protein	626
NannoCCMP1779_2255	H/ACA ribonucleoprotein complex subunit 4	125
NannoCCMP1779_2291	squamous cell carcinoma antigen recognized by T-cells 3-like	250
NannoCCMP1779_34	lysine-specific demethylase rbr-2	27
NannoCCMP1779_3458	Regulator of nonsense transcripts 1-like protein	668;669;671
NannoCCMP1779_3497	ESCRT-related protein CHMP1-like	75
NannoCCMP1779_35	DNA-directed RNA polymerase I subunit 1	498;501
NannoCCMP1779_365	DEAD-box ATP-dependent RNA helicase 20	667
NannoCCMP1779_4307	zinc finger CCCH domain-containing protein 48	289
NannoCCMP1779_444	Protein CHROMATIN REMODELING 5	92
NannoCCMP1779_4733	histone acetyltransferase GCN5	273
NannoCCMP1779_4915	transcription elongation factor TFIIS-like	351
NannoCCMP1779_518	transformation/transcription domain-associated protein-like	1300;2352;2354;2358;2272
NannoCCMP1779_5211	nuclear pore complex protein NUP88	294
NannoCCMP1779_5283	THO complex subunit 1 isoform X1	643
NannoCCMP1779_5563	protein BTR1	60;357
NannoCCMP1779_5795	nucleoside diphosphate kinase 1	10
NannoCCMP1779_6319	MYB family protein	372
NannoCCMP1779_811	nucleolin 2	116
NannoCCMP1779_8165	DNA-directed RNA polymerase II subunit RPB2	1074
NannoCCMP1779_8188	GTP-binding nuclear protein Ran-3	117
NannoCCMP1779_8795	AMP-binding family protein	592
NannoCCMP1779_8825	26S proteasome non-ATPase regulatory subunit 2 homolog A	631;1489
NannoCCMP1779_8902	protein argonaute PNH1-like isoform X2	371;577;607
NannoCCMP1779_9231	DNA polymerase delta catalytic subunit	218;875
NannoCCMP1779_9642	DEAD-box ATP-dependent RNA helicase 24	667
NannoCCMP1779_9983	sensory transduction histidine kinase, putative	410

Cytosol

NannoCCMP1779_10051	ATP-citrate synthase beta chain protein 1	988;1057
NannoCCMP1779_10442	5-oxoprolinase	898;1054
NannoCCMP1779_10476	ATP-dependent 6-phosphofructokinase 3 isoform X2	184
NannoCCMP1779_10721	puromycin-sensitive aminopeptidase-like isoform X1	92;354
NannoCCMP1779_10746	delta-1-pyrroline-5-carboxylate synthase-like	44
NannoCCMP1779_10941	60S ribosomal protein L6-like	72
NannoCCMP1779_10959	calcium-dependent protein kinase 20-like isoform X1	927;929
NannoCCMP1779_11011	T-complex protein 1 subunit gamma	198
NannoCCMP1779_11062	UDP-glucose:glycoprotein glucosyltransferase isoform X1	383
NannoCCMP1779_1119	alpha,alpha-trehalose-phosphate synthase [UDP-forming] 5	307
NannoCCMP1779_1126	T-complex protein 1 subunit theta	210
NannoCCMP1779_11459	xylose isomerase	207
NannoCCMP1779_11463	dehydrogenase/reductase SDR family member 12-like isoform X1	115
NannoCCMP1779_11541	60S ribosomal protein L14-2-like	94
NannoCCMP1779_11631	Heat shock 70 kDa protein 17	165
NannoCCMP1779_11811	Serine hydroxymethyltransferase 2 isoform 1	405
NannoCCMP1779_11814	glutathione reductase, cytosolic	7
NannoCCMP1779_11841	UDP-sugar pyrophospharylase	381
NannoCCMP1779_11842	elongation factor 2	354;444;453;485
NannoCCMP1779_11915	bifunctional riboflavin kinase/FMN phosphatase-like isoform X2	131
NannoCCMP1779_152	DnaJ heat shock family protein	5
NannoCCMP1779_1860	40S ribosomal protein S6	83
NannoCCMP1779_2087	elongation factor 1-beta 1	20
NannoCCMP1779_2146	COP9 signalosome complex subunit 1	52;312
NannoCCMP1779_2504	lysophospholipase nte1	304
NannoCCMP1779_2506	serine/threonine-protein kinase BLUS1 isoform X3	278
NannoCCMP1779_2577	eukaryotic initiation factor 4A-15	30
NannoCCMP1779_2701	60S ribosomal protein L27-3-like	43
NannoCCMP1779_274	bifunctional protein FolD 2-like	272
NannoCCMP1779_2777	conserved hypothetical protein, partial	195
NannoCCMP1779_2887	aldehyde dehydrogenase 22A1	177
NannoCCMP1779_3004	coronin-like protein crn1	720;721
NannoCCMP1779_3124	UDP-sugar pyrophosphorylase	539;737
NannoCCMP1779_3186	dnaJ homolog subfamily B member 4	536
NannoCCMP1779_3202	protein ILITYHIA	584;1207
NannoCCMP1779_3236	glyceraldehyde-3-phosphate dehydrogenase, cytosolic-like	67;134;297
NannoCCMP1779_3263	serine/threonine-protein kinase Nek6-like	215

NannoCCMP1779_3410	Protein decapping 5	35
NannoCCMP1779_3427	pyruvate decarboxylase 4	53
NannoCCMP1779_3593	alpha-soluble NSF attachment protein	213
NannoCCMP1779_3737	coatomer subunit beta-1-like	148;689
NannoCCMP1779_4034	caffeoylshikimate esterase-like	224
NannoCCMP1779_4273	protein arginine N-methyltransferase 2	1233
NannoCCMP1779_442	eukaryotic peptide chain release factor GTP-binding subunit ERF3A	355
NannoCCMP1779_4489	LIMR family protein At5g01460-like	135
NannoCCMP1779_4637	DEAD-box ATP-dependent RNA helicase 27-like	445
NannoCCMP1779_4900	glyceraldehyde-3-phosphate dehydrogenase	183
NannoCCMP1779_4979	transmembrane 9 superfamily member 2-like	105
NannoCCMP1779_5185	Methionine synthase	153
NannoCCMP1779_5187	T-complex protein 1 subunit delta	177;352
NannoCCMP1779_5366	heat shock protein 83	339;554
NannoCCMP1779_5424	translation initiation factor 2	338
NannoCCMP1779_5761	ubiquitin carboxyl-terminal hydrolase 25-like	212
NannoCCMP1779_5782	mannitol-1-phosphate 5-dehydrogenase	285;668
NannoCCMP1779_5939	Galactokinase family protein	46;196
NannoCCMP1779_6003	xanthine dehydrogenase 1	209
NannoCCMP1779_6135	cullin 4	100;361;407
NannoCCMP1779_6290	aspartate--tRNA ligase 2, cytoplasmic-like	361
NannoCCMP1779_6330	Aspartate-semialdehyde dehydrogenase	158
NannoCCMP1779_6658	pyruvate dehydrogenase E1 component alpha subunit	6
NannoCCMP1779_668	leucine aminopeptidase 1-like	446
NannoCCMP1779_6818	eukaryotic translation initiation factor 2 subunit gamma	417
NannoCCMP1779_6819	glutamine synthetase	102;334
NannoCCMP1779_7418	putative transaldolase-like	249
NannoCCMP1779_7748	glutamyl-tRNA reductase	335
NannoCCMP1779_7921	alcohol dehydrogenase 1	309
NannoCCMP1779_817	UDP-glucose 6-dehydrogenase 5-like isoform X2	10;113
NannoCCMP1779_8248	nitrate reductase [NADH]-like	197
NannoCCMP1779_8329	serine--tRNA ligase-like	411
NannoCCMP1779_8545	deoxyhypusine synthase	193
NannoCCMP1779_8799	branched-chain-amino-acid aminotransferase	60
NannoCCMP1779_8806	Cell division control protein 48 homolog D	728
NannoCCMP1779_9138	eukaryotic translation initiation factor 3 subunit K-like	11
NannoCCMP1779_9185	26S protease regulatory subunit 6A homolog	395;408
NannoCCMP1779_937	eukaryotic translation initiation factor 5-like	121
NannoCCMP1779_9780	protein-L-isoaspartate O-methyltransferase 1-like	129

Transmembrane system

NannoCCMP1779_10109	CSC1-like protein isoform X1	115

NannoCCMP1779_10128	Phosphatidylinositol:ceramide inositolphosphotransferase 1	136
NannoCCMP1779_11163	protein transport protein SEC23-like	76
NannoCCMP1779_11306	spermatogenesis-associated protein 20	739
NannoCCMP1779_11360	ABC transporter E family member 2	26;31;48;65;68
NannoCCMP1779_11499	dnaJ protein ERDJ3B	228
NannoCCMP1779_16	probable protein disulfide-isomerase A6	33;39
NannoCCMP1779_1885	AP3-complex subunit beta-A	506
NannoCCMP1779_2036	---NA---	19
NannoCCMP1779_2182	inositol-phosphate phosphatase	339
NannoCCMP1779_236	O-acyltransferase WSD1-like	221
NannoCCMP1779_2702	sodium-coupled neutral amino acid transporter 2	232
NannoCCMP1779_3162	MFS transporter	473;478
NannoCCMP1779_3350	ABC transporter C family member 2-like	646
NannoCCMP1779_3627	11-beta-hydroxysteroid dehydrogenase-like 4A	80
NannoCCMP1779_3772	RING-H2 finger protein ATL52	231
NannoCCMP1779_4091	calcium-transporting ATPase 1, endoplasmic reticulum-type-like	233
NannoCCMP1779_4669	coatomer subunit alpha-1	588;1101
NannoCCMP1779_4679	SPX domain-containing protein 1-like	134
NannoCCMP1779_4998	protein transport protein SEC31 homolog B-like	707
NannoCCMP1779_5460	ABC transporter C family member 4	171
NannoCCMP1779_5478	sucrase-like protein	368
NannoCCMP1779_5704	dnaJ protein homolog	142
NannoCCMP1779_663	SPX domain-containing protein 1-like	429
NannoCCMP1779_6720	6-deoxyerythronolide-b synthase erya1, modules 1 and 2	1109;1959
NannoCCMP1779_6768	DUF21 domain-containing protein isoform X1	69;238
NannoCCMP1779_7486	calcium-transporting ATPase 4, endoplasmic reticulum-type-like	775
NannoCCMP1779_761	dnaJ protein ERDJ2A	356
NannoCCMP1779_771	D-alanyl-D-alanine carboxypeptidase-like	77
NannoCCMP1779_8051	phosphatidylinositol/phosphatidylcholine transfer protein SFH12	154
NannoCCMP1779_8394	ABC transporter-like protein	534
NannoCCMP1779_8561	beta-adaptin-like protein B	307
NannoCCMP1779_8721	temperature-induced lipocalin-1-like	4
NannoCCMP1779_9	calcium-transporting ATPase 2, endoplasmic reticulum-type	286;707;837
NannoCCMP1779_9383	endoplasmin homolog	55
NannoCCMP1779_963	Proteasome subunit alpha type-3	73

Hypothetical proteins

NannoCCMP1779_1052	---NA---	79;144
NannoCCMP1779_10816	---NA---	26

NannoCCMP1779_10886	---NA---	483;545
NannoCCMP1779_11075	---NA---	55
NannoCCMP1779_11134	predicted protein	185;270;297
NannoCCMP1779_11446	---NA---	357
NannoCCMP1779_11516	hypothetical protein F511_09402	9
NannoCCMP1779_1420	---NA---	877
NannoCCMP1779_1518	---NA---	225
NannoCCMP1779_1578	---NA---	460
NannoCCMP1779_1888	---NA---	31
NannoCCMP1779_1904	---NA---	91
NannoCCMP1779_1957	hypothetical protein SELMODRAFT_270941	202
NannoCCMP1779_2086	---NA---	323;359
NannoCCMP1779_2518	---NA---	462
NannoCCMP1779_2626	---NA---	382
NannoCCMP1779_2629	---NA---	44
NannoCCMP1779_2640	---NA---	78
NannoCCMP1779_2879	---NA---	383
NannoCCMP1779_3183	---NA---	46;75;86;89
NannoCCMP1779_3277	---NA---	34
NannoCCMP1779_3769	---NA---	741;860
NannoCCMP1779_4209	---NA---	176
NannoCCMP1779_4283	---NA---	28
NannoCCMP1779_4339	---NA---	189
NannoCCMP1779_4457	---NA---	115
NannoCCMP1779_5278	---NA---	88
NannoCCMP1779_5402	---NA---	350
NannoCCMP1779_5466	---NA---	169
NannoCCMP1779_5683	---NA---	310
NannoCCMP1779_5830	---NA---	355
NannoCCMP1779_6261	predicted protein	187;272
NannoCCMP1779_6836	---NA---	378
NannoCCMP1779_7211	---NA---	7
NannoCCMP1779_7489	---NA---	95
NannoCCMP1779_750	predicted protein	172
NannoCCMP1779_7541	---NA---	16
NannoCCMP1779_7686	---NA---	14
NannoCCMP1779_8313	---NA---	59
NannoCCMP1779_8387	---NA---	83
NannoCCMP1779_8444	---NA---	18
NannoCCMP1779_8456	---NA---	161
NannoCCMP1779_9285	---NA---	34
NannoCCMP1779_9314	---NA---	255
NannoCCMP1779_9351	---NA---	135

NannoCCMP1779_947	---NA---	59
NannoCCMP1779_9705	---NA---	812
NannoCCMP1779_9743	---NA---	816
NannoCCMP1779_9800	---NA---	134
NannoCCMP1779_9993	---NA---	273

Other		
NannoCCMP1779_10312	NAD(P)-binding rossmann-fold protein	120
NannoCCMP1779_10492	isoform 2 of ankyrin repeat domain-containing protein 17	104
NannoCCMP1779_10922	probable aldehyde dehydrogenase isoform X2	25
NannoCCMP1779_10961	protein tesmin/TSO1-like CXC 3	340
NannoCCMP1779_11429	ERBB-3 BINDING PROTEIN 1	240
NannoCCMP1779_11832	peroxisomal (S)-2-hydroxy-acid oxidase GLO1	390
NannoCCMP1779_11851	nicotinate phosphoribosyltransferase 2-like isoform X1	1267
NannoCCMP1779_1692	probable mannitol dehydrogenase	43
NannoCCMP1779_1850	probable calcium-binding protein CML27	1686;1693;2290;3815
NannoCCMP1779_2320	vacuolar-sorting receptor 3-like isoform X1	46
NannoCCMP1779_3972	NADPH-dependent 1-acyldihydroxyacetone phosphate reductase	248;252;262
NannoCCMP1779_4004	protein NAR1	579
NannoCCMP1779_437	probable manganese-transporting ATPase PDR2	1008
NannoCCMP1779_4409	putative formate transporter	96;100
NannoCCMP1779_5843	L-ascorbate peroxidase 3, peroxisomal	6
NannoCCMP1779_6772	PREDICTED: uncharacterized protein LOC8285738	358
NannoCCMP1779_6868	putative dehydrogenase	228
NannoCCMP1779_7255	probable phosphoglucomutase-2 isoform X2	324
NannoCCMP1779_8460	probable carboxylesterase 15	375
NannoCCMP1779_8808	probable polyamine transporter At3g19553	561
NannoCCMP1779_9510	vacuolar protein sorting-associated protein 13	1399
NannoCCMP1779_9534	jmjC domain-containing protein 7	338

Table A3: High-light-treated

Protein ID	**Description**	**Cys-SOH position**
Chloroplast - Photosynthesis		
gene_petJ	cytochrome c6, chloroplastic-like	52
NannoCCMP1779_10228	violaxanthin de-epoxidase, chloroplastic	24;36
NannoCCMP1779_10542	protoporphyrinogen IX oxidase	286
NannoCCMP1779_11417	Aldolase superfamily protein	174
NannoCCMP1779_11954	chlorophyll a-b binding protein 3, chloroplastic-like	71
NannoCCMP1779_2084	ferredoxin--NADP reductase, root isozyme, chloroplastic	499;504

NannoCCMP1779_2223	uroporphyrinogen decarboxylase	202
NannoCCMP1779_349	RuBisCO large subunit-binding protein subunit beta, chloroplastic	75
NannoCCMP1779_3511	magnesium-chelatase subunit ChlH, chloroplastic	17
NannoCCMP1779_3819	RuBisCO large subunit-binding protein subunit alpha	168
NannoCCMP1779_3970	phosphoenolpyruvate carboxylase	361
NannoCCMP1779_4201	LHCX1	162
NannoCCMP1779_4383	delta-aminolevulinic acid dehydratase 1, chloroplastic-like	257
NannoCCMP1779_4980	fructose-1,6-bisphosphatase, chloroplastic	949;1083
NannoCCMP1779_5038	geranylgeranyl diphosphate reductase, chloroplastic	90
NannoCCMP1779_5425	D-3-phosphoglycerate dehydrogenase 2, chloroplastic	38
NannoCCMP1779_6341	nifU-like protein 1, chloroplastic	380
NannoCCMP1779_6650	protochlorophyllide reductase	112;284
NannoCCMP1779_6698	alpha carbonic anhydrase 4	47;57
NannoCCMP1779_6822	zeaxanthin epoxidase	97
NannoCCMP1779_7460	ferredoxin-thioredoxin reductase catalytic chain, chloroplastic	129;131
NannoCCMP1779_7696	D-3-phosphoglycerate dehydrogenase 2, chloroplastic-like	38
NannoCCMP1779_7851	p-type H+-ATPase	48
NannoCCMP1779_7881	2Fe-2S ferredoxin-like superfamily protein	13
NannoCCMP1779_8196	chlorophyll a-b binding protein 13, chloroplastic-like	4
NannoCCMP1779_8678	porphobilinogen deaminase, chloroplastic	284
NannoCCMP1779_9291	superoxide dismutase [Fe], chloroplastic	5
NannoCCMP1779_9742	probable L-ascorbate peroxidase 6	294
NannoCCMP1779_9798	photosynthetic NDH subunit of subcomplex B 3, chloroplastic	78
NannoCCMP1779_9838	retinol dehydrogenase 11	184

Chloroplast - Biosynthesis		
NannoCCMP1779_102	tryptophan synthase beta chain 1	681
NannoCCMP1779_10879	formate dehydrogenase, chloroplastic/mitochondrial	68
NannoCCMP1779_1109	threonine--tRNA ligase, chloroplastic/mitochondrial 2	411
NannoCCMP1779_11497	D-3-phosphoglycerate dehydrogenase 1, chloroplastic-like	44;619
NannoCCMP1779_11837	arogenate dehydrogenase 2, chloroplastic	566
NannoCCMP1779_11892	methionine--tRNA ligase, chloroplastic/mitochondrial	424
NannoCCMP1779_1246	glycine dehydrogenase (decarboxylating) 1, mitochondrial	86
NannoCCMP1779_2708	bifunctional glutamate/aspartate-prephenate aminotransferase	376
NannoCCMP1779_31	arginine--tRNA ligase, chloroplastic/mitochondrial-like isoform X2	409; 591;801
NannoCCMP1779_3532	farnesyl pyrophosphate synthase	274
NannoCCMP1779_4384	digalactosyldiacylglycerol synthase 1, chloroplastic isoform X2	91;323;330

NannoCCMP1779_4622	glutamine--fructose-6-phosphate aminotransferase [isomerizing] 2	72;318;476
NannoCCMP1779_4978	ferredoxin-dependent glutamate synthase, chloroplastic	1270
NannoCCMP1779_4984	anthranilate synthase alpha subunit 2, chloroplastic	796
NannoCCMP1779_5307	phosphomethylpyrimidine synthase, chloroplastic	579; 599; 601
NannoCCMP1779_5740	S-adenosyl-L-methionine-dependent methyltransferase	13
NannoCCMP1779_6371	glutamate synthase 1 [NADH], chloroplastic-like isoform X1	113;116;121
NannoCCMP1779_6372	glutamate synthase 1 [NADH], chloroplastic isoform X1	101
NannoCCMP1779_7110	LL-diaminopimelate aminotransferase, chloroplastic isoform X2	26
NannoCCMP1779_7122	ornithine carbamoyltransferase, chloroplastic-like	229
NannoCCMP1779_8497	3-oxoacyl-[acyl-carrier-protein] synthase I, chloroplastic	85
NannoCCMP1779_9174	probable phosphoribosylformylglycinamidine synthase	714;715;1028
NannoCCMP1779_9295	amidophosphoribosyltransferase, chloroplastic	166

Chloroplast - Metabolism

NannoCCMP1779_10574	pyruvate dehydrogenase E1 component subunit alpha-3, chloroplastic	228;360
NannoCCMP1779_1243	acetyl-coenzyme A synthetase, chloroplastic/glyoxysomal-like	150
NannoCCMP1779_1520	pyruvate, phosphate dikinase 1, chloroplastic	7;519
NannoCCMP1779_1998	plastidic ATP/ADP-transporter	49;152;371
NannoCCMP1779_2758	Double Clp-N motif-containing P-loop nucleoside triphosphate hydrolase	51
NannoCCMP1779_3273	phosphoglycerate kinase, chloroplastic	77
NannoCCMP1779_3874	ATP-dependent Clp protease proteolytic subunit-related protein 4	118
NannoCCMP1779_4504	pyruvate carboxylase	4;633
NannoCCMP1779_4675	NADP-dependent malic enzyme, chloroplastic-like	75;515
NannoCCMP1779_5917	probable ribose-5-phosphate isomerase 3, chloroplastic	161
NannoCCMP1779_6032	pyruvate, phosphate dikinase 1, chloroplastic	460
NannoCCMP1779_6184	nicotinamide adenine dinucleotide transporter 1,	573
NannoCCMP1779_6382	dihydrolipoyl dehydrogenase 1, chloroplastic-like	328
NannoCCMP1779_6562	malonyl CoA-acyl carrier transacylase	334
NannoCCMP1779_6870	plastidic ATP/ADP-transporter-like	108
NannoCCMP1779_7491	casein lytic proteinase B3	951

Chloroplast -Translation

gene_rpl18	50S ribosomal protein L18, chloroplastic-like	38
gene_rpl36	ribosomal protein L36 (plastid)	11;14;27
gene_rps14	ribosomal protein S14 (chloroplast)	63
NannoCCMP1779_1819	ribosomal protein S15 (chloroplast)	11
NannoCCMP1779_2188	translation factor GUF1 homolog, chloroplastic	619;632
NannoCCMP1779_3281	30S ribosomal protein S1, chloroplastic	380
NannoCCMP1779_3598	60S ribosomal protein L10-1	105

NannoCCMP1779_5777	stromal processing peptidase, chloroplastic	82
NannoCCMP1779_6381	elongation factor G-2, chloroplastic	458
NannoCCMP1779_7395	chaperone protein ClpC1, chloroplastic-like	251
NannoCCMP1779_7780	Chaperone protein dnaJ A6 chloroplastic	304

Chloroplast -Transcription

NannoCCMP1779_11353	DEAD-box ATP-dependent RNA helicase 26	286
NannoCCMP1779_29	putative helicase	1413
NannoCCMP1779_2946	DEAD-box ATP-dependent RNA helicase 50	44;59;454;455; 616;666
NannoCCMP1779_833	DNA gyrase subunit B, chloroplastic/mitochondrial	439

Chloroplast - Redox reactions

NannoCCMP1779_2416	Thioredoxin-like protein	132
NannoCCMP1779_5126	thioredoxin F, chloroplastic	119
NannoCCMP1779_5845	putative glutaredoxin-like protein	105;406
NannoCCMP1779_6649	protein ABCI7, chloroplastic	265;450
NannoCCMP1779_6931	peroxiredoxin-2E-2, chloroplastic-like	92
NannoCCMP1779_6935	cytochrome P450 97B2, chloroplastic	355;417;440
NannoCCMP1779_734	glyoxylate/succinic semialdehyde reductase 2	148
NannoCCMP1779_8455	Peroxiredoxin-2E-1, chloroplastic	78
NannoCCMP1779_8541	thioredoxin-like protein aaed1, chloroplastic	105
NannoCCMP1779_8696	2-Cys peroxiredoxin BAS1, chloroplastic	281;284

Chloroplast - Other

gene_psbV	---NA---	62
NannoCCMP1779_10332	uncharacterized aarF domain-containing protein kinase	910
NannoCCMP1779_10579	diaminopimelate epimerase, chloroplastic	53
NannoCCMP1779_10595	heme-binding-like protein At3g10130, chloroplastic	15
NannoCCMP1779_11914	aspartate-semialdehyde dehydrogenase	283
NannoCCMP1779_1519	pyridoxal 5'-phosphate synthase subunit PDX1.1	152
NannoCCMP1779_1996	thylakoid membrane slr0575-like protein	22;104
NannoCCMP1779_2011	S-adenosylmethionine carrier 1, chloroplastic/mitochondrial	30;32;39
NannoCCMP1779_2773	3-isopropylmalate dehydratase large subunit, chloroplastic	353;366;430
NannoCCMP1779_3495	isocitrate dehydrogenase [NADP], chloroplastic/mitochondrial	111
NannoCCMP1779_3703	glutamate--tRNA ligase, chloroplastic/mitochondrial	72;180
NannoCCMP1779_4392	s uncoupled 1	142
NannoCCMP1779_4567	2-isopropylmalate synthase 1	198
NannoCCMP1779_460	pentatricopeptide repeat-containing protein	132
NannoCCMP1779_464	glycerol-3-phosphate dehydrogenase [NAD(+)]	204;307
NannoCCMP1779_5435	28 kDa ribonucleoprotein, chloroplastic	91

NannoCCMP1779_6007	ketol-acid reductoisomerase, chloroplastic	538
NannoCCMP1779_6748	transketolase, chloroplastic	304;645
NannoCCMP1779_6810	thylakoid lumenal 15 kDa protein 1, chloroplastic	239
NannoCCMP1779_7869	3-isopropylmalate dehydrogenase 2, chloroplastic-like	405
NannoCCMP1779_8795	probable acyl-activating enzyme 16, chloroplastic	137
NannoCCMP1779_956	predicted protein	221
NannoCCMP1779_9743	protein translocase subunit SecA, chloroplastic	296;816
NannoCCMP1779_9747	probable protein phosphatase 2C 55	566

Mitochondrion

NannoCCMP1779_10056	succinate dehydrogenase [ubiquinone] flavoprotein subunit, mitochondrial-like	443
NannoCCMP1779_10233	V-type proton ATPase catalytic subunit A	555
NannoCCMP1779_10757	citrate synthase, mitochondrial	63;436
NannoCCMP1779_10769	NADH--cytochrome b5 reductase 1-like isoform X3	387;807
NannoCCMP1779_11966	probable 37S ribosomal protein S5, mitochondrial	305
NannoCCMP1779_1590	electron transfer flavoprotein subunit beta, mitochondrial	122
NannoCCMP1779_1681	Glycine--tRNA ligase mitochondrial 1	685
NannoCCMP1779_1692	probable mannitol dehydrogenase	46
NannoCCMP1779_18	elongation factor G-2, mitochondrial	9
NannoCCMP1779_2069	succinate-semialdehyde dehydrogenase, mitochondrial isoform X2	236;317
NannoCCMP1779_245	cardiolipin synthase (CMP-forming), mitochondrial	31
NannoCCMP1779_2465	cysteine desulfurase, mitochondrial-like	205
NannoCCMP1779_2823	ADP,ATP carrier protein 1, mitochondrial-like	354
NannoCCMP1779_3428	Molecular chaperone of the GrpE family	154
NannoCCMP1779_4346	aspartate aminotransferase, mitochondrial	302
NannoCCMP1779_4352	glycine--tRNA ligase, mitochondrial 1	449;528
NannoCCMP1779_4381	mitochondrial phosphate carrier protein 3, mitochondrial-like	66;74
NannoCCMP1779_5189	SAM-dependent methyltransferase	302
NannoCCMP1779_6181	elongation factor Tu, mitochondrial-like	22
NannoCCMP1779_6229	sulfide:quinone oxidoreductase, mitochondrial	387
NannoCCMP1779_6537	NADH dehydrogenase [ubiquinone] iron-sulfur protein 1 mitochondrial	296;570;584;674
NannoCCMP1779_6983	isovaleryl-CoA dehydrogenase, mitochondrial	279
NannoCCMP1779_6999	dihydrolipoyllysine-residue acetyltransferase of pyruvate dehydrogenase complex	756
NannoCCMP1779_7057	probable mitochondrial-processing peptidase subunit beta, mitochondrial	418
NannoCCMP1779_7784	putative pentatricopeptide repeat-containing protein	256
NannoCCMP1779_8141	succinyl-CoA ligase [ADP-forming] subunit alpha-1, mitochondrial	165
NannoCCMP1779_8190	mitochondrial phosphate carrier protein 3, mitochondrial-like	460
NannoCCMP1779_8242	heat shock 70 kDa protein, mitochondrial	358

NannoCCMP1779_829	chaperonin CPN60-2, mitochondrial	125
NannoCCMP1779_8683	protein Rf1, mitochondrial isoform X3	145;721
NannoCCMP1779_8740	monothiol glutaredoxin-S17	174
NannoCCMP1779_8828	betaine aldehyde dehydrogenase 2, mitochondrial	453
NannoCCMP1779_9552	acetyl-coa carboxylase	84
NannoCCMP1779_9764	succinate dehydrogenase [ubiquinone] iron-sulfur subunit 1, mitochondrial-like	109;251
NannoCCMP1779_9984	ATP synthase subunit beta, mitochondrial	111

Nucleus

NannoCCMP1779_10220	phosphomethylethanolamine N-methyltransferase	438
NannoCCMP1779_10293	DNA-directed RNA polymerase I subunit RPA2-like	1185
NannoCCMP1779_10539	pre-mRNA-processing factor 19 homolog 1-like isoform X1	3
NannoCCMP1779_10557	25S rRNA (cytosine-C(5))-methyltransferase nop2-like	471
NannoCCMP1779_10747	general negative regulator of transcription subunit 3-like isoform X4	100
NannoCCMP1779_10959	calcium-dependent protein kinase 20-like isoform X1	927
NannoCCMP1779_10981	eukaryotic translation initiation factor 2 subunit alpha homolog	22
NannoCCMP1779_11131	splicing factor U2af small subunit B-like	84
NannoCCMP1779_11218	Protein CHROMATIN REMODELING 5	402;1162
NannoCCMP1779_11356	splicing factor 3B subunit 1	1063
NannoCCMP1779_11489	probable glutathione peroxidase 2	29
NannoCCMP1779_11712	DNA-directed RNA polymerases I and III subunit rpac1-like isoform X1	282;285
NannoCCMP1779_177	eukaryotic initiation factor 4A-15-like	165
NannoCCMP1779_1977	proteasome subunit beta type-6-like	65
NannoCCMP1779_2122	cysteine proteinase 15A	308;317
NannoCCMP1779_2174	Histone-lysine N-methyltransferase ASHH2	88
NannoCCMP1779_2893	exportin-2 isoform X1	228
NannoCCMP1779_3007	cleavage stimulating factor 64-like	15;283
NannoCCMP1779_3055	KRR1 small subunit processome component	484
NannoCCMP1779_34	lysine-specific demethylase rbr-2	42;1607;1620;1648;1892;1917;1933
NannoCCMP1779_3497	ESCRT-related protein CHMP1-like	75
NannoCCMP1779_35	DNA-directed RNA polymerase I subunit 1	10;361;498;584
NannoCCMP1779_3589	RNA-binding protein 25 isoform X3	623
NannoCCMP1779_365	DEAD-box ATP-dependent RNA helicase 20	533;569;660;678
NannoCCMP1779_3697	probable ubiquitin-conjugating enzyme E2 16	50
NannoCCMP1779_3714	ubiquitin-like modifier-activating enzyme atg7	153;319;453;744
NannoCCMP1779_392	U4/U6.U5 tri-snRNP-associated protein 2-like	69
NannoCCMP1779_413	transcription factor GTE7-like	273;1045;1317
NannoCCMP1779_4233	Proteasome subunit alpha type-1-A	4

NannoCCMP1779_4342	cyclin-dependent kinase C-2-like	322
NannoCCMP1779_4435	protein CTR9 homolog isoform X2	243
NannoCCMP1779_444	Protein CHROMATIN REMODELING 5	92;1178;1284;1349;1376;1401;1402;1412;1605
NannoCCMP1779_4449	putative DNA ligase 4	145;728
NannoCCMP1779_4637	DEAD-box ATP-dependent RNA helicase 27-like	445
NannoCCMP1779_4710	---NA---	82
NannoCCMP1779_4840	putative DNA-dependent ATPase SNF2H	526;527
NannoCCMP1779_4842	serine/threonine-protein kinase TOR isoform X2	417;663
NannoCCMP1779_4915	transcription elongation factor TFIIS-like	60;323;348
NannoCCMP1779_518	transformation/transcription domain-associated protein-like	2352;2354
NannoCCMP1779_524	transformation/transcription domain-associated protein-like	336
NannoCCMP1779_5283	THO complex subunit 1 isoform X1	183;542
NannoCCMP1779_5286	histone acetyltransferase GCN5	331
NannoCCMP1779_5386	protein BCCIP homolog	11;147;251
NannoCCMP1779_5471	DExH-box ATP-dependent RNA helicase DExH12	616;1787
NannoCCMP1779_6071	Pre-mRNA-splicing factor SLU7	107;110
NannoCCMP1779_634	DEAD-box ATP-dependent RNA helicase 37-like	333
NannoCCMP1779_6377	25S rRNA (cytosine-C(5))-methyltransferase nop2-like	600
NannoCCMP1779_6540	splicing factor 3B subunit 3-like	70;114;350;612;878
NannoCCMP1779_6726	DNA ligase 6 isoform X4	163
NannoCCMP1779_6818	eukaryotic translation initiation factor 2 subunit gamma-like	72
NannoCCMP1779_7568	deoxyribodipyrimidine photo-lyase	350
NannoCCMP1779_7643	DEAD-box ATP-dependent RNA helicase 7	101;305;413;571
NannoCCMP1779_7689	cleavage and polyadenylation specificity factor subunit 3-I-like	184;244
NannoCCMP1779_8165	DNA-directed RNA polymerase II subunit RPB2	1074
NannoCCMP1779_8825	26S proteasome non-ATPase regulatory subunit 2 homolog A	868
NannoCCMP1779_9293	Ras-related protein Rab7	84
NannoCCMP1779_9302	calcium-dependent protein kinase 25	169;335
NannoCCMP1779_963	Proteasome subunit alpha type-3	219
NannoCCMP1779_9864	dead-box atp-dependent rna helicase 38	68

Cytosolic

NannoCCMP1779_10051	ATP-citrate synthase beta chain protein 1	523;543;1053
NannoCCMP1779_10411	probable ubiquitin conjugation factor E4	244;538
NannoCCMP1779_10662	NADP-dependent alkenal double bond reductase P2-like	46;184;189
NannoCCMP1779_10723	plasma membrane ATPase 1-like	424

NannoCCMP1779_10941	60S ribosomal protein L6-like	72
NannoCCMP1779_11098	tRNA synthetase class I (I, L, M and V) family protein	496;745
NannoCCMP1779_11134	predicted protein	192;297;607;715
NannoCCMP1779_11151	aspartate--tRNA ligase 2, cytoplasmic-like	115;234
NannoCCMP1779_11328	Eukaryotic translation initiation factor 4G	703
NannoCCMP1779_11423	Fungal lipase-like domain containing protein	15
NannoCCMP1779_11453	S-adenosyl-l-homocysteine hydrolase A	506;547;745
NannoCCMP1779_11455	alcohol dehydrogenase class-3	106
NannoCCMP1779_11459	xylose isomerase	473
NannoCCMP1779_11488	putative threonyl-tRNA synthetase	318
NannoCCMP1779_11541	60S ribosomal protein L14-2-like	94
NannoCCMP1779_11597	pre-mRNA-splicing factor ATP-dependent RNA helicase DEAH7	719
NannoCCMP1779_11663	glutathione reductase	337
NannoCCMP1779_11808	polyadenylate-binding protein RBP47C	61
NannoCCMP1779_11835	cytosolic phosphoglucose isomerase	167
NannoCCMP1779_11841	UDP-sugar pyrophospharylase	381
NannoCCMP1779_11842	elongation factor 2	346;354;544;649;745
NannoCCMP1779_1325	Eukaryotic translation initiation factor 3 subunit B	307
NannoCCMP1779_1327	cytochrome P450 704C1	174;177
NannoCCMP1779_1372	ubiquitin carboxyl-terminal hydrolase 6	317
NannoCCMP1779_1599	cullin-1 isoform X2	489
NannoCCMP1779_1827	glutamine--tRNA ligase-like	338
NannoCCMP1779_1866	aminopeptidase M1-like	589
NannoCCMP1779_19	Beta-lactamase-like protein	186
NannoCCMP1779_2179	acyl-lipid (9-3)-desaturase-like	437
NannoCCMP1779_2213	pyrophosphate-energized vacuolar membrane proton pump-like	627
NannoCCMP1779_2215	long chain base biosynthesis protein 2a	25;455;682;738
NannoCCMP1779_2255	H/ACA ribonucleoprotein complex subunit 4	12;121;125
NannoCCMP1779_2494	transketolase 1, thiamin-binding protein	36
NannoCCMP1779_2506	serine/threonine-protein kinase BLUS1 isoform X3	34
NannoCCMP1779_2660	beta-glucosidase BoGH3B-like	596;754;865
NannoCCMP1779_2836	Fruit bromelain	156
NannoCCMP1779_2887	aldehyde dehydrogenase 22A1	157;177;480;487
NannoCCMP1779_3041	60S ribosomal protein L3-like	251
NannoCCMP1779_3098	probable copper-transporting ATPase HMA5	321;461;464
NannoCCMP1779_3124	UDP-sugar pyrophosphorylase	470;737
NannoCCMP1779_3202	protein ILITYHIA	748;1585
NannoCCMP1779_3236	glyceraldehyde-3-phosphate dehydrogenase, cytosolic-like	67;134;360
NannoCCMP1779_3247	glyceraldehyde-3-phosphate dehydrogenase, cytosolic	159;305
NannoCCMP1779_3418	eukaryotic translation initiation factor eIF2A family	396

	protein	
NannoCCMP1779_3427	pyruvate decarboxylase 4	511
NannoCCMP1779_3737	coatomer subunit beta-1-like	171;641
NannoCCMP1779_3861	sulfate adenylyltransferase	5
NannoCCMP1779_3972	11-beta-hydroxysteroid dehydrogenase 1B	67;248;260
NannoCCMP1779_3979	long-chain-alcohol oxidase FAO2-like isoform X1	454;846
NannoCCMP1779_4034	caffeoylshikimate esterase-like	224
NannoCCMP1779_4091	calcium-transporting ATPase 1, endoplasmic reticulum-type-like	16;233;958
NannoCCMP1779_4372	40S ribosomal protein S16	150
NannoCCMP1779_4375	ABC transporter G family member 40	222;350;462
NannoCCMP1779_442	peptide chain release factor GTP-binding subunit ERF3A-like	588;597
NannoCCMP1779_4551	N-terminal acetyltransferase A, auxiliary subunit	326;913;1177
NannoCCMP1779_4716	tubulin alpha chain	349
NannoCCMP1779_4766	glutathione reductase	84;89
NannoCCMP1779_4979	transmembrane 9 superfamily member 2-like	448
NannoCCMP1779_5185	Methionine synthase	552
NannoCCMP1779_5187	T-complex protein 1 subunit delta	177
NannoCCMP1779_5387	calmodulin-domain kinase CDPK protein	168
NannoCCMP1779_5389	NADP-dependent glyceraldehyde-3-phosphate dehydrogenase	360;511
NannoCCMP1779_5424	translation initiation factor 2	739
NannoCCMP1779_5478	sucrase-like protein	360;368;388
NannoCCMP1779_5488	S-formylglutathione hydrolase	66
NannoCCMP1779_5491	60S ribosomal protein L34	46
NannoCCMP1779_5562	inner arm dynein, group 5	811;1850;2106;3733;3847;4250
NannoCCMP1779_567	fructose-bisphosphate aldolase cytoplasmic isozyme-like	330
NannoCCMP1779_5759	pyruvate kinase, cytosolic isozyme-like	219
NannoCCMP1779_5795	nucleoside diphosphate kinase 1	60
NannoCCMP1779_5890	putative tRNA pseudouridine synthase isoform X1	103
NannoCCMP1779_5939	Galactokinase family protein	46
NannoCCMP1779_6003	xanthine dehydrogenase 1	209;233;234;243
NannoCCMP1779_6045	glutamate--tRNA ligase, cytoplasmic-like	431
NannoCCMP1779_6209	Eukaryotic initiation factor 4A-8	285
NannoCCMP1779_625	thiol-disulfide oxidoreductase LTO1-like	331;367
NannoCCMP1779_6261	predicted protein	194;609
NannoCCMP1779_6299	elongation factor 1-gamma 2	376
NannoCCMP1779_6346	choline transporter-like protein 2	49;110;380
NannoCCMP1779_6395	6-phosphogluconate dehydrogenase, decarboxylating	358;413
NannoCCMP1779_6422	imidazoleglycerol-phosphate dehydratase	112;420
NannoCCMP1779_6580	eukaryotic translation initiation factor 3 subunit A-like	89

NannoCCMP1779_6615	chaperone protein dnaJ 49-like	11
NannoCCMP1779_6618	26S proteasome regulatory subunit 4 homolog A	406
NannoCCMP1779_668	leucine aminopeptidase 1-like	20;446;655;785
NannoCCMP1779_6718	ubiquitin carboxyl-terminal hydrolase 14	402
NannoCCMP1779_6720	6-deoxyerythronolide-b synthase erya1, modules 1 and 2	2187
NannoCCMP1779_6819	glutamine synthetase	102;120
NannoCCMP1779_7040	30-kDa cleavage and polyadenylation specificity factor 30	122
NannoCCMP1779_7064	phenylalanine--tRNA ligase beta subunit, cytoplasmic-like	360
NannoCCMP1779_7085	serine--tRNA ligase-like	74;360;363
NannoCCMP1779_7121	putative CDP-diacylglycerol--inositol 3-phosphatidyltransferase 2	194
NannoCCMP1779_7188	pyrophosphate-energized membrane proton pump 2-like	112
NannoCCMP1779_72	T-complex protein 1 subunit zeta 1	25;293
NannoCCMP1779_7244	26S proteasome non-ATPase regulatory subunit 10	514;558
NannoCCMP1779_7312	ABC transporter G family member 9-like	6
NannoCCMP1779_7353	Prolyl endopeptidase	382
NannoCCMP1779_7468	eukaryotic translation initiation factor 2 subunit beta	266
NannoCCMP1779_761	dnaJ protein ERDJ2A	356;454
NannoCCMP1779_7852	plasma membrane ATPase 1-like [Dendrobium catenatum]	137;189
NannoCCMP1779_7994	protein VACUOLELESS1	301
NannoCCMP1779_8130	pyruvate kinase, cytosolic isozyme-like	44;334;507
NannoCCMP1779_817	UDP-glucose 6-dehydrogenase 5-like isoform X2	10,28,110;113
NannoCCMP1779_8189	cytosolic Fe-S cluster assembly factor NBP35	230
NannoCCMP1779_8243	probable boron transporter 7	440
NannoCCMP1779_8329	serine--tRNA ligase-like	374
NannoCCMP1779_8641	tetratricopeptide repeat (TPR)-containing protein	781
NannoCCMP1779_8685	proteinaceous rnase p 3	112
NannoCCMP1779_8715	tubulin beta chain	248
NannoCCMP1779_8741	pyruvate kinase, cytosolic isozyme-like	163;236;411
NannoCCMP1779_8794	40S ribosomal protein S7-like	143
NannoCCMP1779_8806	Cell division control protein 48 homolog D	728
NannoCCMP1779_8848	ATPase 11, plasma membrane-type	8
NannoCCMP1779_8891	NADP-specific glutamate dehydrogenase isoform X2	193
NannoCCMP1779_8915	Eukaryotic translation initiation factor 3 subunit 7 (eIF-3)	50;506
NannoCCMP1779_9	calcium-transporting ATPase 2, endoplasmic reticulum-type	707
NannoCCMP1779_9028	microsomal glutathione S-transferase 3-like	163
NannoCCMP1779_9036	eukaryotic translation initiation factor 4G	979;1083
NannoCCMP1779_9046	histone deacetylase 14	172
NannoCCMP1779_908	kinesin-like protein KIN-14Q	499
NannoCCMP1779_9086	predicted protein	286

NannoCCMP1779_9121	26S proteasome non-ATPase regulatory subunit 12 homolog A-like	404
NannoCCMP1779_9139	60S ribosomal protein L37a isoform X1	82
NannoCCMP1779_9154	ubiquitin-activating enzyme E1 1-like	335
NannoCCMP1779_9177	dehydroascorbate reductase like3	91
NannoCCMP1779_9185	26S protease regulatory subunit 6A homolog	241
NannoCCMP1779_9258	ATPase ASNA1 homolog	48
NannoCCMP1779_937	eukaryotic translation initiation factor 5-like	121
NannoCCMP1779_9516	soluble inorganic pyrophosphatase 4	56
NannoCCMP1779_9669	40S ribosomal protein S13	38

Transmembrane system

NannoCCMP1779_10023	---NA---	317
NannoCCMP1779_10606	calnexin like	81
NannoCCMP1779_10745	DNA-directed RNA polymerase II subunit 1	125;127
NannoCCMP1779_11163	protein transport protein SEC23-like	98
NannoCCMP1779_11238	trigger factor type chaperone family protein	17
NannoCCMP1779_11360	ABC transporter E family member 2	26;31;35;39;48;65;71
NannoCCMP1779_11631	Heat shock 70 kDa protein 17	165
NannoCCMP1779_11688	ABC transporter G family member 25	147
NannoCCMP1779_130	---NA---	172
NannoCCMP1779_1420	---NA---	877
NannoCCMP1779_16	probable protein disulfide-isomerase A6	28;37;39
NannoCCMP1779_167	exportin-4 protein	1154
NannoCCMP1779_230	ascorbate peroxidase	130
NannoCCMP1779_2320	vacuolar-sorting receptor 3-like isoform X1	131;144
NannoCCMP1779_236	O-acyltransferase WSD1	117;181;187;221;486
NannoCCMP1779_2461	---NA---	179
NannoCCMP1779_275	hsp70-Hsp90 organizing protein 3-like	160;452
NannoCCMP1779_3492	AP-4 complex subunit epsilon	106
NannoCCMP1779_3541	auxin transport protein BIG	471
NannoCCMP1779_3593	alpha-soluble NSF attachment protein	243
NannoCCMP1779_3772	RING-H2 finger protein ATL52	339
NannoCCMP1779_40	target of Myb protein 1-like	244
NannoCCMP1779_4054	clathrin heavy chain 1	1373
NannoCCMP1779_4263	protein transport protein sec23	23
NannoCCMP1779_4669	coatomer subunit alpha-1	1075;1101
NannoCCMP1779_4679	SPX domain-containing protein 1-like	134
NannoCCMP1779_4712	WD repeat-containing protein 76	16
NannoCCMP1779_4808	random slug protein 5	249
NannoCCMP1779_4998	protein transport protein SEC31 homolog B-like	707
NannoCCMP1779_5045	chaperone protein dnaJ 50	38

NannoCCMP1779_515	protein transport protein Sec24-like At3g07100	284
NannoCCMP1779_5366	heat shock protein 83	339;355;524;554
NannoCCMP1779_5385	putative LOV domain-containing protein	322
NannoCCMP1779_5881	autophagy-related protein 18a-like	158;354
NannoCCMP1779_6011	target of Myb protein 1-like	312
NannoCCMP1779_640	AP-1 complex subunit gamma-2-like	15
NannoCCMP1779_6571	coatomer subunit beta'-2 isoform X1	650
NannoCCMP1779_8372	ABC transporter F family member 5	571
NannoCCMP1779_8561	beta-adaptin-like protein B	168;307;413
NannoCCMP1779_8721	temperature-induced lipocalin-1	5
NannoCCMP1779_9383	endoplasmin homolog	55
NannoCCMP1779_9510	vacuolar protein sorting-associated protein 13	2181

Other

NannoCCMP1779_10078	glutathione S-transferase DHAR2-like	154
NannoCCMP1779_10088	Inositol-3-phosphate synthase	499
NannoCCMP1779_10256	CCR4-NOT transcription complex subunit 1-like	377;610
NannoCCMP1779_10317	nascent polypeptide-associated complex subunit alpha-like protein 1	167
NannoCCMP1779_10442	5-oxoprolinase	898;974
NannoCCMP1779_10492	isoform 2 of ankyrin repeat domain-containing protein 17	104
NannoCCMP1779_10922	probable aldehyde dehydrogenase isoform X2	25
NannoCCMP1779_10945	long chain acyl-CoA synthetase 6, peroxisomal isoform X1	91
NannoCCMP1779_11061	UDP-glucose:glycoprotein glucosyltransferase	756
NannoCCMP1779_11306	spermatogenesis-associated protein 20	495
NannoCCMP1779_11336	protein STRICTOSIDINE SYNTHASE-LIKE 10-like	189
NannoCCMP1779_11425	nad-specific glutamate dehydrogenase	272;323;385
NannoCCMP1779_11454	long chain acyl-CoA synthetase 6, peroxisomal-like isoform X2	37;175;299
NannoCCMP1779_11784	thyroid adenoma-associated protein homolog isoform X2	873
NannoCCMP1779_1585	flagellar radial spoke protein 5 isoform X2	24
NannoCCMP1779_199	carbon catabolite repressor protein 4 homolog 1-like isoform X1	90;99
NannoCCMP1779_2107	cysteine and histidine-rich domain-containing protein RAR1	146;278;283
NannoCCMP1779_2242	probable inositol 3-phosphate synthase isozyme 3	393;455
NannoCCMP1779_2426	peroxisomal catalase	94
NannoCCMP1779_2500	serine hydroxymethyltransferase 4-like	79;354
NannoCCMP1779_274	bifunctional protein FolD 2-like	272
NannoCCMP1779_3004	coronin-like protein crn1	721
NannoCCMP1779_3410	Protein decapping 5	35
NannoCCMP1779_3824	enhancer of mRNA-decapping protein 4-like	136

NannoCCMP1779_4001	long chain acyl-CoA synthetase 7, peroxisomal isoform X1	488
NannoCCMP1779_4004	protein NAR1	159;312;579;583
NannoCCMP1779_4938	programmed cell death 8 (apoptosis-inducing factor)	277
NannoCCMP1779_5081	TBCC domain-containing protein 1-like	14
NannoCCMP1779_5344	bifunctionalglutamate/aspartate-prephenate aminotransferase	17
NannoCCMP1779_5694	glutamate--glyoxylate aminotransferase 2	229;385
NannoCCMP1779_5782	Altronate oxidoreductase, putative	193
NannoCCMP1779_5843	L-ascorbate peroxidase 3, peroxisomal	45
NannoCCMP1779_5967	protein NAR1	91;102;250;253;256;299
NannoCCMP1779_6050	FK506-binding protein 2-like isoform X2	182
NannoCCMP1779_6099	Chalcone isomerase	8;13
NannoCCMP1779_6127	bifunctional purine biosynthesis protein PurH	134
NannoCCMP1779_6355	sphingosine-1-phosphate lyase	357;466
NannoCCMP1779_6430	cysteine and histidine-rich domain-containing protein RAR1	253
NannoCCMP1779_6522	peroxisomal acyl-coenzyme A oxidase 1-like	602
NannoCCMP1779_6945	Malate synthase, glyoxysomal	171
NannoCCMP1779_7101	CBL-interacting serine/threonine-protein kinase 23	214
NannoCCMP1779_8005	bifunctional purine biosynthesis protein PurH	134
NannoCCMP1779_8799	branched-chain-amino-acid aminotransferase	365
NannoCCMP1779_9009	5-oxoprolinase-like isoform X1	1056;1191
NannoCCMP1779_9178	Fumarate hydratase class I, anaerobic, putative	258;352
NannoCCMP1779_9558	12-oxophytodienoate reductase 3	352
NannoCCMP1779_9676	putative Bromodomain-containing protein	368
NannoCCMP1779_9754	metacaspase type I	65

Hypothetical protein

NannoCCMP1779_10040	---NA---	60
NannoCCMP1779_1052	---NA---	79;82;123;141;144
NannoCCMP1779_10721	puromycin-sensitive aminopeptidase-like isoform X1	919;924
NannoCCMP1779_10886	---NA---	545
NannoCCMP1779_11446	---NA---	337;357
NannoCCMP1779_11450	---NA---	54
NannoCCMP1779_1155	oxidoreductase, putative	98
NannoCCMP1779_11571	---NA---	11;1473
NannoCCMP1779_1172	hypothetical protein SELMODRAFT_424234	73
NannoCCMP1779_11948	---NA---	172
NannoCCMP1779_125	heme-binding protein 2	277
NannoCCMP1779_1277	---NA---	433;434
NannoCCMP1779_1324	unknown	174

NannoCCMP1779_1401	---NA---	198
NannoCCMP1779_1404	---NA---	58
NannoCCMP1779_1428	---NA---	148;218;405
NannoCCMP1779_1488	---NA---	259
NannoCCMP1779_1506	---NA---	125
NannoCCMP1779_1508	---NA---	172
NannoCCMP1779_158	---NA---	382
NannoCCMP1779_160	---NA---	550
NannoCCMP1779_1904	---NA---	71
NannoCCMP1779_1907	---NA---	422
NannoCCMP1779_1950	---NA---	169
NannoCCMP1779_2199	---NA---	341
NannoCCMP1779_2260	---NA---	290;387;422
NannoCCMP1779_2291	---NA---	250
NannoCCMP1779_2310	---NA---	121
NannoCCMP1779_233	---NA---	409
NannoCCMP1779_2518	---NA---	271;421;695
NannoCCMP1779_2619	---NA---	35
NannoCCMP1779_2777	---NA---	195
NannoCCMP1779_2904	---NA---	50
NannoCCMP1779_3034	---NA---	53
NannoCCMP1779_3183	---NA---	49
NannoCCMP1779_3343	---NA---	252
NannoCCMP1779_356	---NA---	22
NannoCCMP1779_3670	---NA---	15
NannoCCMP1779_3811	cell number regulator 4-like	212;225
NannoCCMP1779_3873	---NA---	134
NannoCCMP1779_3887	---NA---	887
NannoCCMP1779_3964	---NA---	28
NannoCCMP1779_403	---NA---	105
NannoCCMP1779_4097	---NA---	173
NannoCCMP1779_4115	oxidoreductase, putative	307
NannoCCMP1779_4225	---NA---	15
NannoCCMP1779_4284	---NA---	69
NannoCCMP1779_4448	uncharacterized oxidoreductase At4g09670-like	93;220
NannoCCMP1779_4499	---NA---	161;167;245;270;290;298
NannoCCMP1779_4913	---NA---	7
NannoCCMP1779_4965	---NA---	89
NannoCCMP1779_507	---NA---	157
NannoCCMP1779_5178	---NA---	338
NannoCCMP1779_5402	---NA---	350
NannoCCMP1779_5498	---NA---	371

NannoCCMP1779_5560	---NA---	184
NannoCCMP1779_5683	---NA---	295;316
NannoCCMP1779_5830	---NA---	355
NannoCCMP1779_6051	---NA---	258
NannoCCMP1779_6260	---NA---	130
NannoCCMP1779_6354	---NA---	75
NannoCCMP1779_6367	---NA---	505
NannoCCMP1779_6592	---NA---	168
NannoCCMP1779_6702	---NA---	784
NannoCCMP1779_6764	---NA---	336
NannoCCMP1779_6868	putative dehydrogenase	7
NannoCCMP1779_7210	---NA---	458
NannoCCMP1779_7211	---NA---	7;15
NannoCCMP1779_745	uncharacterized protein LOC110673803	102
NannoCCMP1779_7541	---NA---	42
NannoCCMP1779_771	---NA---	61;426
NannoCCMP1779_7937	---NA---	74
NannoCCMP1779_8176	---NA---	482;490
NannoCCMP1779_8387	---NA---	83
NannoCCMP1779_8620	---NA---	40
NannoCCMP1779_8788	---NA---	56;76;105
NannoCCMP1779_8950	---NA---	100
NannoCCMP1779_9006	---NA---	1056;1191;1733;1961;2178
NannoCCMP1779_9495	---NA---	244
NannoCCMP1779_9646	---NA---	10
NannoCCMP1779_9705	---NA---	812
NannoCCMP1779_9946	---NA---	10;18
NannoCCMP1779_9983	---NA---	410
NannoCCMP1779_9993	---NA---	273

Appendix B

Full list of Cys-SOH modified proteins from *A. thaliana* chloroplast

All repeat sequences were removed for clarity. This list is all of the proteins identified from at least one LC-MS/MS run, based on either the dimedone label or oxygen mass shift. Isoform numbers included when Cys-SOH location differs between isoforms.

Table B1: Dark-treated plants

Gene ID	Gene Name	Description	Cys-SOH position(s)
AT1G09100.1	RPT5B	26S proteasome AAA-ATPase subunit RPT5B	105
AT2G32730.1		26S proteasome regulatory complex,Rpn2/Psmd1 subunit	161
AT1G45000.1		AAA-type ATPase protein	353
AT1G27450.1	APT1	adenine phosphoribosyl transferase 1	215
AT1G27450.2	APT1	adenine phosphoribosyl transferase 1	155
AT1G27450.3	APT1	adenine phosphoribosyl transferase 1	256
AT1G70580.1	AOAT2	alanine-2-oxoglutarate aminotransferase 2	377
AT4G01800.1	AGY1	Albino or Glassy Yellow 1	621
AT2G01140.1		Aldolase	187
AT2G30970.1	ASP1	aspartate aminotransferase 1	293
AT1G11910.1	APA1	aspartic proteinase A1	19
AT1G17260.1	AHA10	autoinhibited H(+)-ATPase isoform 10	441
AT2G10940.1		Bifunctional inhibitor/lipid-transfer protein/ 2S albumin	279
AT5G07340.1		Calreticulin protein	309
AT5G07340.2		Calreticulin protein	317
AT3G01500.1	CA1	carbonic anhydrase 1	203
AT5G14740.1	CA2	carbonic anhydrase 2	272;275
AT1G20630.1	CAT1	catalase 1	420
AT3G26740.1	CCL	CCR-like	132
AT5G05170.1	CESA3	Cellulose synthase protein	62
AT5G16910.1	CSLD2	cellulose-synthase like D2	735
AT3G15190.1		chloroplast 30S ribosomal protein S20; putative	78
AT3G53460.4	CP29	chloroplast RNA-binding protein 29	182
AT3G48870.1	HSP93-III	Clp ATPase	109
AT3G48870.2	HSP93-III	Clp ATPase	78
AT3G48870.1	HSP93-III	Clp ATPase	30
AT2G24200.1		Cytosol aminopeptidase protein	305
AT3G56940.2	CRD1	dicarboxylate diiron protein; putative (Crd1)	165
AT3G56940.2	CRD1	dicarboxylate diiron protein; putative (Crd1)	222
AT3G56940.2	CRD1	dicarboxylate diiron protein; putative (Crd1)	63
AT5G46470.1	RPS6	disease resistance protein (TIR-NBS-LRR class)	361
AT2G24420.1		DNA repair ATPase-related	415
AT2G44430.1		DNA-binding bromodomain-containing protein	93

AT5G22060.1	J2	DNAJ homologue 2	149
AT3G44110.1	ATJ	DNAJ homologue 3	194
AT5G25100.1		Endomembrane protein 70 protein	68
AT5G05740.1	EGY2	ethylene-dependent gravitropism-deficient and yellow-green-like 2	167
AT3G61820.1		Eukaryotic aspartyl protease protein	195
AT1G03220.1		Eukaryotic aspartyl protease protein	102
AT4G30950.1	FAD6	fatty acid desaturase 6	413
AT2G26140.1	ftsh4	FTSH protease 4	320
AT5G63570.1	GSA1	glutamate-1-semialdehyde-2;1-aminomutase	33
AT3G04120.1	GAPC	glyceraldehyde-3-phosphate dehydrogenase C subunit 1	159
AT2G05380.1	GRP3S	glycine-rich protein 3 short isoform	92;99
AT1G07930.1		GTP binding Elongation factor Tu protein	150
AT1G07930.1		GTP binding Elongation factor Tu protein	151
AT4G39520.1		GTP-binding protein-related	145
AT3G48420.1		Haloacid dehalogenase-like hydrolase (HAD)	66
AT1G56410.1	ERD2	heat shock protein 70 (Hsp 70) protein	319
ATCG01060.1	PSAC	iron-sulfur cluster binding;electron carriers	54;58
ATCG01060.1	PSAC	iron-sulfur cluster binding;electron carriers	48
ATCG01060.1	PSAC	iron-sulfur cluster binding;electron carriers	51
ATCG01060.1	PSAC	iron-sulfur cluster binding;electron carriers	11
ATCG01060.1	PSAC	iron-sulfur cluster binding;electron carriers	17
AT4G00630.1	KEA2	K+ efflux antiporter 2	268
AT1G49750.1		Leucine-rich repeat (LRR) protein	407
AT3G20820.1		Leucine-rich repeat (LRR) protein	99
AT3G17240.1	LPD2	lipoamide dehydrogenase 2	82;87
AT3G45140.1	LOX2	lipoxygenase 2	611
AT3G16000.1	MFP1	MAR binding filament-like protein 1	471
AT4G37910.1	mtHsc70-1	mitochondrial heat shock protein 70-1	367
AT4G37910.1	mtHsc70-1	mitochondrial heat shock protein 70-1	364
AT1G80030.1		Molecular chaperone Hsp40/DnaJ protein	265
AT5G53580.1		NAD(P)-linked oxidoreductase	310
AT5G37510.1	CI76	NADH-ubiquinone dehydrogenase	218
ATCG01090.1	NDHI	NADPH dehydrogenases	67
AT2G15620.1	NIR1	nitrite reductase 1	505
AT1G08550.1	NPQ1	non-photochemical quenching 1	140
AT1G08550.1	NPQ1	non-photochemical quenching 1	134
AT1G12800.1		Nucleic acid-binding; OB-fold-like protein	587
AT1G12800.1		Nucleic acid-binding; OB-fold-like protein	588
AT1G12250.1		Pentapeptide repeat-containing protein	58
AT4G34830.1	MRL1	Pentatricopeptide repeat (PPR)	822
AT3G06050.1	PRXIIF	peroxiredoxin IIF	114
AT5G48880.1	KAT5	peroxisomal 3-keto-acyl-CoA thiolase 2	360

AT2G33150.1	KAT2	peroxisomal 3-ketoacyl-CoA thiolase 3	417
AT5G14040.1	PHT3;1	phosphate transporter 3;1	270
AT5G14040.1	PHT3;1	phosphate transporter 3;1	149
AT4G03280.1	PETC	photosynthetic electron transfer C	175
AT4G02770.1	PSAD-1	photosystem I subunit D-1	135
AT1G03130.1	PSAD-2	photosystem I subunit D-2	131
AT3G50820.1	PSBO2	photosystem II subunit O-2	61
AT2G47860.1		Phototropic-responsive NPH3 protein	179
AT2G47860.2		Phototropic-responsive NPH3 protein	61
AT2G47860.3		Phototropic-responsive NPH3 protein	202
AT3G17360.1	POK1	phragmoplast orienting kinesin 1	573
AT4G14210.1	PDS3	phytoene desaturase 3	500
AT4G14210.1	PDS3	phytoene desaturase 3	503
AT5G15430.1		Plant calmodulin-binding protein-related	101
AT5G08050.1		Protein of unknown function (DUF1118)	7
AT3G25800.1	PDF1	protein phosphatase 2A subunit A2	308
AT3G55330.1	PPL1	PsbP-like protein 1	48
AT1G74470.1		Pyridine nucleotide-disulphide oxidoreductase protein	415
AT1G61580.1	ARP2	R-protein L3 B	331
AT4G20360.1	RABE1b	RAB GTPase homolog E1B	451
AT3G16100.1	RABG3c	RAB GTPase homolog G3C	84
AT3G05530.1	RPT5A	regulatory particle triple-A ATPase 5A	106
AT1G06190.1		Rho termination factor	24
AT1G06190.1		Rho termination factor	62
AT5G19370.1		rhodanese-like/ PPIC-type PPIASE domain-containing protein	67
AT3G04400.2	emb2171	Ribosomal protein L14p/L23e protein	41
AT5G22440.1		Ribosomal protein L1p/L10e	203
ATCG00905.1	RPS12C	ribosomal protein S12C	27
AT2G40590.1		Ribosomal protein S26e protein	29
AT1G23410.1		Ribosomal protein S27a / Ubiquitin protein	141
AT3G04230.1		Ribosomal protein S5 domain 2-like	25
AT5G18380.1		Ribosomal protein S5 domain 2-like	127
AT2G07732.1		Ribulose bisphosphate carboxylase large chain; catalytic domain	10
ATMG00280.1	ORF110A	Ribulose bisphosphate carboxylase large chain; catalytic domain	10
ATCG00490.1	RBCL	ribulose-bisphosphate carboxylases	427
AT3G26420.1	ATRZ-1A	RNA-binding (RRM/RBD/RNP motifs) protein	123
AT2G39730.1	RCA	rubisco activase	223
AT2G39730.1	RCA	rubisco activase	224
AT2G39730.1	RCA	rubisco activase	282
AT4G13940.1	HOG1	S-adenosyl-L-homocysteine hydrolase	42
AT4G18030.1		S-adenosyl-L-methionine-dependent methyltransferases	119

AT1G75520.1	SRS5	SHI-related sequence 5	144
AT1G75520.1	SRS5	SHI-related sequence 5	145
AT1G48410.1	AGO1	Stabilizer of iron transporter SufD / Polynucleotidyl transferase	696;707
AT2G36390.1	SBE2.1	starch branching enzyme 2.1	820
AT3G13470.1		TCP-1/cpn60 chaperonin protein	40
AT5G28740.1		Tetratricopeptide repeat (TPR)-like	700
AT1G15510.1	ATECB2	Tetratricopeptide repeat (TPR)-like	862
AT5G03880.1		Thioredoxin protein	173
AT4G14713.1	PPD1	TIFY domain/Divergent CCT motif protein	271
AT2G45290.1		Transketolase	509
AT5G39830.1	DEGP8	Trypsin protein with PDZ domain	27
AT3G62250.1	UBQ5	ubiquitin 5	121
AT3G32930.1		unknown protein	187
AT4G14723.1		unknown protein	66
AT5G55610.2		unknown protein	263
AT5G02160.1		unknown protein	84
AT3G55250.1		unknown protein	200
AT2G14740.1	VSR3	vaculolar sorting receptor 3	529
AT1G14610.1	TWN2	valyl-tRNA synthetase / valine--tRNA ligase (VALRS)	433
AT2G06850.1	XTH4	xyloglucan endotransglucosylase/hydrolase 4	290
AT1G52300.1		Zinc-binding ribosomal protein protein	19

Table B2: LL-grown plants

Gene ID	Gene name	Description	Cys-SOH position
Photosynthesis			
AT3G01500.1	CA1	carbonic anhydrase 1	90
AT3G01500.2	CA1	carbonic anhydrase 1	167
AT3G01500.3	CA1	carbonic anhydrase 1	167
AT5G14740.5	CA2	carbonic anhydrase 2	283
AT3G54890	LHCA1	chlorophyll a-b binding protein 6	91
AT5G66190	FNR1	ferredoxin-NADP[+]-oxidoreductase 1	178
AT4G38970	FBA2	fructose-bisphosphate aldolase 2	79
AT1G08550	NPQ1	non-photochemical quenching 1	120
AT1G08550	NPQ1	non-photochemical quenching 1	159
AT1G08550	NPQ1	non-photochemical quenching 1	163
AT1G08550	NPQ1	non-photochemical quenching 1	178
AT4G22890		PGR5-LIKE A	303
ATCG01060	PSAC	photosystem I subunit VII	54
AT4G14210	PDS3	phytoene desaturase 3	310
AT4G14210	PDS3	phytoene desaturase 3	503

AT4G14210	PDS3	phytoene desaturase 3	500
AT5G17230.3	PSY	PHYTOENE SYNTHASE	183
AT1G03630	POR C	protochlorophyllide oxidoreductase C	280
AT1G19150	LHCA6	PSI type II chlorophyll a/b-binding protein	58
AT1G74470		Pyridine nucleotide-disulfide oxidoreductase protein	415
AT3G17930	DAC	B6f complex assembly	63

Redox process

AT3G02360		6-phosphogluconate dehydrogenase protein	375
AT5G62530	ALDH12A1	aldehyde dehydrogenase 12A1	168
AT1G20630	CAT1	catalase 1	420
AT1G13090	CYP71B28	cytochrome P450, 71, sub B, polypeptide 28	93
AT4G00360	CYP86A2	cytochrome P450, 86, sub A, polypeptide 2	69
AT4G00360	CYP86A2	cytochrome P450, 86, sub A, polypeptide 2	85
AT4G30950	FAD6	fatty acid desaturase 6	413
AT1G58290	HEMA1	Glutamyl-tRNA reductase protein	302
AT4G16155		lipoamide dehydrogenase 1	108
AT3G52880.2	MDAR1	monodehydroascorbate reductase 1	45
AT1G63940.1	MDAR6	monodehydroascorbate reductase 6	119
AT1G63940.2	MDAR6	monodehydroascorbate reductase 6	126
AT4G30210	ATR2	P450 reductase 2	602
AT1G71500		Rieske (2Fe-2S) domain-containing protein	141
AT1G24180	IAR4	Thiamin diphosphate-binding fold (THDP-binding) protein	147

Response to stimulus

AT1G49240	ACT8	actin 8	287
AT1G11910	APA1	aspartic proteinase A1	19
AT1G11910	APA1	aspartic proteinase A1	342
AT1G11910	APA1	aspartic proteinase A1	425
AT4G23650	CDPK6	calcium-dependent protein kinase 6	193
AT5G61790	CNX1	calnexin 1	307
AT5G07340.1		Calreticulin protein	309
AT5G07340.2		Calreticulin protein	317
AT1G22450	COX6B	cytochrome C oxidase 6B	147
AT5G22060.1	J2	DNAJ homologue 2	165
AT3G44110.1	J3	DNAJ homologue 3	151
AT3G44110.1	J3	DNAJ homologue 3	167
AT3G44110.2	J3	DNAJ homologue 3	167
AT3G44110.2	J3	DNAJ homologue 3	183
AT1G11860		Glycine cleavage T-protein	75
AT2G33210.1	HSP60-2	heat shock protein 60-2	305
AT2G33210.1	HSP60-2	heat shock protein 60-2	377

AT2G33210.2	HSP60-2	heat shock protein 60-2	372
AT1G56410	ERD2	heat shock protein 70 (Hsp 70) protein	326
AT5G52640	HSP1.4	HEAT SHOCK PROTEIN 81.4	550
AT4G37910	HSP70-1	heat shock protein 70-1	364
AT2G47860.1	SETH6	Phototropic-responsive NPH3 protein	179
AT2G47860.2	SETH6	Phototropic-responsive NPH3 protein	61
AT2G47860.3	SETH6	Phototropic-responsive NPH3 protein	202
AT5G26000	TGG1	thioglucoside glucohydrolase 1	91
AT5G26000	TGG1	thioglucoside glucohydrolase 1	449

Translation

AT2G32940	AGO6	Argonaute protein	132
AT1G43170	RP1	ribosomal protein 1	73
AT2G17360		Ribosomal protein S4 (RPS4A) protein	41
AT2G36170		60S ribosomal protein L40-1	99
AT2G40510		Ribosomal protein S26e protein	26
AT2G40510		Ribosomal protein S26e protein	29
AT2G40510		Ribosomal protein S26e protein	33
AT3G52590	UBQ1	ubiquitin extension protein 1	99
AT5G22440		Ribosomal protein L1p/L10e	203
ATCG00800		ribosomal protein S3	42

Metabolic process

AT3G48870.1	HSP93-III	Clp ATPase	320
AT3G48870.2	HSP93-III	Clp ATPase	289
AT5G50920	CLPC1	CLPC homologue 1	299
AT3G02350	GAUT9	galacturonosyltransferase 9	557
AT2G19860.1	HXK2	hexokinase 2	399
AT2G19860.1	HXK2	hexokinase 2	48
AT2G19860.2	HXK2	hexokinase 2	290
AT4G38690		PLC-like phosphodiesterases protein	281
AT4G38690		PLC-like phosphodiesterases protein	286
AT4G38690		PLC-like phosphodiesterases protein	306
AT2G32415		Polynucleotidyl transferase, ribonuclease H fold protein	532
AT4G13940	HOG1	S-adenosyl-L-homocysteine hydrolase	42
AT1G48600.1	PMEAMT	S-adenosyl-L-methionine-dependent methyltransferases	192
AT1G48600.2	PMEAMT	S-adenosyl-L-methionine-dependent methyltransferases	208
AT1G62290		Saposin-like aspartyl protease protein	387
AT1G66970.2	SVL2	SHV3-like 2	69

Sturctural component

AT3G46520	ACT12	actin-12	287

AT1G18450	ARP2	actin-related protein 4	348
AT5G05170	CEV1	Cellulose synthase protein	42
AT5G05170	CEV1	Cellulose synthase protein	47
AT5G05170	CEV1	Cellulose synthase protein	62
AT5G05170	CEV1	Cellulose synthase protein	65
AT5G20490.1	XIK	Myosin protein with Dil domain-containing protein	783
AT5G20490.2	XIK	Myosin protein with Dil domain-containing protein	703
AT1G14850	NUP155	nucleoporin 155	114
AT1G14850	NUP155	nucleoporin 155	125

Transport

AT4G28390	AAC3	ADP/ATP carrier 3	129
AT1G25490	RCN1	ARM repeat protein	226
AT4G30190.2	HA2	H[+]-ATPase 2	574
AT4G02510	TOC159	translocon at the outer envelope of chloroplasts 159	1064
AT1G70610	ABCB26	transporter associated with antigen processing protein 1	186
AT1G70610	ABCB26	transporter associated with antigen processing protein 1	192

Other

AT2G13360	AGT	alanine:glyoxylate aminotransferase	297
AT2G24420		DNA repair ATPase-like protein	415
AT1G29670		GDSL-like Lipase/Acylhydrolase protein	299
AT4G39520		GTP-binding protein-like protein	143
AT4G39520		GTP-binding protein-like protein	145
AT5G65720.1	NFS1	nitrogen fixation S (NIFS)-like 1	304
AT5G65720.2	NFS1	nitrogen fixation S (NIFS)-like 1	176
AT1G12800		Nucleic acid-binding, OB-fold-like protein	587
AT3G58160	XIJ	P-loop containing nucleoside triphosphate hydrolases	509
AT3G15140		Polynucleotidyl transferase, ribonuclease H-like	83
AT5G07640		RING/U-box protein	283
ATCG00180	RPOC1	RNA polymerase beta' subunit	558
AT1G60650	RZ1B	RNA-binding (RRM/RBD/RNP motifs) protein	120
AT4G18030		S-adenosyl-L-methionine-dependent methyltransferases	119
AT5G28740		Tetratricopeptide repeat (TPR)-like protein	700
AT3G52850	VR1	vacuolar sorting receptor homolog 1	529
AT3G60600.2	VAP27-1	vesicle associated protein	213

Hypothetical Proteins

AT2G42100		Actin-like ATPase protein	288
AT3G22120		cell wall-plasma membrane linker protein	322
AT5G13410		FKBP-like peptidyl-prolyl cis-trans isomerase protein	50

AT4G24330	hypothetical protein (DUF1682)	255
AT1G49750	Leucine-rich repeat (LRR) protein	407
AT3G20820	Leucine-rich repeat (LRR) protein	99
AT5G15980	Pentatricopeptide repeat (PPR) protein	514

Table B3: HL-treated plants

Gene ID	Gene name	Description	Cys-SOH position
Photosynthesis			
AT3G07480		2Fe-2S ferredoxin-like protein	135
AT1G08520	ALBINA 1	Magnesium chelatase	371
AT4G04640	ATPC1	ATPase, F1 complex, gamma subunit protein	249
AT3G55250	PDE329	calcium homeostasis regulator; PSI assembly	126
AT5G14740.5	CA2	carbonic anhydrase 2	283
AT5G14740.5	CA2	carbonic anhydrase 2	294
AT3G47860	LCNP	chloroplastic lipocalin	38
AT3G47860	LCNP	chloroplastic lipocalin	224
AT1G03475	LIN2	Coproporphyrinogen III oxidase	379
AT3G01480	CYP38	cyclophilin 38	28
AT3G10370	SDP6	FAD-dependent oxidoreductase family protein	569
AT1G20020	FNR2	ferredoxin-NADP[+]-oxidoreductase 2	150
AT2G01140	FBA3	Fructose-bisphosphate aldolase	187
AT1G64770	NDF2	NDH-dependent cyclic electron flow 1	319
AT1G08550	NPQ1	non-photochemical quenching 1	120
AT1G08550	NPQ1	non-photochemical quenching 1	159
AT4G30210	ATR2	P450 reductase 2;	602
AT5G64040	PSAN	photosystem I reaction center subunit PSI-N	126
ATCG01060	PSAC	photosystem I subunit VII	54
ATCG01060	PSAC	photosystem I subunit VII	11
ATCG01060	PSAC	photosystem I subunit VII	17
AT2G20890	PSB29	photosystem II reaction center PSB29 protein	284
AT3G50820	PSBO2	photosystem II subunit O-2	48
AT4G14210	PDS3	phytoene desaturase 3	500
AT4G14210	PDS3	phytoene desaturase 3	503
AT1G19150	LHCA6	PSI type II chlorophyll a/b-binding protein	58
AT1G61520	LHCA3	PSI type III chlorophyll a/b-binding protein	8
AT1G74470		Pyridine nucleotide-disulfide oxidoreductase family protein	415
ATCG00490	RBCL	ribulose-1,5-bisphosphate carboxylase/oxygenase large subunit	427
ATCG00490	RBCL	ribulose-1,5-bisphosphate carboxylase/oxygenase large subunit	247
Redox process			
AT2G25450		2-oxoglutarate (2OG) and Fe(II)-dependent oxygenase protein	213

AT2G25450		2-oxoglutarate (2OG) and Fe(II)-dependent oxygenase protein	215
AT5G65750		2-oxoglutarate dehydrogenase, E1 component	40
AT5G62530	P5CDH	aldehyde dehydrogenase 12A1	168
AT5G42650	AOS	allene oxide synthase	381
AT3G63520	CCD1	carotenoid cleavage dioxygenase 1	332
AT1G20630	CAT1	catalase 1	420
AT1G20630	CAT1	catalase 1	413
AT4G33010	GLDP1	glycine decarboxylase P-protein 1	664
AT2G26080	GLDP2	glycine decarboxylase P-protein 2	670
AT2G26080	GLDP2	glycine decarboxylase P-protein 2	575
AT5G37510.2	EMB1467	NADH-ubiquinone dehydrogenase	738
AT5G37510.1	EMB1467	NADH-ubiquinone dehydrogenase	335
AT5G37510.1	EMB1467	NADH-ubiquinone dehydrogenase	95
AT2G02050		NADH-ubiquinone oxidoreductase B18 subunit	61
AT4G25130	MSRA4	peptide met sulfoxide reductase 4	250
AT4G22010	SKS4	SKU5 similar 4	530
AT3G27380	SDH2-1	succinate dehydrogenase 2-1	121
AT5G40650	SDH2-2	succinate dehydrogenase 2-2	120
AT5G04590	SIR	sulfite reductase	198
AT5G03880		Thioredoxin family protein	273
AT2G24820	TIC55-II	translocon at the inner envelope membrane of chloroplasts 55-II	148
AT3G26060	PRXQ	Thioredoxin protein	116

Translation

AT5G03940	CPSRP54	chloroplast signal recognition particle 54 kDa subunit	14
AT3G61240		DEA(D/H)-box RNA helicase family protein	412
AT3G58510		DEA(D/H)-box RNA helicase family protein	243
AT2G45810		DEA(D/H)-box RNA helicase family protein	442
AT4G00660	RH8	RNAhelicase-like 8	419
AT4G29060	EMB2726	elongation factor Ts family protein	27
AT1G07920	EF-Tu	GTP binding Elongation factor Tu family protein	151
AT4G35250	HCF244	NAD(P)-binding Rossmann-fold protein	205
AT4G20360	RABE1b	RAB GTPase homolog E1B	27
AT2G32220		Ribosomal L27e protein family	70
AT3G25920		ribosomal protein L15	111
AT3G63490		Ribosomal protein L1p/L10e family	323
AT2G42740		ribosomal protein large subunit 16A	146
AT5G30510		ribosomal protein S1	70
ATCG01230		ribosomal protein S12	34
ATCG00065		ribosomal protein S12	34
ATCG00905		ribosomal protein S12	34
AT2G40510		Ribosomal protein S26e family protein	23
AT2G40510		Ribosomal protein S26e family protein	26

AT1G23410		Ribosomal protein S27a / Ubiquitin family protein	126
ATCG00800		ribosomal protein S3	42
AT3G62250	UBQ5	ubiquitin 5	121
AT4G19210	ABCE2	RNAse l inhibitor protein 2	25
AT1G52300		Zinc-binding ribosomal protein family protein	19
AT3G16080		Zinc-binding ribosomal protein family protein	22

Response to stimulus

AT1G11910	APA1	aspartic proteinase A1	19
AT1G11910	APA1	aspartic proteinase A1	425
AT3G53230	CDC48B	ATPase, AAA-type, CDC48 protein	74
AT2G25140	CLPB4	casein lytic proteinase B4	276
AT5G26742.2	emb1138	DEAD box RNA helicase (RH3)	742
AT5G26742.3	emb1138	DEAD box RNA helicase (RH3)	649
AT5G55070		Dihydrolipoamide succinyltransferase	60
AT2G17060		Disease resistance protein (TIR-NBS-LRR class) family	1068
AT3G44110	J3	DNAJ homologue 3	191
AT1G03230		Eukaryotic aspartyl protease family protein	87
AT5G63840	RSW3/PSL5	Glycosyl hydrolases family 31 protein	29
AT1G56410	ERD2	heat shock protein 70 (Hsp 70) family protein	326
AT4G37910		heat shock protein 70-1	364
AT3G07770	Hsp89.1	HEAT SHOCK PROTEIN 89.1	636
AT1G79920	Hsp91	heat shock protein 91	368
AT5G60660	PIP2;4	plasma membrane intrinsic protein 2;4	138
AT2G16850	PIP2;8	plasma membrane intrinsic protein 2;8	129
AT1G02130	RA-5	RAS 5	23
AT1G06190	RHON1	Rho termination factor	24

Metabolic processes

ATCG00500	ACCD	acetyl-CoA carboxylase beta subunit	247
AT1G70580	AOAT2	alanine-2-oxoglutarate aminotransferase 2	377
AT5G08670		ATP synthase alpha/beta family protein	87
AT1G17260	AHA10	autoinhibited H[+]-ATPase isoform 10	336
AT5G50920	CLCP1	CLPC homologue 1	39
AT3G61820		Eukaryotic aspartyl protease family protein	195
AT4G23940	FtsHi1	FtsH extracellular protease family	722
AT1G06430	FTSH8	FTSH protease 8	7
AT1G23310	GGT1	glutamate:glyoxylate aminotransferase	18
AT3G48420		Haloacid dehalogenase-like hydrolase (HAD) protein	66
AT3G48420		Haloacid dehalogenase-like hydrolase (HAD) protein	83
AT4G35260	IDH1	isocitrate dehydrogenase 1	344
AT1G77590	LACS9	long chain acyl-CoA synthetase 9	622

AT3G47520	MDH	malate dehydrogenase	333
AT2G36880	MAT3	methionine adenosyltransferase 3	31
AT5G65720	NFS1	nitrogen fixation S (NIFS)-like 1	24
AT2G32415.2		Polynucleotidyl transferase, ribonuclease H fold protein	532
AT1G78570	RHM1	rhamnose biosynthesis 1	534
AT3G45480		RING/U-box protein with C6HC-type zinc finger	281
AT1G66970.1	SVL2	SHV3-like 2	411
AT1G66970.2	SVL2	SHV3-like 2	433
AT2G20990	SYTA	synaptotagmin A	90
AT5G39320	UDG4	UDP-glucose 6-dehydrogenase family protein	284

Phosphorylation

AT1G27630	CYCT1;3	cyclin T 1;3	262
AT1G31230	AK-HSDH	aspartate kinase-homoserine dehydrogenase i	521
AT1G21250	WAK1	cell wall-associated kinase	311
AT1G21250	WAK1	cell wall-associated kinase	327
AT1G61360.2		S-locus lectin protein kinase family protein	366
AT1G61360.1		S-locus lectin protein kinase family protein	447
AT1G21230	WAK5	wall associated kinase 5	249
AT1G19390		Wall-associated kinase family protein	704
AT3G48870.1	HSP93-III	Clp ATPase	109
AT3G48870.2	HSP93-III	Clp ATPase	78

Transport

AT1G65260	VIPP1	plastid transcriptionally active 4	65
AT4G28390	AAC3	ADP/ATP carrier 3	129
AT3G08530		Clathrin, heavy chain	1583
AT4G25450	ABCB28	non-intrinsic ABC protein 8	122
AT5G47200	RAB1A	RAB GTPase homolog 1A	23
AT4G17530	RAB1C	RAB GTPase homolog 1C	23
AT3G53610	RAB8	RAB GTPase homolog 8	30
AT3G46060	RAB8A	RAB GTPase homolog 8A	30
AT5G03520	RAB8C	RAB GTPase homolog 8C	30
AT3G09900	RABE1E	RAB GTPase homolog E1E	30
AT2G10940		Bifunctional inhibitor/lipid-transfer 2S albumin protein	238

Structure

AT3G19820	DWF1	cell elongation protein / DWARF1 / DIMINUTO (DIM)	86
AT2G06850	XTH4	xyloglucan endotransglucosylase/hydrolase 4	290
AT5G62350		Plant invertase/pectin methylesterase inhibitor protein	109
AT5G05170	CEV1	Cellulose synthase family protein	561
AT3G16000	MFP1	MAR binding filament-like protein 1	229
AT3G16000	MFP1	MAR binding filament-like protein 1	471

Other

AT3G32930		6,7-dimethyl-8-ribityllumazine synthase	187
AT3G10690	GYRA	DNA GYRASE A	770
AT2G24420		DNA repair ATPase-like protein	415
AT2G01970		Endomembrane protein 70 protein family	102
AT4G28250	EXPB3	expansin B3	89
AT1G29670		GDSL-like Lipase/Acylhydrolase protein	298
AT1G79340	MC4	metacaspase 4	32
AT1G03090	MCCA	methylcrotonyl-CoA carboxylase alpha chain	37
AT4G27680		P-loop containing nucleoside triphosphate hydrolases protein	296
AT5G13770		Pentatricopeptide repeat (PPR-like) protein	45
AT2G02230	PP2-B1	phloem protein 2-B1	173
AT5G64030		S-adenosyl-L-methionine-dependent methyltransferases protein	495
AT5G64030		S-adenosyl-L-methionine-dependent methyltransferases protein	549
AT4G10440		S-adenosyl-L-methionine-dependent methyltransferases protein	551
AT4G18030		S-adenosyl-L-methionine-dependent methyltransferases protein	119
AT1G73600		S-adenosyl-L-methionine-dependent methyltransferases protein	19
AT3G17390	MTO3	S-adenosylmethionine synthetase family protein	31
AT3G17390	MTO3	S-adenosylmethionine synthetase family protein	161

Hypothetical protein

AT5G02160	---NA---	84
AT3G52610	GATA zinc finger protein	348
AT2G05380.1	glycine-rich protein 3 short isoform	92
AT2G05380.2	glycine-rich protein 3 short isoform	78
AT1G04470	hypothetical protein (DUF810)	643
AT2G07732	hypothetical protein ArthMp025	79
AT2G07732	hypothetical protein ArthMp025	53
AT1G33600	Leucine-rich repeat (LRR) family protein	467
AT3G20820	Leucine-rich repeat (LRR) family protein	99
AT1G49750	Leucine-rich repeat (LRR) family protein	407
AT5G03900	Iron-sulfur cluster biosynthesis family protein	99
AT1G01320	Tetratricopeptide repeat (TPR)-like protein	228
AT4G28080	Tetratricopeptide repeat (TPR)-like protein	404
AT5G28740	Tetratricopeptide repeat (TPR)-like protein	700
AT3G13160	Tetratricopeptide repeat (TPR)-like protein	340
AT4G28080	Tetratricopeptide repeat (TPR)-like protein	179
AT5G14030	translocon-associated protein beta (TRAPB) family protein	174
AT3G25805	transmembrane protein	63

AT2G14720	vacuolar sorting receptor 4	324
AT3G52850	vacuolar sorting receptor homolog 1	524
AT3G18890	NAD(P)-binding Rossmann-fold protein	148
AT3G18890	NAD(P)-binding Rossmann-fold protein	5
AT3G11730	Ras-related small GTP-binding family protein	23
AT5G59840	Ras-related small GTP-binding family protein	30